Analyzing the Effect of Different Aggregation Approaches on Remotely Sensed Data

Rahul Raj

January, 2009

Analyzing the Effect of Different Aggregation Approaches on Remotely Sensed Data

by

Rahul Raj

Thesis submitted to Indian Institute of Remote Sensing (IIRS) and International Institute for Geo-information Science and Earth Observation (ITC) in partial fulfilment of the requirements for the Joint Master in Geoinformatics.

Thesis Assessment Board:

Chairman	**:**	Prof. Dr. Ir. Alfred Stein
External Examiner	**:**	Dr. V. K. Sehgal
IIRS Member	**:**	Dr. Sameer saran Mr. P.L.N. Raju

Supervisors:	IIRS	**:**	Dr. Yogesh Kant
	ITC	**:**	Dr. Nicholas Hamm

INTERNATIONAL INSTITUTE FOR GEO-INFORMATION SCIENCE AND EARTH OBSERVATION ENSCHEDE, THE NETHERLANDS

&

INDIAN INSTITUTE OF REMOTE SENSING, NATIONAL REMOTE SENSING CENTRE (NRSC), ISRO, DEPARTMENT OF SPACE, DEHRADUN, INDIA

I certify that although I may have conferred with others in preparing for this assignment, and drawn upon a range of sources cited in this work, the content of this thesis report is my original work.

Signed …….

(Name)

Disclaimer

This document describes work undertaken as part of a programme of study at the International Institute for Geo-information Science and Earth Observation. All views and opinions expressed therein remain the sole responsibility of the author, and do not necessarily represent those of the institute.

Dedicated to My Parents

ACKNOWLEDGEMENTS

This thesis is the end of my long journey in obtaining my degree in Geoinformatics. I have not travelled in a vacuum in this journey. There are some people who made this journey easier with words of encouragement and more intellectually satisfying by offering different places to look to expand my theories and ideas.

I would like to express my deep and sincere gratitude to my ITC supervisor, Dr. Nicholas Hamm. His wide knowledge and logical way of thinking have been of great value for me. His understanding, constructive criticism, encouraging and personal guidance have provided a good basis for the present thesis.

I am deeply grateful to my IIRS supervisor, Dr. Yogesh Kant for his detailed and constructive comments, and for his important support throughout this work. His encouraging words brought my path into the light when I was standing in dark.

I warmly thank Dr. V.K Dadhwal, Dean, Indian Institute of Remote Sensing for his special interest and valuable suggestions at all the stages of research work.

My special thanks to Mr. P.L.N. Raju, In-charge Department of Geoinformatics, and Dr. Sameer Saran, course coordinator IIRS-ITC Joint Study Program IIRS, Dehradun, who provided me nice infrastructure and environment to carry-out the present study and gave me untiring help during my difficult moments.

My special expression of appreciation and love is given to Dr. C. Jeganathan, who gave me direction to make a proposal on this research work. I can not forget his constructive ideas, support and motivation during this research work. He is a person having a soft corner for everybody. He is my idol.

I have furthermore to thank Ms Vandita Srivastava and Mrs Shefali Agarwal for stimulating suggestions during this research work.

I would also like to gratefully acknowledge the support of my friends and colleagues, Shashi, Alka, Naveen, Navneet, Anurag, Gaurav, Jitendra, in IIRS. They helped me immensely by giving me encouragement and friendship. Especially I am thankful to Amitava and V. S. Pandey for countless hour spent discussing fruitful ideas over cups of coffee at the campus.

Last but not the least; I owe my loving thanks to my mother Mrs Renu Kumari, my father Mr Birendra Prasad, my brothers Bipul Raj and Atul Raj, my sister Mrs Nandita verma. Whose constant encouragement and love I have relied throughout my time at the Academy. Without their support it would have been impossible for me to finish this work.

ABSTRACT

Spatial aggregation is widely used in the studies, such as land use/cover monitoring, ecological resource management, that is carried out at regional, national and global level. Spatial aggregation divides the input grid of fine resolution raster image into blocks and the value for each block is determined to generate coarse resolution aggregated grid. Spatial aggregation of classified image is called categorical aggregation and spatial aggregation of continuous image is called numerical aggregation. Both aggregation approaches produce changes in fine resolution image in different way, which is based on the aggregation logic used by them. Present study examined the effect of both categorical and numerical aggregation approaches. Under categorical aggregation approach, the effect of majority rule-based (MRB), random rule-based (RRB) and point centered distance weighted moving window method (PDW) was analyzed. Under categorical aggregation approach, the effect of mean and central pixel resampling was addressed. Most of the previous studies to assess the effect of aggregation were carried out using land-cover classes. The present study evaluated the effect of aggregation using land use/cover classes to report the generality of results. The LISS-III image (23.5m) was aggregated to level 70.5m, 117.5m and 164.5m before and after classifying it.

The change in class proportions, aggregation index (AI) and square pixel index (SqP) with respect to reference image were used to assess the effect of aggregation approaches. The calibration based model is useful to correct the area of classes with respect to reference area, which is distorted due to coarse resolution. The effect of MRB and mean approach on deriving the calibration based model was also addressed. The local variance of each class was also computed to assess the effect of numerical aggregation approaches. As the RRB approach is based on random selection of class from input grid, so it produces different realizations of aggregated image. PDW approach is based on selection of different parameters values, so it also produces different realizations by changing the parameters values. The variability in realizations of RRB and PDW were reported by assessing their effect on class proportions, AI and SqP value.

Results indicated that RRB, PDW and CPR approach preserved the class proportion with decreasing spatial resolutions. MRB increased the proportion of dominant class and decreased all other class proportions. On the contrary, mean approach increased the proportion of class that was not dominant in landscape. MRB increased the AI value of dominant class and decreased AI value of other classes. RRB, PDW and CPR decreased AI value of all classes, but slope of decrease was less in the case of mean aggregation approach. RRB, PDW and CPR approach produced low distortion in shape complexity of all classes than MRB and mean approach and thus carried spatial information regarding shape complexity better than MRB and mean approach. As the RRB, PDW and CPR maintained the class proportions so these approaches were not used to derive calibration based model. It was found that MRB responded better to derive calibration based model than mean approach. Graph of local variance curve showed that mean approach decreased the local variance of each class; on the contrary CPR approach produced strong increase in local variance. For the different realizations, RRB responded in similar manner, but PDW produced variability that is best minimized by choosing its one of the parameters ‘weight = 2’.

The work attempted here was to analyze the effect of both categorical and numerical aggregation approaches in depth so that understanding of their effects can help to select appropriate aggregation approach for particular study.

Key words: Aggregation, Majority rule-based, Random rule-based, Point centered distance weighted moving window method, Mean, Central pixel resampling, Aggregation Index, Square Pixel Index, Calibration based model, Local variance.

Table of contents

1. INTRODUCTION 1

1.1. IMPORTANCE OF SPATIAL AGGREGATION OF SATELLITE DATA 1
1.2. SPATIAL AGGREGATION APPROACHES AND THEIR EFFECTS 2
1.3. NEED FOR A CALIBRATION BASED MODEL 2
1.4. RESEARCH IDENTIFICATION 2
1.5. RESEARCH OBJECTIVES 4
1.6. RESEARCH QUESTIONS 4

2. REVIEW OF LITERATURE 5

2.1. SCALE DEFINITIONS 5
2.2. AGGREGATION OF CLASSIFIED IMAGE 6
2.3. AGGREGATION OF CONTINUOUS IMAGE 11

3. STUDY AREA & DATA PROCESSING 13

3.1. STUDY AREA 13
3.2. DATA USED 14
3.3. PROCESSING OF SATELLITE DATA 14

4. METHODOLOGY 15

4.1. METHEDOLOGY FLOW CHART 15
4.1.1. Implementation of categorical aggregation approaches 15
4.1.2. Implementation of numerical aggregation approaches 16
4.1.3. Brief explanation of flow chart 16
4.2. SUPERVISED FUZZY C-MEAN CLASSIFICATION 17
4.3. ACCURACY ASSESSMENT OF CLASSIFIED IMAGES 19
4.4. AGGREGATION APPROACHES 19
4.4.1. Categorical aggregation approaches 19
4.4.2. Numerical aggregation approaches 23
4.5. LANDSCAPE METRICS TO ASSESS SPATIAL PROPERTIES 24
4.5.1. Aggregation Index (AI) 25
4.5.2. Square Pixel (SqP) 26
4.6. CALIBRATION BASED MODEL FOR AREA CORRECTION 26
4.7. STATISTICAL PROPERTY OF IMAGES AT CLASS LEVEL 27

5. RESULTS & DISCUSSIONS 29

5.1. CLASSIFICATION ACCURACY 29
5.2. ANALYSIS OF APPLIED AGGREGATION APPROACHES 30
5.2.1. Class proportions 30
5.2.2. Aggregation Index 33
5.2.3. Square pixel Index (SqP) 35
5.2.4. Calibration based model (slope estimator) for area correction 38
5.2.5. Local variance of classes 42
5.3. REALIZATIONS OF RRB AND PDW AGGREGATION APPROACH 44
5.4. SUMMARY OF RESULTS 49

6. CONCLUSIONS & RECOMMENDATIONS 51

7. REFERENCES 55

APPENDIX 1 58

CLASS PROPORTIONS OBSERVED FOR EACH AGGREGATION APPROACH AT EACH AGGREGATION LEVEL 58
AGGREGATION INDEX OF EACH CLASS FOR EACH AGGREGATION APPROACH AT EACH AGGREGATION LEVEL 58
SQUARE PIXEL INDEX OF EACH CLASS FOR EACH AGGREGATION APPROACH AT EACH AGGREGATION LEVEL 59
SLOPE ESTIMATOR ASSESSMENT OF CLASS PROPORTIONS FOR MAJORITY RULE-BASED AND MEAN AGGREGATION APPROACH AT EACH AGGREGATION LEVEL..... 59
TOTAL ERROR (TE) BEFORE AND AFTER APPLYING SLOPE ESTIMATOR METHOD..... 60
LOCAL VARIANCE OF EACH CLASS FOR MEAN AND CPR APPROACH AT EACH AGGREGATION LEVEL..... 60
STANDARD DEVIATION OF PERCENT CHANGE IN CLASS PROPORTIONS, AGGREGATION INDEX AND SQUARE PIXEL INDEX 60
RRB realizations..... 60
PDW realizations using 100 random number seeds 61

APPENDIX 2 62

CODE OF MAJORITY RULE-BASED AGGREGATION APPROACH 62
CODE OF RANDOM RULE-BASED AGGREGATION APPROACH 65
EXPLANATION OF PDW AGGREGATION APPROACH..... 67
CODE OF CENTRAL PIXEL RESAMPLING APPROACH..... 71
CODE OF AGGREGATION INDEX 73
SOME LIMITATIONS OF CODE..... 75

List of Figure

FIGURE 2.1 METHODOLOGY ADOPTED BY MOODY (1998) TO APPLY SLOPE ESTIMATOR METHOD 7
FIGURE 2.2 METHODOLOGY ADOPTED BY GARDNER *ET AL.* (2008) TO ASSESS THE EFFECT OF PDW APPROACH 9
FIGURE 3.1 LOCATION OF STUDY AREA AND CORRESPONDING LISS-III IMAGE 13
FIGURE 4.1 FLOW DIAGRAM SHOWING IMPLEMENTATION OF CATEGORICAL AGGREGATION APPROACHES 15
FIGURE 4.2 FLOW DIAGRAM SHOWING IMPLEMENTATION OF NUMERICAL AGGREGATION APPROACHES 16
FIGURE 4.3 MRB AGGREGATION APPROACH 20
FIGURE 4.4 RRB AGGREGATION APPROACH 21
FIGURE 4.5 AGGREGATION BY PDW (SOURCE PDW DOCUMENTATION) 22
FIGURE 4.6 DISTRIBUTION OF SAMPLING NET FOR N = 9 AND R = 0 23
FIGURE 4.7 MEAN AGGREGATION APPROACH 24
FIGURE 4.8 CPR AGGREGATION APPROACH 24
FIGURE 5.1 A) LISS-III CONTINUOUS IMAGE B) LISS-III CLASSIFIED IMAGE 30
FIGURE 5.2 CLASS PROPORTIONS OF CLASSIFIED LISS-III IMAGE AGGREGATED TO AGGREGATION LEVEL 3, 5 & 4 USING THE APPROACHES A) MAJORITY RULE-BASED B) RANDOM RULE-BASED C) POINT CENTERED, DISTANCE WEIGHTED, AND MOVING WINDOW METHOD D) MEAN E) CENTRAL PIXEL RESAMPLING 32
FIGURE 5.3 AI OF EACH CLASS IN CLASSIFIED LISS-III IMAGE AGGREGATED TO AGGREGATION LEVEL 3, 5 & 4 USING THE APPROACHES A) MAJORITY RULE-BASED B) RANDOM RULE-BASED C) POINT CENTERED, DISTANCE WEIGHTED, AND MOVING WINDOW METHOD D) MEAN E) CENTRAL PIXEL RESAMPLING 34
FIGURE 5.4 SQP OF EACH CLASS IN CLASSIFIED LISS-III IMAGE AGGREGATED TO AGGREGATION LEVEL 3, 5 & 4 USING THE APPROACHES A) MAJORITY RULE-BASED B) RANDOM RULE-BASED C) POINT CENTERED, DISTANCE WEIGHTED, AND MOVING WINDOW METHOD D) MEAN E) CENTRAL PIXEL RESAMPLING 36
FIGURE 5.5 TOTAL ERROR PRODUCED BEFORE AND AFTER APPLYING SLOPE ESTIMATOR METHOD FOR MRB 38
FIGURE 5.6 PERFORMANCE OF SLOPE ESTIMATOR METHOD FOR EACH CLASS DISTORTED BY MRB APPROACH AT A) AGGREGATION LEVEL 3 B) AGGREGATION LEVEL 5 C) AGGREGATION LEVEL 7 39
FIGURE 5.7 TOTAL ERROR PRODUCED BEFORE AND AFTER APPLYING SLOPE ESTIMATOR METHOD FOR MEAN 40
FIGURE 5.8 PERFORMANCE OF SLOPE ESTIMATOR METHOD FOR EACH CLASS DISTORTED BY MEAN APPROACH AT A) AGGREGATION LEVEL 3 B) AGGREGATION LEVEL 5 C) AGGREGATION LEVEL 7 41
FIGURE 5.9 LOCAL VARIANCE OF EACH CLASS FOR MEAN APPROACH AT AGGREGATION LEVEL 3, 5 AND 7 42
FIGURE 5.10 LOCAL VARIANCE OF EACH CLASS FOR CPR APPROACH AT AGGREGATION LEVEL 3, 5 AND 7 43
FIGURE 5.11 VARIABILITY IN EACH CLASS PROPORTION DUE TO DIFFERENT RRB REALIZATIONS AT AGGREGATION LEVELS 3, 5 & 7 44
FIGURE 5.12 VARIABILITY IN AI OF EACH CLASS DUE TO DIFFERENT RRB REALIZATIONS AT AGGREGATION LEVELS 3, 5 & 7 45
FIGURE 5.13 VARIABILITY IN SQP OF EACH CLASS DUE TO DIFFERENT RRB REALIZATIONS AT AGGREGATION LEVELS 3, 5, 7 46
FIGURE 5.14 AGGREGATION INDEX OF EACH CLASS AT AGGREGATION LEVEL 3, 5 AND 7 FOR CHOICES OF W, 0, 1 & 2 47
FIGURE 5.15 VARIABILITY IN EACH CLASS PROPORTION DUE TO DIFFERENT PDW REALIZATIONS AT AGGREGATION LEVELS 3, 5 & 7 47
FIGURE 5.16 VARIABILITY IN AI OF EACH CLASS DUE TO DIFFERENT PDW REALIZATIONS AT AGGREGATION LEVELS 3, 5 & 7 48
FIGURE 5.17 VARIABILITY IN SQP OF EACH CLASS DUE TO DIFFERENT PDW REALIZATIONS AT AGGREGATION LEVEL 3, 5 & 7 48

List of Tables

TABLE 3.1 LISS-III BAND INFORMATION 14

TABLE 4.1 AGGREGATION LEVELS AND CORRESPONDING RESOLUTION 16

TABLE 5.1 CLASSIFICATION ACCURACY OF LISS-III BASE IMAGE AND ALL AGGREGATED IMAGES 29

1. Introduction

1.1. Importance of spatial aggregation of satellite data

Many Geographic Information System (GIS) and Remote sensing related studies such as monitoring of landscape patterns, face problems in the availability of remotely sensed data (RS data) at specific resolution. The data available for particular study rarely fit perfectly the scale at which the process being studied, or the scales at which decisions are needed (Quattrochi *et al.* 1997). As for example if decision makers are to implement a policy that requires general pattern of land-cover (Stein *et al.* 2001) and there is availability of RS data at the resolution finer than that required by policy model, then it is more feasible to aggregate available data to the required resolution rather than looking for the data from external sources, which is more time consuming and not a cost effective.

An application of geographic information system frequently requires the integration of RS data obtained at different spatial resolution (Turner *et al.* 1989). Combining information from multiple scales of measurement (spatial resolution or grain size) is an essential part of global change and landscape dynamic research (Cullinan *et al.* 1992). Integration of RS data obtained at different resolution is possible only when they are brought to the same level or resolution. Spatial aggregation is often used to rescale the data before integration.

Large spatial extent of landscape and multiple resolution satellite data are often used to examine the issues of biodiversity, wildlife conservation, and landscape change. These involve the use of RS data covering large area and aggregation of RS data from finer resolution to coarse resolution (Rastetter *et al.* 1992, Leibowitz *et al.* 1999 in He *et al.* 2002).

According to Bian *et al.* (1999), spatial characteristics (spatial patterns, spatial autocorrelation, etc) at corresponding scales is represented by spatial aggregation of RS data available at fine resolution. Spatial aggregation is widely used for "scaling up" environmental analysis or model from local to regional or global scales in the field of global studies.

Fine resolution reference image can be used in the validation of global land cover datasets (Moody *et al.* 1995), for this purpose it is required to aggregate fine resolution reference map to the corresponding coarse resolution global land cover dataset. Aggregation of fine resolution data is used to achieve the characterization of land surface boundary for a grid cell (50- 100Km) of General Circulation Model (Gupta *et al.* 2000, 2002).

Aggregation of fine resolution data is also used to derive a calibration based models for the correction of area estimated from coarse resolution land-cover data (Moody *et al.* 1996, Moody. 1998). The model is developed between the fine resolution and the coarse resolution RS data which in turn is obtained by spatial aggregation of fine resolution RS data. This model is used to correct area estimates of land-cover when only coarse resolution RS data is available.

1.2. Spatial aggregation approaches and their effects

Two types of approaches are used for aggregating fine resolution RS data. One approach is based on numerical aggregation in which the mathematical method such as mean, median central pixel resampling (Bian *et al.* 1999) is applied on the input grid DN values and the result is assigned to the output aggregated grid. Another approach is based on the categorical aggregation that assigns the class label to output grid by logical processing on input grid categories such as selection of frequently occurring class, random selection of class from input grid (He *et al.* 2002).

Change in spatial properties of land-cover classes is observed by spatial aggregation of fine resolution RS data. Landscape metrics (mean patch size, contagion, fractal dimension, landscape shape index, aggregation index, square pixel, etc) are frequently used to quantify and compare the spatial properties of different classes at a given spatial resolution or same class at different spatial resolutions (O'Neill *et al.* 1988, Turner *et al.* 1989, Moody *et al.* 1995, Frohn *et al.* 1998, He *et al.* 2000, 2002, Wu *et al.* 2002, Saura *et al.* 2004, Frohn *et al.* 2006, Gardner *et al.* 2008). In other words landscape metrics are important for assessing the effect of aggregation approaches. For example, aggregation level (clumpiness that is assessed by aggregation index) of dominant class increases with decreasing spatial resolution using majority rule-based (MRB) aggregation approach. This shows MRB generalizes the spatial pattern of dominant class (He *et al.* 2000).

1.3. Need for a calibration based model

According to Moody *et al.* (1996, 1998), many problems of Earth system science (models of net primary productivity, biogeochemical cycling) and ecological resources management depend on the reliable (with respect to ground or reference fine resolution RS data) measurement of land cover data. Earth system science and ecological resource management related fields of enquiry have been increasingly focused at global scale by many researchers. Coarse resolution RS data is generally used in global scale studies but proportional accuracy of land cover data derived from it, is affected by the coarse grid. Areal accuracy of global land-cover data is also important as it is used to monitor the location, extent and changes of major vegetation assemblage. Calibration based model provides a posterior (after classification) correction of land-cover area estimate derived from coarse resolution RS data with respect to that derived from fine resolution RS data. Model is developed between the fine resolution and coarse resolution RS data and it is used later when only coarse resolution RS data are available.

1.4. Research identification

The spatial scale related issues are studied under the term- modifiable areal unit problems (MAUP) that is composed of zoning and scale problems. Zoning problems refer to the variation in results when areal units are combined into different zones in different ways at the same scale. Scale problems refer to the variation in results when the areal units are represented as small numbers of large areal units by changing grain size or resolution (Quattrochi *et al.* 1997, Wu *et al*. 2002).

In the proposed work, scale problems has been taken into account, where numerical and categorical aggregation has been used to aggregate fine resolution data to achieve coarse resolution. The evaluation of the effects on aggregated data caused by either numerical or categorical aggregation has been studied elsewhere (Moody *et al.* 1995, Bian *et al.* 1999, Gupta *et al.* 2000, 2002, He *et al.* 2002, Gardner *et al*. 2008). In these studies, impact of categorical aggregation has been quantified by taking spatial properties (such as mean patch size, fractal dimension, edge density, aggregation index) of land-

cover classes. The impact of numerical aggregation has been quantified by taking statistical distribution (mean and standard deviation of aggregated data) of aggregated data, but the impact of numerical aggregation on spatial properties of class has not been addressed in these studies. Derivation of calibration based model is also related to the scaling problems. Majority rule-based or averaging of DN values aggregation approach has been used to derive it (Moody *et al.* 1996, Moody 1998). In their studies, behaviour of other aggregation approaches to derive the calibration based model was not tested.

The proposed work examined the impact of both numerical and categorical aggregation approach on spatial properties (assessed by landscape metrics) and class proportions as well as on deriving calibration based model.

Random rule-based (RRB) categorical aggregation approach is based on random selection of class from the input grid of fine resolution classified RS data and then assignment of randomly selected class to the desired coarse grid output (He *et al.* 2002). As it is based on random selection, different outputs for the same coarse resolution level are realized each time the RRB is run on the fine input grid. Variability in output has not been addressed previously. The proposed work focused on this issue also.

Point-centered, distance weighted, moving window method (PDW) categorical aggregation (as well as disaggregation) approach has been developed by Gardner *et al.* (2008). The aggregated output of PDW depends on three parameters; n (number of sample points), r (resolution of sample points) and w (weight of sample points from center). PDW sets sample points around centre of input grid of fine resolution classified RS data, calculates normalized frequency distribution f of sampled class types, randomly select one class from f and assigns it to the desired coarse grid output. As this algorithm is also based on random selection of a class from f, random number seed concept has also been used in this algorithm to avoid the variability in output for the same coarse resolution level. But use of different random number seeds may give the variability in output. The proposed work pointed out variability in output produced by PDW using different random number seed as well as choice of different parameter values.

When numerical aggregation is used, through different aggregation levels the change in statistical properties (mean, median, standard deviation, etc) is also observed (Bian *et al.* 1999). In the proposed work, statistical property has been also considered to quantify the aggregation effect in the case of numerical aggregation approaches.

The aim of proposed work is to evaluate the numerical and categorical aggregation approaches by taking following indicators into consideration

1. Change in class proportion through aggregation levels
2. Change in spatial properties through aggregation levels
3. Change in statistical property through aggregation levels only in the case of numerical aggregation approach
4. Impact of aggregation approaches to derive calibration based model for area correction

1.5. Research objectives

The main objective of this research is to analyze the effect of different algorithms (majority rule-based, random rule-based, PDW, mean, central pixel resampling) on aggregation of fine resolution remotely sensed data by taking into consideration of their impact on spatial, statistical properties of aggregated image and derivation of calibration based model for area correction across aggregation levels.
The sub objective of this research is to evaluate the variability in outputs of PDW and RRB aggregation approach.

1.6. Research questions

For the fulfilment of objectives, present study aims to answer the following questions:

1. As a function of resolution and aggregation approaches and aggregation levels, what changes are observed in land use/cover class proportions?
2. How do the spatial properties of land use/cover class change using different aggregation approaches through aggregation levels?
3. What variations are found in statistical property of continuous aggregated image through aggregation levels?
4. What is the impact of different aggregation approaches on deriving calibration based model for area correction?
5. Is it possible to optimize the PDW parameters?
6. What variability is found in different realization of random rule aggregation approach on classified image?

2. Review of literature

2.1. Scale definitions

Geographic information systems (GIS) and remote sensing have opened a gate to handle multiscale representation of remotely sensed data. Integration and use of multiscale data in GIS are often needed in the area of global change studies, to represent spatial properties that can be revealed at particular scale, to understand the spatial processes through information from range of scales (Quattrochi *et al.* 1997). The issue of scale has prompted interest from scientists from different disciplines, which leads to emergence of new era of science, called science of scale. (Marceau *et al.* 1999). The meaning of scale is treated differently in various perspectives. Its meaning can be acknowledged broadly into three categories viz spatial, temporal and spatio-temporal scale. Four connotations of spatial scale have been suggested (Quattrochi *et al.* 1997).

1. Cartographic scale – It is the ratio of distance on a map to the corresponding distance on a ground. A large scale map provides more detailed information of ground than small scale map.
2. Geographic scale – It refers to the spatial extent of study area. A large geographic scale means a large scale study covering large area than small geographic scale which shows small scale study covering small area. Geographic scale is also termed as observational scale or simply extent in ecology (Turner *et al.* 1989).
3. Operational scale – It refers to the scale at which certain phenomenon or processes operate in the environment. For example, migration pattern of residents from downtown to suburbs can be best observed by the population change at city-specific level than at regional or state levels that may cause existence of different migration patterns. Above example also shows that phenomenon exist at one scale may not exist at another scale.
4. Measurement scale – It refers to the smallest distinguishable parts of an object or features in spatial data. Remotely sensed data (RS data or image) encapsulate the measurement scale as a pixel size. It is also termed as spatial resolution or grain (Turner *et al.* 1989). In ecology, measurement scale is also used for sampling interval.

Remote sensing has opened a new era of science and technology to provide a synoptic view of landscape in different section of electro-magnetic radiation with range of spatial resolution (~1m to ~1000m). Different spatial resolution has its own importance for the different domains of remote sensing application such as forestry, hydrology and landscape ecology. For example coarse resolution data is important for monitoring the landscape pattern at a large scale.

Remotely sensed data is composed of an array of square cells also called a grid. Size of physical features or their operational scales cannot be always represented by the size of the grid cell generated by sensors. The grid can be aggregated to coarse resolutions to match dominant operational scales (Quattrochi *et al.* 1997).

Aggregation of RS data reveals the general patterns of geographic features and that is why it is used in global scale studies in which general pattern of features are required. The other importance of aggregation has been explained earlier in introduction part.

Aggregation of fine resolution image to coarsen its resolution changes the spatial and statistical properties of data. The statistical properties are related to the DN values and number of bands present in

image. For example spread of DN values in different bands can be assessed by their standard deviation. The spatial properties can be related to the land use/ land cover classes. Landscape metrics are used to assess the spatial properties of classes. For example, the aggregation index reflects the clumpiness of classes present in landscape (He *et al.* 2000, 2002, Bogaert *et al.* 2002). Change in spatial and statistical properties depend upon the features presents in image and aggregation method used. Aggregation can be applied on thematic (called categorical aggregation) as well as continuous image (called numerical aggregation). There are wide ranges of literature in which effect of different aggregation approaches on image and effect on landscape metrics by coarsening image resolution have been addressed.

2.2. Aggregation of classified image

Moody *et al.* (1994) in their study used a polygon grids (aggregation grid) overlaid on per pixel class map of 30 m TM image (class – barren, brush, hardwood, conifer, water) and most frequently occurring class type among 30m TM pixels within that polygon grid is assigned to each grid cell of polygon grid. This aggregation technique is called as majority rule-based (MRB) categorical aggregation approach. Different cell size of polygon grid was overlaid to get coarse resolution thematic image of 90, 150, 240, 510, 1020, 3000 and 6000m from 30m base class map. The obtained coarse resolution class maps were used to assess the areal proportional error (with respect to the areal proportions derived from 30m class map) of land cover classes due to spatial resolution. At 90m resolution low error in areal proportion of all classes was observed, although barren class showed highest proportional error due to its scattered pattern. Proportion of conifer class (dominant class, 50 % in original scene) increased with aggregation levels and showed large proportion error than any other classes. Proportion of brush decreased strongly (20 % of scene). Hardwood, water, and barren decreased with resolution but their proportions are relatively maintained throughout the aggregation sequence. Development of regression relationship was recommended to estimate fine resolution class proportions from coarse resolution class proportions in order to handle change in class proportions resulting from a change in spatial resolution.

Moody *et al.* (1995) proposed multiple-linear and tree based regression techniques to assess the influence of landscape spatial characteristics (assessed by spatial measures) on land cover proportion estimation errors as land-cover map are aggregated to coarser scales. Four land-cover classes namely barren, brush, hardwood, conifer and water were derived from 30m TM image and MRB approach was used to get coarse land cover data at resolution of 90, 150, 240, 510 and 1020m. Spatial measures like Shannon index, variance/mean ratio, initial class proportions (present in 30m image), mean patch size, mean interpatch distance were considered as independent variables and proportion estimation error due to aggregation as dependent variable, for regression analysis. Multiple-linear regression showed that increase in patch size, variance/mean ratio and initial proportions of cover types caused the proportion estimation error of those cover types to move in positive direction through aggregation levels. Regression tree model was developed separately to split the dependent variable into increasingly homogeneous subsets based on independent variables and resolution. It was observed that regression tree model better captures the resolution dependent trends in proportion estimation error than multiple-linear regression model. Finally it was suggested that understanding the influence of spatial characteristic on proportion estimation errors with increasing aggregation levels may be used to quantify the errors expected in coarse scale surface representation or to preserve this information across scales.

Some work has been done to make the class proportions measured from coarse resolution image nearer to that measured from fine or reference resolution image that represents true surface. It may be called area correction of class proportions measured from coarse resolution image. Moody *et al.* (1996) com-

pared two calibration based area correction models, inverse estimator and slope estimator. Inverse estimator method includes class transition probabilities between coarse and fine resolution (reference) image, which is multiplied by coarse resolution class proportions to get fine resolution class proportions. Slope estimator is based on relationship between coarse and fine resolution class proportions via linear or regression modelling. Slope and intercept value of regression line is used for coarse resolution area correction. Four classes (barren, brush, hardwood, conifer and water) and four aggregation levels (150m, 240m, 510m and 1020m) using MRB aggregation approach were derived from 30m TM reference image. Calibration based models were developed separately for each aggregation level using reference image. Another site having same classes was taken for validation of calibration based models. Performance of models for each level was tested by "total error" that is sum of difference between the reference class proportions and class proportions at that level after correction. The inverse estimator method produced better result for area correction at the coarse scales (large aggregation levels) than slope estimator method. It was observed that inverse estimator performed better than slope estimator method with less value of total error for validation site at 1020m, but this method performed poorly for fine scales (small aggregation level). In general, the slope estimator produced improvement in coarse resolution proportions for all aggregation levels. It was suggested to incorporate the spatial characteristics of landscape with slope estimator method to improve its performance. Moody (1998) incorporated some spatial measures (that quantify spatial characteristics of landscape) namely entropy, range, variance, contrast and Shannon index with slope estimator method. Figure 2.1 shows methodology adopted by Moody.

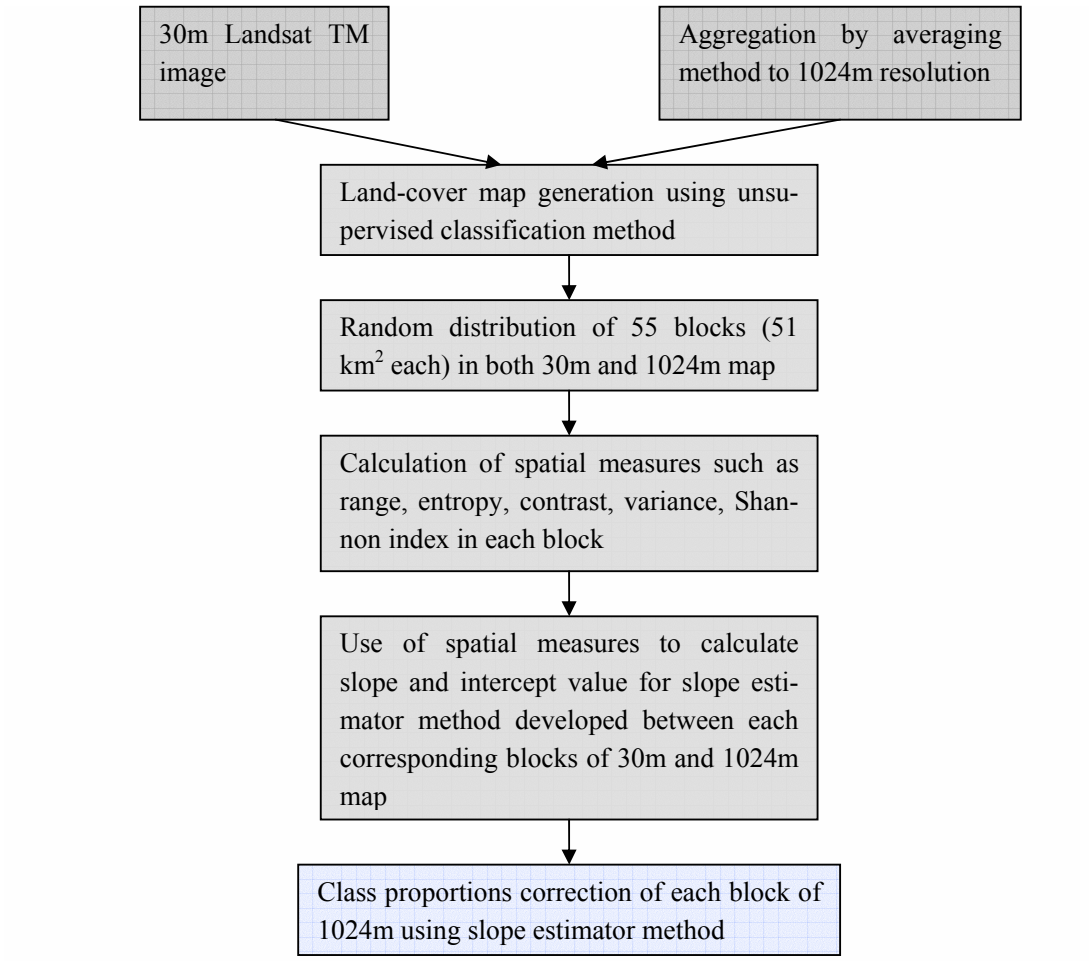

Figure 2.1 Methodology adopted by Moody (1998) to apply slope estimator method

30m TM image was taken as reference image and 1024m image was obtained by taking the average of spectral value within 34×34 windows of 30m pixels in each band. Both images were classified into four classes using unsupervised classification method, same as mentioned above and 55 samples blocks were defined in each image. Spatial measures were estimated for each block and then used to estimate the slope and intercept values of regression line that relates the 30m and 1024m class proportions in each sample block, instead of direct measuring their values from regression line. These values were used for correction of class proportions estimated from 1024m aggregated image in each block. It was observed that mean value of total error of each block after correction (0.18) became lower than that before correction (0.24). Slope estimator methods performed worst for the classes that make up less than about 20% of a sample block. For such cases, model based on non linear regression was suggested.

The effect of categorical aggregation such as MRB and random rule-based (RRB) on spatial properties of land-cover classes has also been addressed by He *et al.* (2002). RRB is based on random selection of class from the specified cells of input grid and assigning it to the aggregated output grid. In their study, four land-cover classes namely Maple (26%, dominant class), mixed deciduous and coniferous forest (17%, mid common class), water and oak (5% and 4%, least common classes) were derived from 30m TM image and MRB and RRB approaches were used separately to get coarse land cover data at resolution ranging from 90m to 990m by increment of 60m. Landscape metrics such as average patch size, fractal dimension and aggregation index (AI) were used to assess the effect of aggregation approaches. AI of least common class decreased and dominant and mid common classes increased across aggregation levels in the case of MRB aggregation approach. RRB caused decrease in AI of all classes, but more rapidly for highly aggregated class (water) than other classes. Average patch size of all classes increased, but the fractal dimension of all classes decreased across aggregation levels in the case of both MRB and RRB approaches. But, all classes exhibited linear decrease in fractal dimension for RRB approach.

A new method called point- centered, distance weighted, moving window approach (PDW) was developed by Gardner *et al.* (2008). It can be used to either increase (aggregation) or decrease (disaggregation) the pixel size of classified image. It means PDW can rescale map in two directions. It Sets sample points around center of input grid, calculate normalized frequency distribution, f, of sampled cover types, randomly select cover type from f and assign it to output grid. This approach preserves the class proportions through aggregation levels. Rescaling by PDW is based on choice of sampling scheme that includes the selection of three parameters, n – number of sample points, r – resolution of sample points, w – distance weighting for estimating f to decrease the influence of points that are large distance from center of input grid. Variability in three landscape metric area-weighted average patch size (S), total amount of edge (G), the number of habitat patches (A) were addressed and total of three experiments were performed to assess the effect of PDW on rescaling process. Figure 2.2 show the methodology adopted in this work to assess the effect of PDW approach. The first experiment examined the effect of different sampling schemes by changing n, r and w to rescale the first multifractal map (It shows realistic landscape pattern and allows the user to systematically vary resolution and cover type proportion 'p') from 30m to 15m and second multifractal map from 15m to 30m. Each multifractal map was generated with single cover type (p = 0.5). It was observed that different sampling schemes did not affect 'S'. Maximum of 3% and 8% change in 'S' was observed in the case of aggregating and disaggregating multifractal maps respectively. Increase in n and r produced corresponding increase in 'A' and 'G', while increase in w caused 'A' and 'G' to decline. The second experiment involved the aggregation of 10 m multifractal map (having single cover type) to maps with resolution

from 15 to 40m and disaggregation of 40m multifractal map (having single cover type) to maps with resolution from 35 to 10m by increments of 5m.

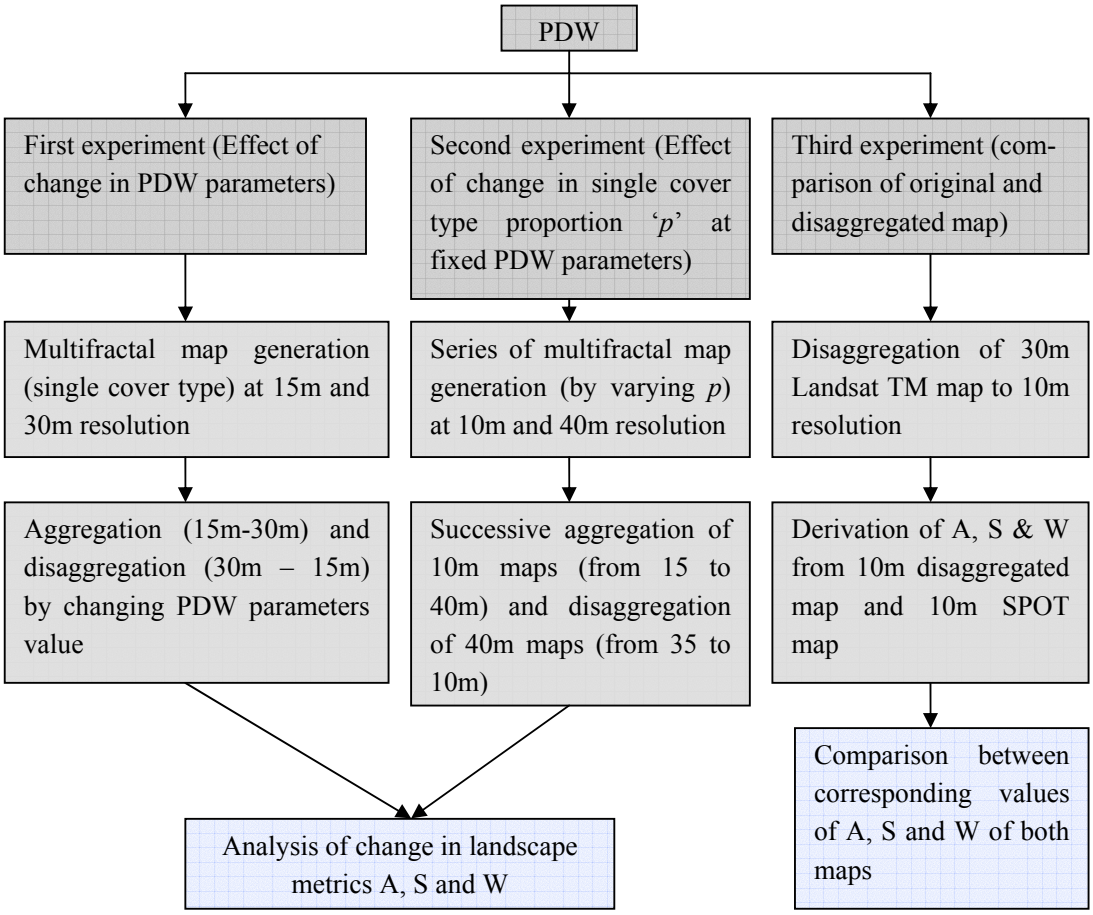

Figure 2.2 Methodology adopted by Gardner *et al.* (2008) to assess the effect of PDW approach

All these maps were also generated by changing the fraction of single cover type, *p*, ranging from 0.1 to 0.9 by increment of 0.1. Sampling net was kept fix in these rescaling processes. For all values of *p*, aggregation produced increase in 'G' and 'A', disaggregation produced decrease in 'G' and 'A', but 'S' remained relatively constant. The third experiment involved the disaggregation of 30m Landsat maps to 10m and comparing of 'G', 'S', and 'A' from disaggregated map to map of same region derived from 10m SPOT image. Sampling scheme was kept fix at n =9, w =1 and r =10m. Metric values derived from 10m disaggregated map closely matched the metric values for 10m SPOT maps. Also the close resemblance was found in misclassification rate of disaggregated map and 10m SPOT map. As the PDW rescaling process depends on the selection of sampling scheme, therefore the use of optimization technique was suggested to select n, r and w for particular landscape attributes.

Some research works have also addressed the effect on different landscape metrics due to categorical aggregation. Turner *et al.* (1989) examined the effect on three landscape metrics diversity, dominance and contagion index (similar to aggregation index) as the resolution of categorical map is coarsened by MRB approach. They found that diversity index decreased linearly with decreasing resolution. But dominance and contagion did not show consistency through decreasing resolution. Both increase and decrease in their values was observed through decreasing resolution, thereby exhibited a non linear response.

Wickham *et al.* (1995) analysed diversity and evenness metrics for cover types and evenness metrics for edge types. These metrics were estimated from land cover images at spatial resolution of 4, 12, 28 and 80m. These images were obtained by converting vector land cover data digitized from areal photograph to raster format using ARC/INFO POLYGRID runtime that assigns to a pixel the land cover value comprising most of the pixel area. It was found that both diversity and evenness metrics are predictable over the 4 to 80m pixel range and showed nearly constant trend up to 80m pixel size.

Wu *et al.* (2002) investigated the response of 19 landscape metrics to increasing pixel size at the landscape level. MRB approach was used in their study to aggregate the pixels of 30m Landsat land use and land cover map. According to the responses of 19 landscape metrics with increasing pixel size, landscape metrics were divided into three categories. Type I metrics include 13 metrics. Some of them are number of patches, edge density, area-weighted mean patch fractal dimension, square pixel index, largest patch index. These metrics showed predictable response and simple scaling relation (represented by linear, power-law equation that relates landscape metrics with pixel size) with increasing pixel sizes. Type II metrics include patch richness, patch richness density and shannon diversity index. These metrics did not show unique simple scaling relationship and decreased in a staircase-like fashion with increasing pixel size. Type III metrics include contagion, landscape fractal dimension, mean patch shape index and mean patch fractal dimension. These metrics exhibited an erratic response with increasing pixel size and the shape of their response curves was sensitive to the specific landscape pattern. Wu (2004) in his study also examined the response of 17 landscape metrics to increasing pixel size at the class level. MRB approach was used again to aggregate the pixels of 30m Landsat land use and land cover map in order to obtain different coarse resolution maps. Two categories were found for landscape metrics calculated at class level. The first category exhibited consistence scaling relationship with respect to increasing pixel size. Some of metrics of this category are number of patches, edge density, square pixel, landscape shape index. The second category exhibited unpredictable behaviour with no consistent scaling relationship. This category includes class area, mean patch shape index, double log fractal dimension.

These studies examined the response of landscape metrics with decreasing resolution and aggregation of fine resolution classified image was used to obtain different coarse resolution classified image. These studies did not focus the correspondence between landscape metrics derived from aggregated classified image at some level and that derived directly from classified image of actual satellite data at the same resolution. Saura (2004) addressed these issues by taking six landscape metrics, number of patches (NP), mean patch size (MPS), edge length (EL), largest patch index (LPI), landscape division (LD) and patch cohesion (PC) index. These metrics were computed at class level from the 180m classified image derived from the aggregation of 30m Landsat TM classified image using MRB approach and that derived from the image obtained by resampling of WIFS image to 180m. No resemblance was found between the corresponding values of NP, MPS and EL derived from these two classified images, but LPI, LD and PC did not show a systematic difference. Different coarse resolution classified images were also obtained by the aggregation of 30m TM classified image using MRB approach and it was found that LPI and MPS tend to increase and LD decreased with increasing pixel size. LPI and LD showed a similar variation trend as a function of spatial resolution. NP and EL decreased rapidly with increasing pixel size. It was also concluded that among the six indices LD and LPI are most suitable for direct comparison of landscape fragmentation using image with different spatial resolution.

The definition and mathematical formula of above mentioned Landscape metrics can be found in the concerned journals.

2.3. Aggregation of continuous image

The average or mean based numerical aggregation method average the DN values of specified input cells of fine resolution image and assign the result to one cell to get coarse resolution image. To assess the effect of aggregation, Bian (1997) used mean based aggregation approach to aggregate 30m biomass index image and 30m DEM data. 33×33 and 75×75 pixels aggregation of both images was performed separately to coarsen their resolution. Resolution obtained by 75-pixel aggregation was equivalent to the dominant operational scale (the average distance of 60-80 pixels from a ridge feature to an adjacent valley feature in elevation data) of elevation data. It was found that small scaled features (linear feature such as shrubs) present in biomass index image were filtered out during aggregation and net elevation patterns emerged. Aggregation of elevation data did not reveal any new pattern. A linear regression was applied at original 30m resolution and each aggregation level to relate biomass index as the dependent variable to elevation as the independent variable. Steady increase in R^2 value was observed up to 75-pixel resolution, which showed that elevation alone was sufficient to provide an explanation of biomass variation at coarse resolutions. Variance of both biomass and elevation data decreased across aggregation levels, that explained smoothing effect caused by the mean based aggregation method.

Other numerical aggregation methods include median aggregation method and central pixel resampling. In median aggregation method, median of DN values of specified input cells of fine resolution image is assigned to one coarse resolution output cell. Under central pixel aggregation method, the DN value of coarse resolution cell is assigned by taking central pixel DN value of specified input cells of fine resolution image. Bian *et al.* (1999) in their study evaluated the effect caused by mean, median and central pixel aggregation method. Thirty realizations of simulated images of resolution 30m (512×512 pixels) were generated with two predefined spatial autocorrelation structure having range of 30 and 10 pixels. These aggregation methods were applied on the each realization of simulated images to get ten aggregation levels using different pixels aggregation ranging from 3×3 to 81×81 pixels window. Mean values of aggregated images exhibited a constant trend across aggregation levels in the case of mean and median aggregation method, but standard deviation values showed a non linear decreasing trend. The decreasing rate of standard deviation was higher and remained constant up to around 10×10 pixels window aggregation. This rate became slower by further increase in pixels window and standard deviation tended towards stabilization. Central pixel aggregation approach caused a fluctuating trend of both mean and standard deviation values of aggregated images about those of original 30m simulated image with increase in range of variation across aggregation levels. By visual interpretation of aggregated images generated by these three aggregation approach, it was found that mean and median method produced almost identical aggregated images. Central pixel method maintained the contrast and basic pattern of original 30m image within spatial autocorrelation range better than other two methods. To study the aggregation error, error images were created in the case of each aggregation approach. To create error image, aggregated value of each pixels window was subtracted from each pixel value of that window. In this way, error image maintained the original size of 512×512 pixels. In the case of mean and median aggregation approach, mean values of error images varied about zero value and range of variation slightly increased across aggregation levels. Standard deviation values started approaching the constant level after 30×30 pixels aggregation. Central pixel showed greater magnitude and variation in mean and standard deviation values of error images than the other two methods. These variations were large at aggregation levels greater than the spatial autocorrelation range. On the basis of all these observation, it was suggested that spatial autocorrelation ranges is helpful to choose appropriate aggregation level that can help confine the magnitude of errors

produced by aggregation method. Also the knowledge of trend of errors through aggregation can help assess the accuracy of outcome of model in which aggregated data are used.

The effect of K-average and fractal based aggregation approach were addressed by Gupta *et al.* (2000). Mean and median aggregation approach were also addressed. "In the case of K- average method, the average of three nearest gray levels in the case of 2×2 integration and six nearest gray levels in the case of 3×3 integration size were computed". To apply the fractal based aggregation, fractal dimension component was computed and added to mean of DN values of specified pixels window to get aggregated value. To assess the effect on class proportions due to aggregation, LISS II (36.2m) and LISS I (72.5) were aggregated separately to different levels by mean method. Maximum likelihood classification was used to classify images at each aggregation levels. Decrease in proportions of all classes was observed, but for low reflectance feature (water), there was sudden drop of 40 % in proportion. In both cases, decrease in class proportions was observed as an increase in proportion of unclassified pixels. To assess the effect of aggregation on correlation coefficient, LISS II image (4-bands) was aggregated to 72.5m resolution by mean, median, K-average, fractal based method separately and correlated with observed pixel values from LISS I image (72.5m, 4-bands) in all bands for all cover types. It was found that fractal method gave best correlations for agriculture, water than other methods. Barren land exhibited better correlation for fractal method in blue and green band. In red and NIR band, little higher correlation was observed for barren land (having low reflectance value) in the case of other methods, but it was due to noise that was also getting correlated. For sparse vegetation and shadow, K-average and mean method exhibited better correlation than fractal in all bands, but noise due to shadow again contributed here in correlation coefficient. As the fractal method eliminated the noise, which could not be eliminated by other methods, the fractal method was addressed better than other methods for low reflectance cover types (barren land and sparse vegetation). For hill without vegetation, correlation values observed in blue and green bands were comparable for all methods.

Gupta *et al.* (2002) again analysed the effect of aggregation on correlation coefficient for frequency domain aggregation. For which, the high frequency component in Fourier Transform of the 36.5m LISS II image was removed and after that inverse Fourier transform was performed. Then the Fourier transform LISS II image was aggregated to 72.5m using mean and fractal method. This method provided a high correlation between aggregated LISS II image and LISS I image for mixed class (having tobacco, banana, water and barren land) also in case of both aggregation methods, which showed that frequency domain aggregation can handle the heterogeneity in aggregated image. For other classes having single feature (such as marshy land, turbid water), fractal method exhibited better correlation value over mean method.

3. Study area & Data processing

This chapter explores the study area, data used, their pre-processing. Section 3.1 describes the study area, section 3.2 describes the remotely sensed data used and section 3.3 describes the processing of remotely sensed data.

3.1. Study area

The study area lies between 30.78^0 N to 30.98^0 N and 75.20^0 E to 75.41^0 E. which covers the part of three districts of state Punjab (India) namely are Ludhiana, Firozpur and Moga. The study area is situated in almost center part of Punjab. Climate of the area is usually dry except a brief spell of Monsoon season, a very hot summer and bracing winter. The total annual rainfall is 600-700 cm and about 70% of the rainfall is received during the period of July to September. The topography of the area is typical representative of an alluvial plain and due to this agriculture is the main practice of livelihoods in the area. Major crops of the area are rice and cotton in Kharif season (summer). During Rabi season (winter), the major crops productions are wheat and potato.

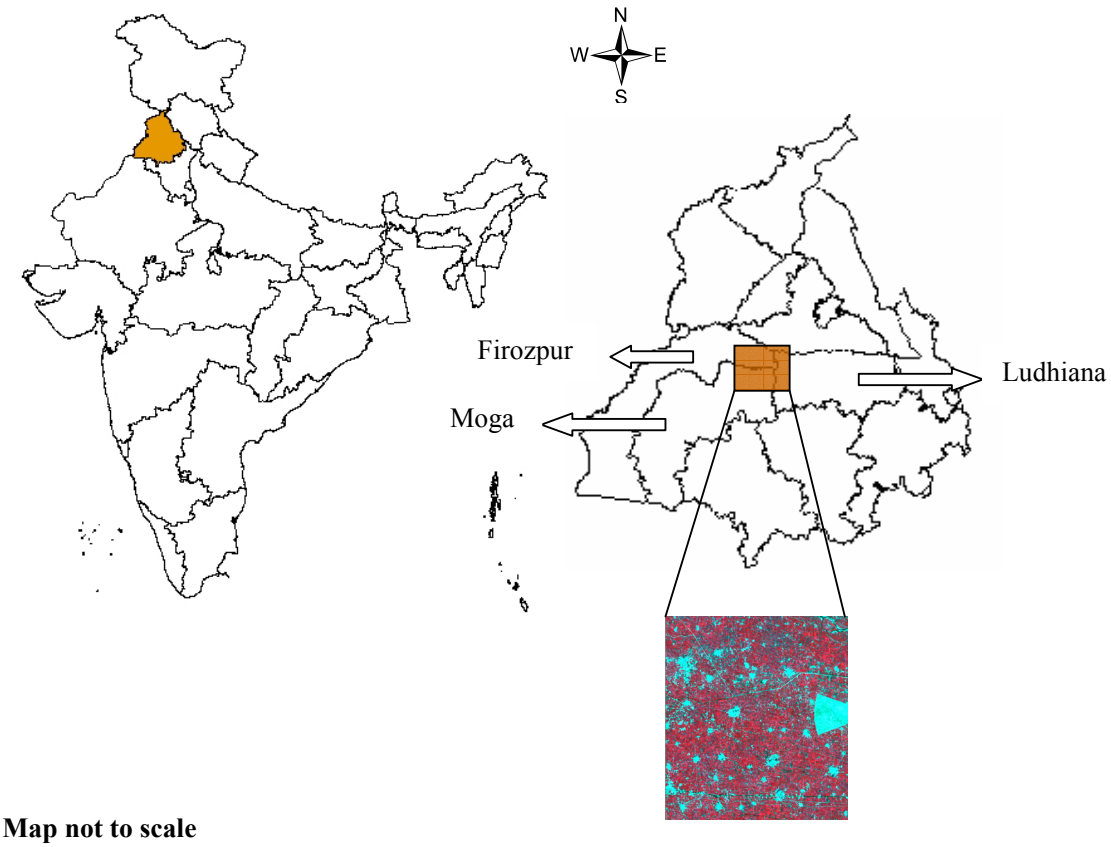

Map not to scale

Figure 3.1 Location of study area and corresponding LISS-III image

Figure 3.1 shows the location of study area and its corresponding LISS-III image. Study area comprises approximately 72% agriculture fields, 16% Fallow lands, 12% settlement and 0.35 % water body. All classes are present in distributed pattern of large number of complex shaped patches having variety of sizes. The areal extent of study area covers 43404 hectares. Prior field knowledge of the area and availability of satellite image was the criteria of selection of study area.

3.2. Data used

LISS-III is a medium resolution Linear Imaging Self Scanner on board IRS – P6 (RESOURCESAT 1) satellite built by ISRO, India. It operates in four spectral bands. Out of which two are in visible band (green and red), one in near infra red (NIR) band and last one in short wave infrared (SWIR) band with 23.5 m spatial resolution. In this study, satellite image over study area acquired by LISS-III sensor has been taken as a reference/ base image. Different aggregation approaches have been applied on LISS-III image to get a coarse spatial resolution levels. The acquisition date of LISS-III image is 23rd January 2008. The spectral characteristics of the LISS-III image are listed in table 1.1.

Table 3.1 LISS-III band information

Band	Wave length (μm)	Spatial Resolution (m)	Radiometric Resolution
Band1(Green)	0.52 – 0.59	23.5	Unsigned 8 bit
Band2(Red)	0.62-0.68	23.5	Unsigned 8 bit
Band3(NIR)	0.77-0.86	23.5	Unsigned 8 bit
Band4(SWIR)	1.55-1.70	23.5	Unsigned 8 bit

3.3. Processing of satellite data

LISS-III image was provided as a video data in Band Interleaved by Line (BIL) format and it was imported in using ERDAS Imagine software using its header information. Due to the curvature of earth, satellite image is subjected to distortions. Therefore, before the LISS-III image could be used for further processing, it is necessary to geometrically correct it. LISS-III image was geometrically registered with respect Survey of India toposheets No. 44N/1 and 44N/5 at scale 1: 50,000 scale. The permanent features like road crossing, canal crossing and turnings were selected on both image and toposheets for ground control points. A total of 100 GCPs were selected for final geometric registration of LISS-III in UTM projection with WGS 84 North spheroid and datum and zone 43. The root mean square error during geo registration was not more than half pixel. Finally square subset of geo-registered LISS-III image (shown in figure 3-1) was taken for further processing. The reason behind taking the square subset was to avoid the effect of 'NoData' value cells from aggregation.

4. Methodology

In present research, 23.5m LISS III image has been considered as a fine resolution image. This is considered as reference or base image. Categorical aggregation approaches have been applied on land use and land cover map of LISS III image to get the aggregation levels as shown in table 1. Numerical aggregation approaches have been applied directly on LISS III image to get same aggregation levels as shown in table 4.1 and then land use and land cover classification was performed on images obtained at each level. Figure 4.1 & 4.4 explains the methodology of present work. First part deals with categorical aggregation and second part deals with numerical aggregation approaches.

4.1. Methedology flow chart

4.1.1. Implementation of categorical aggregation approaches

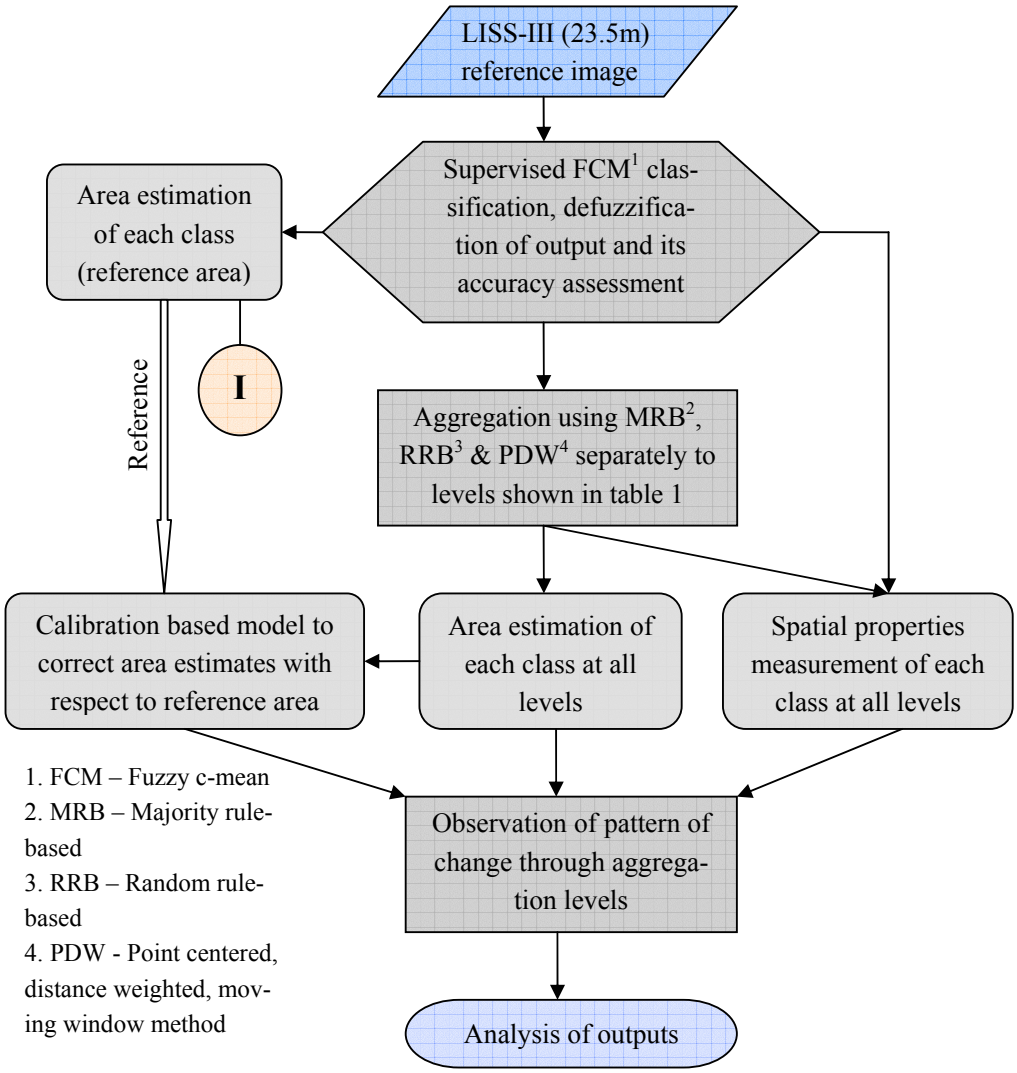

Figure 4.1 Flow diagram showing implementation of categorical aggregation approaches

4.1.2. Implementation of numerical aggregation approaches

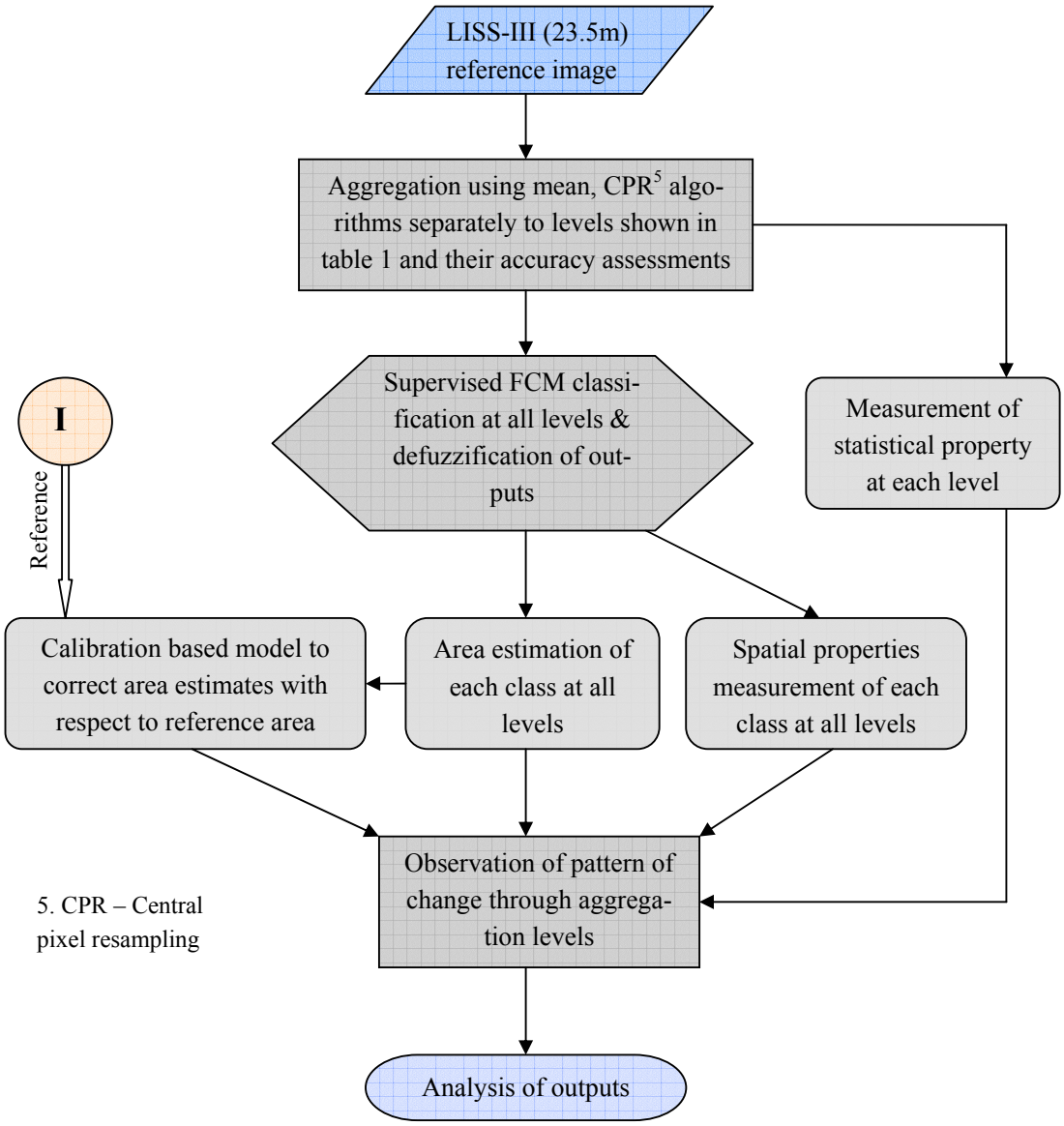

Figure 4.2 Flow diagram showing implementation of numerical aggregation approaches

4.1.3. Brief explanation of flow chart

Table 4.1 Aggregation levels and corresponding resolution

Aggregation level	3	5	7
Resolution	70.5m	117.5m	164.5m

Comment - To obtain each level, 23.5 m pixels of LISS III image (may be regarded as reference level) were aggregated using different pixels window.

1. Categorical aggregation approach – LISS-III (23.5m) continuous image was classified using supervised FCM algorithm. The soft output of FCM was defuzzified to get per pixel land use and land cover

class map, whose accuracy assessment was done using same LISS-III continuous image. The area of each class was calculated and taken as a reference area. Aggregation approaches namely majority rule-based, random rule-based (He et al. 2002) and Point-centered, distance-weighted, moving window method (Gardner et al. 2008) were separately applied to aggregate the classified image to achieve third, fifth and seventh aggregation levels that correspond to resolution of 70.5m, 117.5m, 164.5m. To achieve each level, LISS III classified image (23.5m) was aggregated directly using 3×3, 5×5, 7×7 window size instead of using previous aggregation level. It is called independent aggregation scheme as opposed to the iterative aggregation scheme in which the aggregation to the next level is based on the already-aggregated image of initial fine resolution image that would introduce more errors (Wu *et al.* 2002, 2004). Value of following indicators were calculated from LISS- III classified image and obtained aggregated classified images in the case of each aggregation approach.

a) Area of each class in terms of class proportion.
b) Corrected proportion of each class using calibration based model. (explained in section 4.6)
c) Spatial properties of each class (explained in section 4.5)

Pattern of change across aggregation levels of all above indicators were used to analyze the effect of MRB, RRB and PDW categorical aggregation approach.

2. Numerical aggregation approaches -- First coarse resolution images (70.5m, 117.5m, 164.5m) were achieved by directly aggregating pixel values of LISS III image using Mean and Central pixel resampling (Bian et al. 1999) aggregation approaches. Independent aggregation was also used in this case. Each obtained image was classified using FCM algorithm and defuzzified to get per pixel land use and land cover class map. Accuracy assessment of classified images at each aggregation level was done by considering the aggregated continuous images at the corresponding levels as a reference data. The value of indicators explained at a, b and c were calculated for each obtained image to assess numerical aggregation effect. One other indicator was also calculated in this case as follows
d) Statistical property of LISS III image and all obtained aggregated images at all aggregation levels for each algorithm (explained in section 4.7)

Pattern of change across aggregation levels of indicators a, b, c and d were used to analyze the effect of Mean and CPR aggregation approach.

Detailed explanation of FCM classification, all aggregation approaches and indicators are explained in subsequent sections.

4.2. Supervised fuzzy c-mean classification

Fuzzy c-mean is soft classification technique to classify remotely sensed image in which partial belongingness (fuzzy membership) of each class in image is assigned to each pixel. FCM algorithm is based on following steps (Lucieer, 2004):

1. Objects to be classified are randomly assigned into *c* cluster.
2. The center of each cluster is calculated as the weighted average of attribute (pixel value) of the objects.
3. Objects are reallocated among the classes according to the relative similarity between objects and clusters that is based on distance measures by Euclidean distance or Mahalanobis distance.
4. Reallocation proceeds by iteration until the similar objects are grouped together in a cluster.

The membership of the i^{th} object to the c^{th} cluster of n number of classes gives their degree of affinity with the centroid of the class and it is defined as:

$$\mu_{ic} = \frac{1}{\sum_{c'=1}^{n} \left(\frac{d_{ic}^{2}}{d_{ic'}^{2}} \right)^{\frac{-1}{(q-1)}}} \qquad \textbf{Eq 4.1}$$

Where d is the distance measure used for similarity and q is the fuzzy exponent that determines the level of fuzziness or class overlap. If the value of $q = 1$ then it is essentially the hard clustering [Bezdek, 1984] and no overlap is allowed. This FCM clustering algorithm is unsupervised, but it can be made supervised by providing training data. In this case the class centroid are determined by training data. This reduces the clustering algorithm to a one step calculation that results in fuzzy membership value for each pixel in each of defined classed.

Fuzzy based classifiers are suitable when there is confusion in class definition and it gives better result than traditional hard classifiers such as MLC (Tso *et al.* 2001). In the LISS-III image, four dominant land use/ land cover classes were identified; water body, agriculture field, fallow land and settlement. It was found that there is class confusion among different classes, for example agriculture with fallow land and water with fallow land in that image. For this reason, supervised FCM classification approach was used to classify the LISS-III image into above mentioned four classes. Supervised FCM classification was performed in PARBAT software developed by Arco Lucieer (Lucieer, 2003). Training data for each class is provided by generating Region of interest (ROI) using ENVI software. PARBAT facilitates the user to choose both Euclidean distance or Mahalanobis distance and value of q for classification. Foddy (1996) stated that in most of the clustering cases q =2.0 produce the accurate fuzzy classification result. Kumar *et. al.* (2007), in their study, found that FCM with Euclidean distance performs better in comparison to the Mahalanobis distance. So for this research FCM with Euclidean distance and $q = 2$ were adopted to classify LISS-III image. FCM classifier using PARBAT generates fractional image for each class, which shows the fuzzy membership value of that class in each pixel of image. It also generates the defuzzified output in which class label of maximum membership value in each pixel is assigned to that pixel. This gives per pixel classified image. In this work, defuzzified output of LISS-III has been taken as the categorical aggregation approaches, calibration based model approach and estimation of spatial properties can be carried out only using per pixel classified image. Furthermore, it is difficult to assess the accuracy of those fractional images in comparison to the ground truth/reference data (Foody, 2002). To report the accuracy of fuzzy classified image, defuzzification approach was adopted and per pixel classified image was generated from those fractional images (Gopal *et al.* 1994).

Supervised FCM classification approach was also used to classify the images obtained at each aggregation levels using numerical aggregation approaches and per pixel classified images were obtained due to the same reason mentioned above.

4.3. Accuracy assessment of classified images

Fine resolution image can be taken as reference data for classification accuracy assessment of coarse resolution image. In this case, the classification accuracy of coarse resolution image may be affected by the difference in resolution. Fine resolution image may contain lot of heterogeneity and the classification accuracy will not reflect the accuracy at coarse scale. For this reason, accuracy assessment of LISS-III classified image (reference image) and all classified images obtained after classification of aggregated images in the case of numerical aggregation approaches was judged against the images at corresponding resolutions. ERDAS Imagine software was used to address the classification accuracy by visual interpretation.

Furthermore, the main objective of the research is to analyze the effect of different aggregation approaches. In the case of numerical aggregation approaches, it is necessary to reduce or quantify the effect of classification on aggregated images. If the original aggregated image is used for accuracy assessment then only it is possible to quantify the effect of FCM classifier on particular aggregation level. Instead of it, if another fine resolution dataset is used as reference data then accuracy or performance of a classifier is not judged against the aggregated image as the resolution is also a factor of accuracy. To resolve this issue here original aggregated image was used as reference data in order to address the effect of FCM classification at that particular aggregation level.

4.4. Aggregation approaches

23.5m LISS-III classified image was aggregated to get classified images at coarse resolution 70.5, 117.5 and 165.5 m. It was achieved by running 3×3, 5×5, 7×7 window on LISS-III classified image row wise starting from upper left corner. A single class was selected among classes assigned to LISS-III pixels within specified window size in order to assign it to aggregated pixel. Selection of class is based on different categorical aggregation approaches, which have been described in section 4.4.1.1, 4.4.1.2 and 4.4.1.3.

In the case of numerical aggregation, each band of LISS-III continuous image was aggregated to coarse resolution 70.5, 117.5 and 165.5m separately. It was achieved by running 3×3, 5×5, 7×7 window on each band of LISS-III. DN value of aggregated pixel was estimated by mathematical processing or selection of DN values of LISS-III pixels within specified window size. Assignment of DN values to aggregated pixel is based on different numerical aggregation approaches, which have been described in section 4.4.2.1 and 4.4.2.2.

4.4.1. Categorical aggregation approaches

4.4.1.1. Majority rule-based (MRB)

MRB is a type of categorical aggregation approach. It is applied on fine resolution classified image to get coarse resolution classified image. MRB is based on the selection of the most frequently occurring class (major class) from the specified pixels of input fine resolution grid. This is then assigned to the one pixel of output aggregated coarse resolution grid. It is based on the assumption that dominant classes will contribute more to represent landscape at coarse resolution than other classes. Figure 4.3 shows nine pixels (3×3 pixels window) of input grid of 23.5m LISS III classified image with class labels 1, 2 and 3.

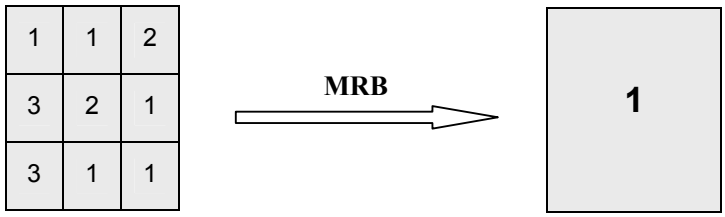

Figure 4.3 MRB aggregation approach

Five pixels are acquired by class 1, that make it major class in nine pixels of input grid. MRB aggregates these nine pixels to get one pixel of resolution 70.5m by selecting class 1 from it and then assigning class 1 to one pixel of output grid.

MRB aggregation approach can be applied in ERDAS using the option
Interpreter -> Utilities -> Aggie
But when there are two major classes within specified pixels of input grid, a class label having low in value is assigned to one pixel of output grid. For example, if out of nine pixels in figure 3, four pixels have label 3 and four pixels have label 2, then no major class is found and label 2 is assigned to the output aggregated pixel. There is no valid reason behind it. In ERDAS, one can also give priority of any class to be selected. But it will create bias.

In ARC MAP, MRB can be achieved as for example by first running following commands in command line
BlockStatistics <input raster> <output raster> "Rectangle 3 3 Cell" MAJORITY DATA

That assigns majority class label to each of nine pixels of input grid and then grid is resampled using nearest neighbour with cell factor 3. If there are two major classes in nine pixels of input grid, then 'NoData' is assigned to output aggregated pixel. It will create holes in image that will affect the measurement of spatial properties.

In order to resolve these two problems, a code has been written in the R programming language to apply MRB aggregation approach in this work. It provides the random selection of class among two or more major classes, if they are present in specified pixels of input grid. Otherwise major class will be selected. It will not create any hole in image and will remove the bias to select class between two or more major classes. Developed MRB code accepts the ASCII format of classified image and generates aggregated output in ASCII format at desired aggregation level.

4.4.1.2. Random rule-based aggregation approach (RRB)

RRB is another type of categorical aggregation approach that is applied on fine resolution classified image to coarsen its resolution. It is based on random selection of class among the classes present in specified pixels of input grid. Selected class is then assigned to one pixel of output aggregated coarse resolution grid. Figure 4.4 shows the RRB approach applied on nine pixels of input grid of LISS-III classified image with class label 1, 2 and 3 to get pixel at 70.5m resolution.

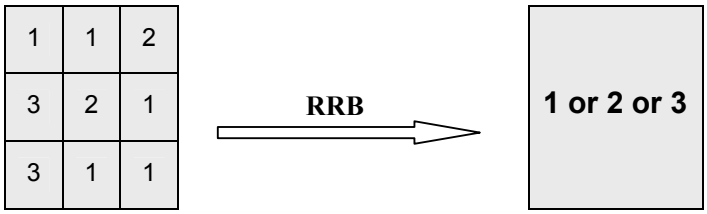

Figure 4.4 RRB aggregation approach

Randomly selected class among these classes are assigned to the output aggregated pixel, but the probability that the class is selected to present an aggregated pixel is proportional to its presence in input data (He *et al.* 2002). RRB is based on the assumption that it may preserve the class proportions through aggregation levels.

Code has been developed in the R programming language to apply RRB aggregation approach for present work. It accepts the ASCII format of classified image for aggregation and generates output in ASCII format at desired aggregation level.
As the RRB is based on random selection of class, different realizations of output aggregated classified image at same coarse resolution may be achieved. Different realizations may differ in class proportions and spatial properties. In order to assess the variability in realization, RRB has been applied 100 times on LISS-III classified image to get 100 realizations of aggregated output at each aggregation level (Table 4.1). Then class proportions and spatial properties have been estimated for each realization and their variations have been reported. In order to assess the general effect of RRB through aggregation levels, only one realization has been considered for each aggregation level.

4.4.1.3. Point-centered, Distance-weighted, moving window method (PDW)

PDW is also a type of categorical aggregation approach proposed by Gardner *et al.* (2008). It can be used to either decrease (aggregation) or increase (disaggregation) classified image resolution. PDW is based on four step process for changing resolution. Figure 4.5 shows the aggregation of nine pixels of fine resolution classified image by PDW to get coarsen resolution pixel. The four steps are as follows.

1. The center point, C_{ij} is located on the coarse resolution pixel (crosshair in Figure 4.5(1)). The location of C_{ij} is expressed in real dimension (decimal fraction of meters) rather than as integer value of grid coordinated.

2. A set of n sampling points (sampling net) are placed on original fine resolution pixel with a center of sampling points at location C_{ij} (Figure 4.5(2)). The sampling points may be of any number and resolution r that is the distance between two points in sampling net. Figure 5 shows the $n = 9$ and r equal to fine resolution pixel size.

3. The types and frequency of classes at the sampling points are enumerated and corresponding cumulative frequency distribution f is estimated (Figure 4.5(3)).

4. Finally the random selection of class from f is performed and selected class is assigned to coarse resolution pixel located at C_{ij} (Figure 4.5(4)).

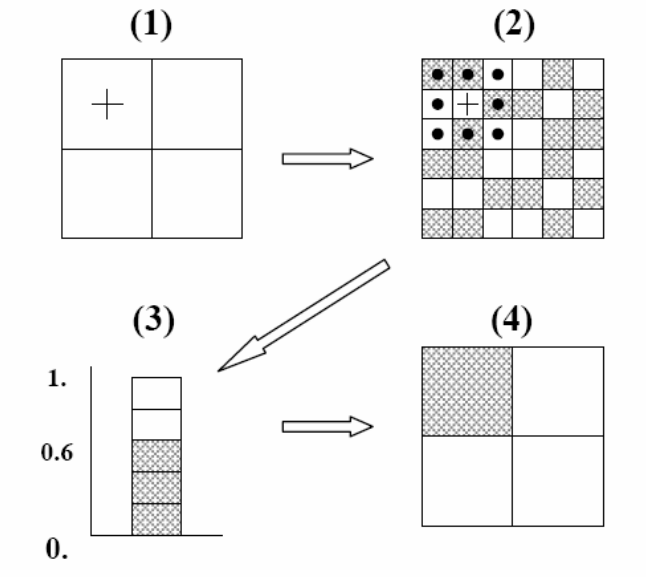

Figure 4.5 Aggregation by PDW (source PDW documentation)

PDW allows the assignment of weight *w* to the points in sampling net in order to decrease the influence of points from center C_{ij}. Three alternative distance-weighted sampling methods can be used: no weighting (all points have equal effect), simple inverse distance weighting, or inverse squared distance weighting. Both PDW and RRB approach use the random selection logic to select class from input grid, therefore in this respect there is similarity between both approaches. However the PDW approach incorporates various parameters to generate output, which is not present in RRB approach. This differentiates PDW from RRB approach.

All the steps written above are based on PDW documentation. More detailed explanation of PDW approach was provided in appendix.

PDW approach was applied by using its Window™ executable downloaded from the website www.al.umces.edu/PDW.htm . This executable uses a command line interface. PDW executable accepts the ASCII format of classified image with no header information and generate coarse resolution classified image in ASCII format. During execution, the choice of *n*, *r* and *w* are entered. Output of PDW depends on the choice of these parameters. There are eight choices for *n*; 1, 5, 9, 13, 21, 25, 45 and 49. If the value for *r* is set to 0, then distance between points of sampling net will be equal to the fine resolution pixel size, otherwise different integer value of *r* can be selected. If value of *r* is taken less than fine resolution pixel size, the points in sampling net may overlap to each other.

The value of *r* can be taken greater than fine resolution pixel size. But if it is not a multiple of fine resolution pixel size, sampling points may again overlap to each other (based on PDW source code). For this reason *r* should be taken 0 or multiple of fine resolution pixel size. There are three choice for *w*; 0(no weight), 1 (inverse distance weight) and 2(inverse squared distance weight). As the assignment of class to coarse resolution pixel is based on random selection of class from *f*, random number seed is also given during execution to avoid the different realization of aggregated classified image at same coarse resolution due to random selection. Value of random number seed should be negative and less than 2^{10}(PDW documentation). Different outputs can be realized by changing random number seed.

In present work, *n* = 9 and *r* = 0 has been taken in the case of aggregation of 23.5m LISS-III classified image to get the resolution of 70.5m (aggregation level 3). It is due to the reason that these choices of n and *r* will distribute the points of sampling net to nine LISS-III pixels (3×3 pixels window) that will aggregate to one 70.5m pixel. Light and dark grey colour in Figure 4.6 represents this distribution. Dark grey colour shows the center of sampling net.

1	1	2
3	**2**	1
3	1	1

Figure 4.6 Distribution of sampling net for n = 9 and r = 0

In this manner, sampling points will not go outside from the support size (70.5m) of coarse resolution pixel and assignment of class in output aggregated pixel (70.5m) will be the result of processing of classes present only within this 3×3 pixels window. In this way, any analysis of output aggregated classified image will be the representative of measurement scale that is being considered.
For the similar reason, n = 25 and r = 0 has been taken to obtain aggregation level 5 (117.5m) using 5×5 LISS-III pixels window and n = 49 and r = 0 has been taken to obtain aggregation level 7 (167.50) using 7×7 LISS-III pixels window.

But the choice of *w* and random number seed can still give different realization of output aggregated classified image at the same aggregation level. In order obtain different realizations at aggregation level 3; hundred random number seeds were generated in R Programming. For each choice of *w* (0, 1 and 2) and random number seed, aggregated output was generated by PDW. The choice of *n* and *r* has been kept fixed as described above. This process generated a total of 300 realizations for aggregation level 3. The similar process was applied to generate 300 realizations for each of aggregation level 5 and 7. In this way, a total of 900 realizations were generated by PDW. Different realizations may differ in class proportions and spatial properties, which were estimated for each realization to assess the variability in PDW output for each aggregation level. To assess the general effect of PDW through aggregation levels, w = 1 and random number seed = -17161817 (given in PDW documentation) has been taken for each aggregation level.

4.4.2. Numerical aggregation approaches

4.4.2.1. Mean aggregation approach

Mean or average is a type of numerical aggregation approach that is applied on continuous image. It estimates the mean of DN values over specified pixels of input grid and assigns the result in one pixel of output coarse resolution grid. It is based on the assumption that pixel or reflectance value for any ground area will be the integrated reflectance value of all objects over the corresponding area on the ground (Bian *et al.* 1999). Figure 4.7 shows the mean approach applied to nine red band pixels of LISS-II image to get 70.5m coarse resolution red band pixel.

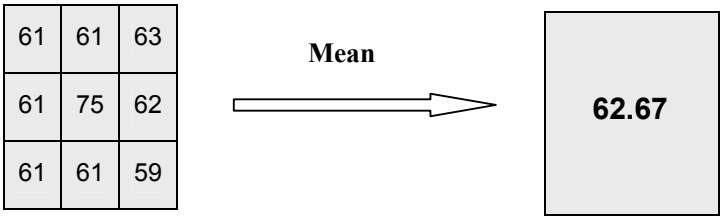

Figure 4.7 Mean aggregation approach

Mean aggregation approach was applied to each band of LISS-III image separately and then coarse resolution bands were stacked to get RGB image at all aggregation levels 3, 5 and 7. This approach was implemented in this work through code developed in the R- programming language that accept the ASCII format of each band of image and generates output in ASCII format at desired aggregation level.

4.4.2.2. Central pixel resampling

CPR is also a type of numerical aggregation approach. It selects an original central pixel value of specified pixels of input grid and assigns it to one pixel of output coarse resolution grid (Bian *et al.* 1999). It is suitable to obtain a coarse resolution image at resolution, which is odd multiple of resolution of fine grided image as it involves the selection of central pixel. The assumption behind CPR may be thought in terms of sensor characteristics. Remote sensors receive the radiation from certain area of ground (regarded as perfect square piece) that is called instantaneous field of view, IFOV. Sensor present non-linear point spread function; it means that the objects located near the center of IFOV contribute more strongly to the output signal than those farther from it (Saura 2004). CPR nearly follows the same assumption by assigning the radiance value of central object of input grid to coarse resolution pixel at which this central object may be regarded as strongly contributing object to radiance value. Figure 4.8 shows the CPR approach applied to nine red band pixels of LISS-II image to get 70.5m coarse resolution red band pixel.

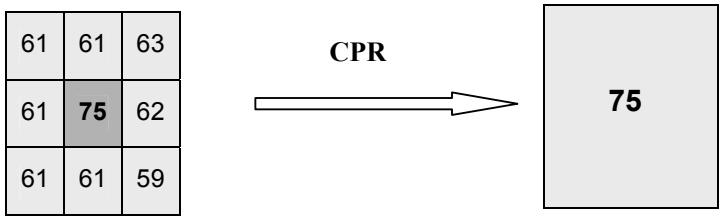

Figure 4.8 CPR aggregation approach

CPR aggregation approach was applied to each band of LISS-III image separately and then coarse resolution bands were stacked to get RGB image at all aggregation levels 3, 5 and 7. This approach was implemented in this work through code developed in R- programming language that accept the ASCII format of each band of image and generates aggregated output of each band in ASCII format.

4.5. Landscape metrics to assess spatial properties

Landscape metrics are used to quantify the spatial properties such as clumpiness, complexity of land use/ cover class or patch in landscape. As the classified image is aggregated, the change in spatial properties can be observed. Therefore landscape metrics are useful to assess the effect of spatial aggregation. There is wide variety of landscape metrics but many of them are correlated with each other.

Riitters *et al.* (1995) examined 55 landscape metrics to show their statistical dependency and independency. They concluded that the information contained in the 55 metrics can be communicated by following few metrics; Dominance, Contagion, Fractal Dimension using Perimeter/Area ratio, Average Patch Perimeter/Area ratio, Number of attribute classes. Dominance index is a measure of dominance that denotes either the landscape is dominated by one/few class or there are many classes in landscape having approximately equal proportions (O'Neill *et al.* 1988). Dominance index exhibited an inconsistence result through different aggregation levels of categorical image (Turner *et al.* 1989). Hence it is not suitable to assess the spatial aggregation effect. Contagion index (CI) measure the degree to which spatial pattern of landscape is aggregated or clumped and Fractal dimension (FD) index capture the shape complexity of spatial patterns (O'Neill *et al.* 1988). Spatial aggregation produces generalization of landscape or changes the spatial patterning that affects its clumpiness or shape complexity. Therefore these indices may be used to capture the spatial changes through aggregation levels. He *et al.* (2000) introduced a new index to quantify degree of clumpiness of spatial patterns and named it Aggregation index (AI). In their study, they showed that CI does not always reflect the clumpiness of spatial patterns as its measurement depends on landscape composition. CI exhibited less contagion for the more clumped landscape. It was found that AI reflected the clumpiness more precisely than CI. AI is a class specific index that can measure clumpiness of spatial patterns within a single class in landscape. AI index can also be used to measure overall landscape clumpiness. But CI only measures the clumpiness of overall landscape. AI showed an advantage over CI as it is independent of landscape composition. Inconsistence result of CI through aggregation levels was also reported by Turner *et al.* (1989), Riitters *et al.* (1995), and Li *et al.* (2004).

FD index can be used to measure the shape complexity of spatial patterns at class level as well as landscape level. It is based on the assumption of power law relationship between perimeter and area. For a single class, it is measured by means of linear regression in which ln(parameter) is plotted against ln(Area) for all patches in class. Two times the slope of regression line is regarded as fractal dimension of that class. Frohn (1997) examined the problems in the measurement of FD and also the advantage of Square Pixel Index (SqP) that also measure the shape complexity. They showed that perimeter area regression to estimate FD creates a number of problems including goodness of fit of regression line, spread of data and need of adequate number of patches. Value of FD was estimated less than its theoretical minimum value (that is 1) in the case when there were availability of small number of patches and a very limited range of perimeter/area values among patches. It was also observed that two landscapes having similar pattern exhibited a large difference in FD value. None of these problems were faced in using SqP as it does not assume power law relationship between perimeter and area. Li *et al.* (2004) also reported the inconsistence result of FD but predictable and consistence behaviour of SqP through aggregation levels was found by Frohn *et al.* (2006).

Due to all above mentioned facts, AI and SqP has been taken in present work to quantify the spatial properties of class such as clumpiness and shape complexity at each level of spatial aggregation.

4.5.1. Aggregation Index (AI)

AI is a class specific index that measures the aggregation level or clumpiness of particular class in landscape present in raster data (He *et al.* 2000) AI for class '*i*' is formulated as:

$$AI_i = e_{i,i} / \max\_e_{i,i} \qquad \textbf{Eq 4.2}$$

Where $e_{i,i}$ is the total edge shared by class *i* itself and $max\_e_{i,i}$ is the largest possible number of shared edges for class *i* . The shared edges are counted only once in AI. In raster data, if A_i is the area of class *i* , n is the side of theoretical largest integer square formed by the number of pixels of class *i* and m = $A_i - n^2$, then the largest possible number of shared edges for class *i* , $max\_e_{i,i}$ will take one of the following forms:

$$max\_e_{i,i} = 2n(n-1), \quad \text{when } m = 0$$
$$max\_e_{i,i} = 2n(n-1)+2m-1, \quad \text{when } m < n, \text{ or}$$
$$max\_e_{i,i} = 2n(n-1)+2m-2, \quad \text{when } m \geq 0$$

The value of AI_i lies between 0 and 1. AI assumes that a class with the highest level of clumpiness (AI = 1) is comprised of pixels sharing the most possible edges. AI = 0 shows the class is completely disaggregated having pixels sharing no edges and lowest level of clumpiness is exhibited.

In this work, a code has been written in R programming language to measure the AI of each class at all spatial aggregation levels including reference level. The input to this code is provided as ASCII format of classified image.

4.5.2. Square Pixel (SqP)

SqP is an alternative to fractal dimension to quantify the shape complexity of class. The SqP considers the perimeter area relationship for raster data structure and normalizes the ratio of perimeter and area to value between 0 (perfect square) and 1(maximum perimeter, edge deviation from that of a perfect square (Frohn 1997). It is formulated as:

$$SqP = 1 - (4 \times A^{1/2} / P) \qquad \textbf{Eq 4.3}$$

Where, P is the total perimeter of all pixels and A is the total area of all pixels of a particular class.
In this present work, total perimeter and area of each class at all spatial aggregation levels including reference level was estimated using computer software program for spatial pattern analysis, FRAGSTAT (McGarigal *et al.* 2002). Then SqP of each class has been estimated by using the formula given above.

4.6. Calibration based model for area correction

Change in class area is observed as the image is aggregated from finer resolution to get coarser resolution. These changes depend upon the proportion of class which is present in fine resolution image. Calibration based model is a tool to correct area of class, which is distorted due to the aggregation effect. It modifies the area of each class to make it closer to reference area estimates (which is present, initially in the fine resolution image). The Calibration method is based on the slope estimator method, also called as direct estimator method (Moody et al, 1996; Moody, 1998).

Slope estimator method

It is based on the regression model that establishes the relationship between the estimated class proportion from coarse resolution image and the actual class proportion obtained from finer resolution image/ reference data. (Moody et al, 1996)

$$P_{ir} = \beta_0 + \beta_1 P_{i0} + error \qquad \textbf{Eq 4.4}$$

Where

P_{ir} -- Proportion of class 'i' at resolution 'r'
P_{i0} -- Proportion of class 'i' at reference/ finer resolution image
β_0 -- Intercept of proportion transition line (explained below)
β_1 -- Slope of proportion transition line (explained below)

Equation 4.4 can be rearranged as

$$P_{i0} = (P_{ir} - \beta_0) / \beta_1 \qquad \textbf{Eq 4.5}$$

It is an inverted model by which actual class proportion can be estimated when only coarse resolution estimates of class proportion is available.

In this present work, both finer and coarser resolution image was divided into same nine sub regions. Actual (fine) and coarse resolution class proportion of each class was calculated in each sub region. It gives the number of class proportion pairs for each class. Coarse resolution proportion of all classes in all sub regions was regressed against that estimated for finer resolution. Proportion transition line is the best fit line obtained after regression of estimated coarse resolution proportions on actual class proportions. β_0 and β_1 are the intercept and slope of best fit line respectively. Proportion transition line relates the actual and coarse resolution proportions.
Same β_0 and β_1 are used for all class 'i' in the inverted model represented by equation 4.5.

Separate calibration model was developed for each coarse resolution image at all aggregation levels in the case of each aggregation approach. This model relates the actual or reference class proportion in LISS-III image and estimated class proportion from coarse resolution image.

In order to assess the success of calibration based model at each aggregation level, total error was estimated according to following formula.

$$TE_r = \sum_{i=1}^{n} \left| Pir - Pio \right| \qquad \textbf{Eq 4.6}$$

Where, 'TE_r' represents the total error at resolution 'r'.

4.7. Statistical property of images at class level

Local variance method

Texture analysis of digital image provides a measure of surface property such as coarseness, smoothness and regularity. Heterogeneity of the scene under observation is affected by the different resolution of images covering that scene and can be measured using texture analysis (Quattrochi *et al.* 1997). Higher textural value reflects greater degree of heterogeneity in scene under observation. In other words, statistical measure like texture analysis indicates the spatial variability in images. If the satellite

images are aggregated to higher level using different numerical aggregation approaches, then it can be expected that it will affect the heterogeneity or variability of different scene in images in different manner. Texture analysis method can provides a useful means to assess the effect of different numerical aggregation approaches. Local variance is one of the methods in texture analysis. It was proposed by Woodcock and Strahler (1987). In this method, 3×3 window passes through the entire image. Each pixel of image is considered at its center. The variance of nine pixel values (within 3×3 window) is calculated at each position of this window. Finally the average of these variance values is calculated over the entire image to estimate the local variance. It indicates the local variability in the image. In order to show the heterogeneity of particular scene in image, local variance should be calculated for that scene. In this work, local variance of each class has been calculated for each aggregated images using Mean and CPR approach as well as base LISS-III image. It indicated the change in heterogeneity of each class from that present in base image. The following steps have been followed to calculate local variance of each class.

1. Variance image of LISS-III NIR band was created using the code written in R-programming language. NIR band was used for the calculation of local variance as it contains maximum information regarding most of the objects present on Earth surface. It gives maximum reflectance for vegetation (agriculture) which is the most dominating class in image. At the same time it shows minimum reflectance value for fallow land and then water. It shows moderate reflectance for areas covered by settlement. Therefore, maximum variability in NIR band is found. Woodcock and Strahler (1987) aggregated the red band of Thematic Mapper (contains maximum variability among all bands) by mean approach and examined the change in local variance with decrease in resolution.

2. Classified LISS-III image was used to generate binary image by assigning ‘1’ value to one class, say agriculture, and ‘0’ to other classes. This binary image was overlaid on the variance image to extract the values of variances that fall within agriculture class. Finally the average of these values was taken to compute that local variance of agriculture class. In this way, local variance of other classes (settlement, fallow land and water) was computed.

The same steps was used to calculate the local variance of each class at aggregation level 3,5 & 7 in the case of both Mean and CPR approach.

5. Results & Discussions

This chapter deals with the results of objectives undertaken in the study. Section 5.1 shows the result of classification accuracy. Section 5.2 explores the impact of aggregation approaches on class proportions, Aggregation Index, Square Pixel Index and local variance. Section 5.3 shows the variation in different realizations of RRB and PDW.

5.1. Classification accuracy

FCM classification accuracy of LISS-III base image was assessed with respect to the same LISS-III image. ERDAS Imaging software was used to generate 600 random points (150 points per class) over classified image as recommended by Congalton (1991) that the number of testing pixels for accuracy assessment should be large enough than the training sample size used to perform supervise classification. At each point, class correspondence and confusion between the classified and raw image was visually observed to report the overall classification accuracy with user and producer accuracy for water, agriculture field, fallow land and settlement. Similarly, 600 random points were also used to calculate the overall classification accuracy of each aggregated image with respect to the raw image at the same resolution in the case of numerical aggregation approach. Table 5.1 shows the overall classification accuracy with user and producer accuracy (UA and PA) of each class for LISS-III image and all aggregated images (at aggregation level 3, 5 and 7) obtained using Mean and CPR aggregation approach.

Table 5.1 Classification accuracy of LISS-III base image and all aggregated images

	LISS-III		**MEAN**						**CPR**					
			3		5		7		3		5		7	
	UA	PA	UA	PA	UA	PA	UA	PA	UA	PA	UA	PA	UA	PA
Water (%)	83	94.4	85	93.4	80	90.9	80	86.9	85	94.4	84.3	96.7	82.5	97.1
Agriculture (%)	89.8	92	89.6	92.3	88.9	93.5	88.4	93.6	89.3	91.9	88.7	93.7	88.9	93.4
Fallow (%)	80.2	68.2	79.7	70.1	74.6	68.2	74.2	66.9	76.9	67.3	76.8	66.7	76.1	64.5
Settlement (%)	91.1	94.1	83.6	85.7	88.5	80.2	86.4	79.2	88.5	90	90.4	85.5	89.9	87.9
Overall Accuracy	**86.83%**		**85.33%**		**84.83%**		**84.33%**		**85.67%**		**86%**		**86.17%**	
Kappa statistics	**0.8161**		**0.7960**		**0.7607**		**0.7274**		**0.80**		**0.7904**		**0.7685**	

The uses of same classifier (FCM), accuracy assessment of classified output of aggregated image with respect to the image at same resolution using 600 random points and approximate consistency in overall accuracy (Table 5.1), ensure that the effect of FCM classifier on class proportions and landscape metrics is low. The major effect is contributed by the numerical aggregation approaches used to aggregate LISS-III image.

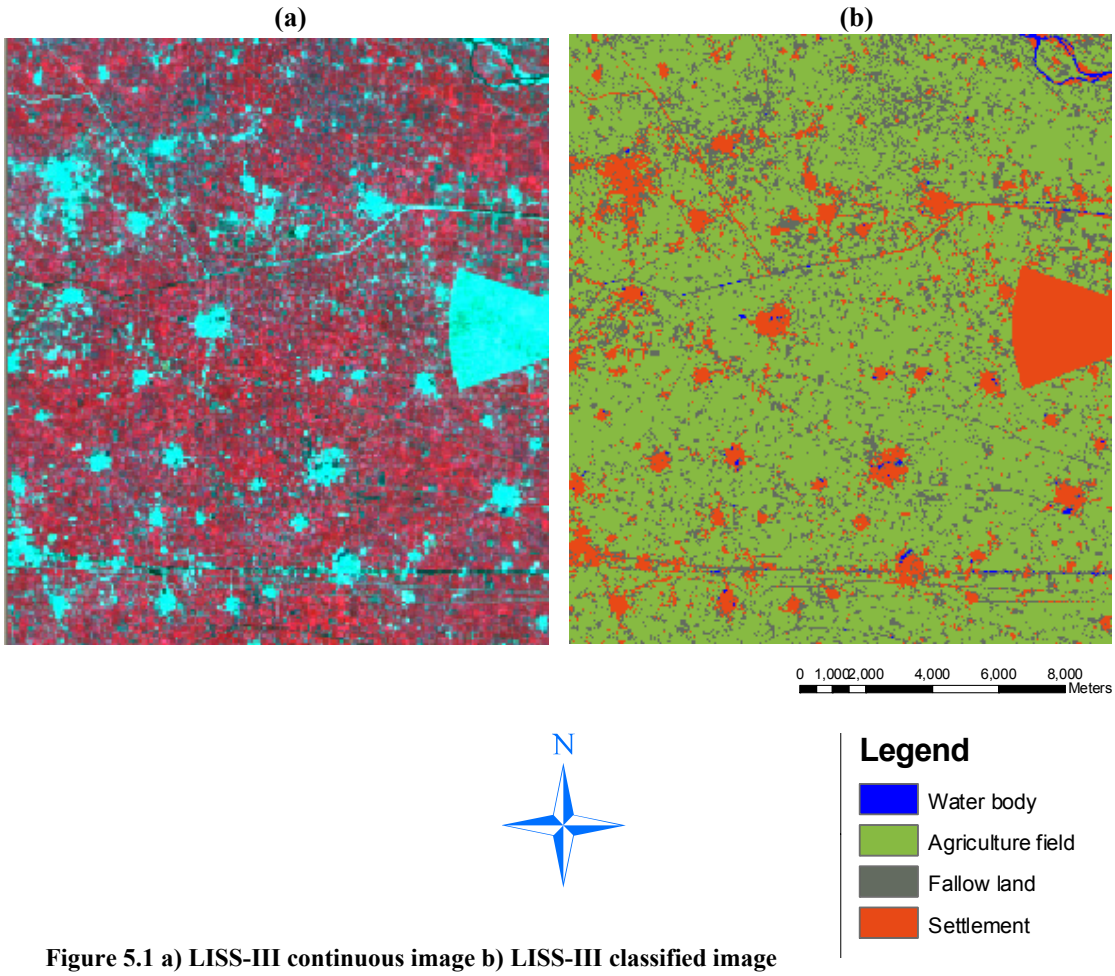

Figure 5.1 a) LISS-III continuous image b) LISS-III classified image

5.2. Analysis of applied aggregation approaches

Effect of MRB, RRB, PDW, mean and CPR approaches in aggregating the fine resolution image (LISS-III image) was analysed by observing their impact on class proportions, AI of each class, SqP index of each class, calibration based model for class proportions correction at three aggregation levels (Table 4.1). The increase or decrease in class proportions, AI and SqP value at different aggregation levels were calculated with respect to that present in base image. Assessment of local variance values showed the change in texture due to mean and CPR approach. Different aggregation approaches uses the different logic or mathematical processing to aggregate the image and therefore they produced diverse trends in these indicators.

5.2.1. Class proportions

Four major land use/cover classes were derived from the classified LISS-III image (base image) in first level classification scheme. Agriculture class was comprised of about 72% of the landscape and it was the most common (dominant) and most clumped class type. Fallow and settlement were moderately common class type and comprised of about 16% and 12% of the landscape respectively. Fallow was most dispersed class type distributed in small patches over the landscape, but the settlement class occurred as a clumped structure in landscape (Figure 5.1b). Water was the least common class and it con-

tributed only 0.3% of the landscape. In this study, class percentage was treated as a class proportion. Aggregation level '1' in Figure 5.2 shows the class proportion of base image. When the MRB aggregation approach was applied to classified LISS-III image, proportion of agriculture, the dominant class, exhibited an increasing trend across aggregation levels (Figure 5.2a). The increase was less (about 5%) at aggregation level 3, but it raised with increasing level of aggregation and about 13% increase in agriculture proportion was observed at aggregation level 7. Proportion of moderately common classes exhibited a decreasing trend through aggregation levels, but the slope of decrease for settlement class was much less than fallow class (Figure 5.2a). The decrease in fallow, water and settlement class proportion was 53%, 44% and 10% respectively at aggregation level 7. The small distributed patches of fallow class in base image reduced the chance of being it a major class in specified cell of input grid with increasing levels of aggregation. It resulted in significant decrease (53%) in fallow class proportion. For the same reason, significant decrease in water proportion was observed. It is not apparent from Figure 5.2a as water class proportion is small (0.3%) with respect to other classes. In general MRB approach made the dominant class more dominant and decrease in other moderate and least common class proportions. These decreases in proportions were compensated by increase in dominant class proportion. These findings were consistence with the results reported elsewhere where the effect of MRB aggregation was analysed to coarsen the resolution of land-cover map of Landsat TM image (Moody *et al.* 1995, He *et al.* 2002).

RRB and PDW aggregation approaches relatively maintained each class proportions through aggregation levels (Figure 5.2 b & c) with a maximum variation of less than 2% except in the case of water class. Approximately no variation in agriculture class proportion (± 0.1%) was observed in both approaches. RRB caused the decrease of about 2% in fallow class proportion and increase of about 2% in settlement at aggregation level 5. At other levels, only about ± 0.5% variations in these classes were observed, but PDW caused the variation of ± 0.3% in these classes at all aggregation levels. Proportion of water class is distorted more by PDW and about 14% decrease was observed at aggregation level 7, which was 7.5% increase in the case of RRB. For other levels also, RRB showed less variation in water class than PDW. Both RRB and PDW are based on random selection of class from the specified cell of input grid. RRB randomly selects the class directly from classes in input grid, but PDW randomly selects it from the cumulative frequency distribution of the classes in specified cells of input grid. In both cases, random selection makes the probability for selecting class to represent an aggregated area directly proportional to its presence in the input data. Due to this reason, both approaches, in general, made no significant distortion in class proportions and preserved it with increasing level of aggregation. Proportion of class, present in abundance (agriculture) was preserved more accurately than other classes in both approaches. Significant variation in water proportion is due to low percentage in base image than other classes. Overall PDW preserved the class proportions more precisely than RRB. The characteristic of RRB and PDW approach to preserve the class proportions was also reported by He *et al.* (2002) and Gardner *et al.* (2008).

Mean aggregation approach exhibited an increasing and decreasing trend in class proportion, but affected differently the class proportions than MRB (Figure 5.2d). At each aggregation level, fallow class showed a successive increment of about 20% to its previous level and increased by 56 % at aggregation level 7. Proportion of agriculture class was not greatly affected by mean aggregation approach and only 2% successive decrease in its proportion was observed at each aggregation level. Proportion of settlement class decreased much and it became 31% lower than its proportion in base image at aggregation level 7. Water class proportion exhibited a higher decrease of 29% at aggregation level 3 than other levels, however the rate of decrease was slower than that observed for settlement classes.

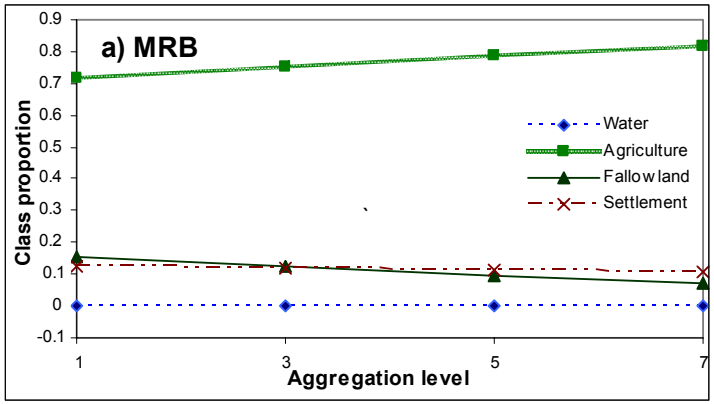

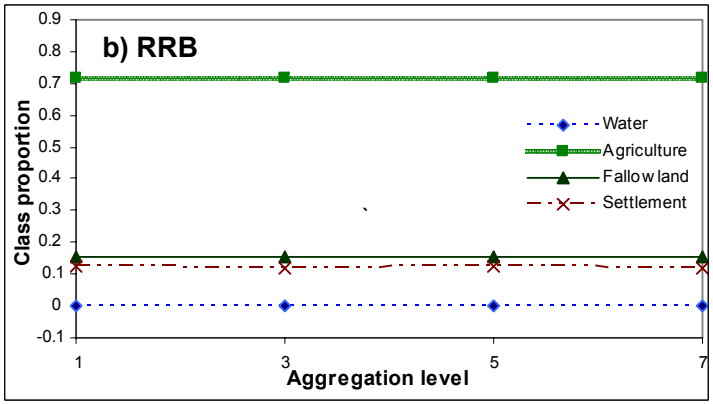

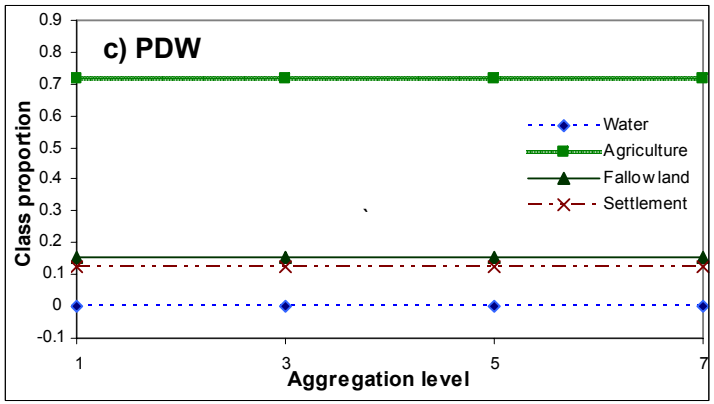

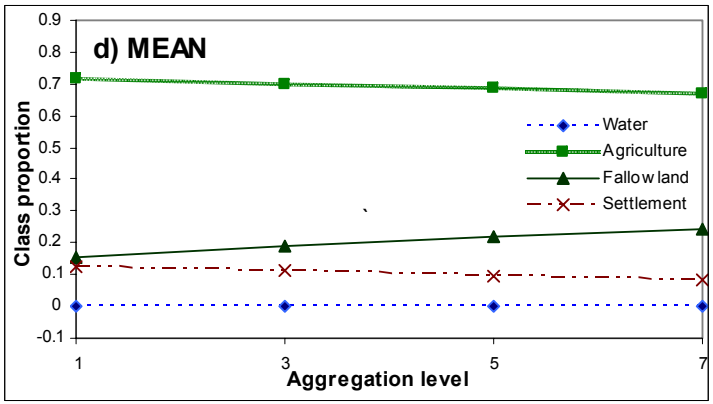

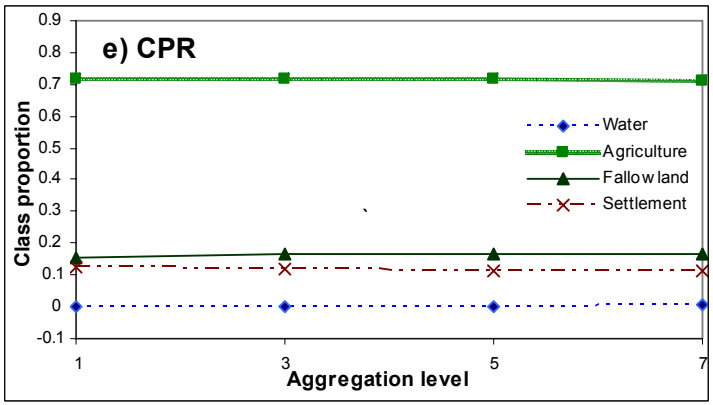

Figure 5.2 Class proportions of classified LISS-III image aggregated to aggregation level 3, 5 & 4 using the approaches a) majority rule-based b) random rule-based c) Point centered, distance weighted, and moving window method d) mean e) central pixel resampling

Loss in proportions of settlement class mostly contributed to increase in fallow class proportion but less than the loss in dominant agriculture class proportion. It may be due to the reason that there are large number of very small patches of settlement and agriculture class surrounded by the fallow class in the landscape (Figure 5.1a). Mean of DN values at these areas filtered out or reduced the effect of these small patches and resulted in DN values close to the fallow class reflectance. As the water class is only 0.3% of landscape, therefore the decrease in its proportion did not significantly contribute to increase in fallow class proportion. In general, mean approach made the increase in proportion of one class (fallow class, i.e. not a dominant class) while there was decrease in proportions of other classes, which was not in the case of MRB, where increase in dominant class proportion was observed. Gupta *et al.* (2000) also observed that mean aggregation approach decreased the each class proportion of LISS-II land-cover map and it caused increase in proportion under unclassified category.

CPR aggregation approach exhibited nearly similar trend in class proportions as it was observed in the case of PDW and RRB. CPR did not change significantly the class proportions with increasing level of aggregation (Figure 5.2e). Proportion of agriculture class varied less than 1% through aggregation levels. Maximum of only 8% increase in fallow class proportion was noticed at aggregation level 7. Proportion of settlement class decreased through aggregation levels, but it was not more than 6%. Water class proportion showed a significant increase of about 15% at aggregation level 7, but its proportion did not change more than 4% up to aggregation level 5. Overall, CPR approach maintained the class proportions. A probability, that a DN values of particular class will lie at the center of specified cells of input grid (odd window), corresponds nearly to the fraction in which all pixels of landscape reduce after aggregation. It made the CPR approach to retain the class proportions with increasing level of aggregation.

5.2.2. Aggregation Index

AI value of a class reflects that how much clumped or aggregated spatial pattern is presented by that class in landscape. Aggregation level 1 in Figure 5.3 shows the AI value of all classes in base image. AI value of the agriculture class was highest (0.92). It reflected that agriculture class was present in highest aggregated spatial pattern at base image than that of other classes. Settlement class had AI value of 0.81, which showed its less aggregated spatial pattern than agriculture class. AI value of fallow and water class was nearly equal (0.61 and 0.62), which showed their nearly same, but less aggregated spatial pattern than other classes at base image. These classes were present in landscape with large number of small patches, which were dispersed over whole space (Figure 5.1b). It resulted in their small and equal AI values.

When base image was aggregated with MRB approach, AI of agriculture first decreased at level 3 with very small amount (4%). It was possibly due to interruption of small patches of other classes on its aggregated pattern. As aggregation level increased, MRB made the dominant class more clumped that resulted in increase in AI of agriculture (Figure 5.3a). AI of fallow and water class decreased in same manner through aggregation levels and showed a same aggregated spatial pattern at each level. About 55% decrease in their AI values was observed at aggregation level 7. It reflected that MRB made the dispersed classes more disaggregated. AI of settlement class also decreases through aggregation level, but the slope of decrease was lower than that observed in the case of fallow and water class as more aggregated spatial pattern was exhibited by settlement class than these classes in base image. The slope of decrease in AI values was more up to aggregation level 3, but it became moderate through further decrease in spatial resolution. Overall, the aggregation index of dominant class increased and moderately and least common classes decreased due to MRB aggregation approach.

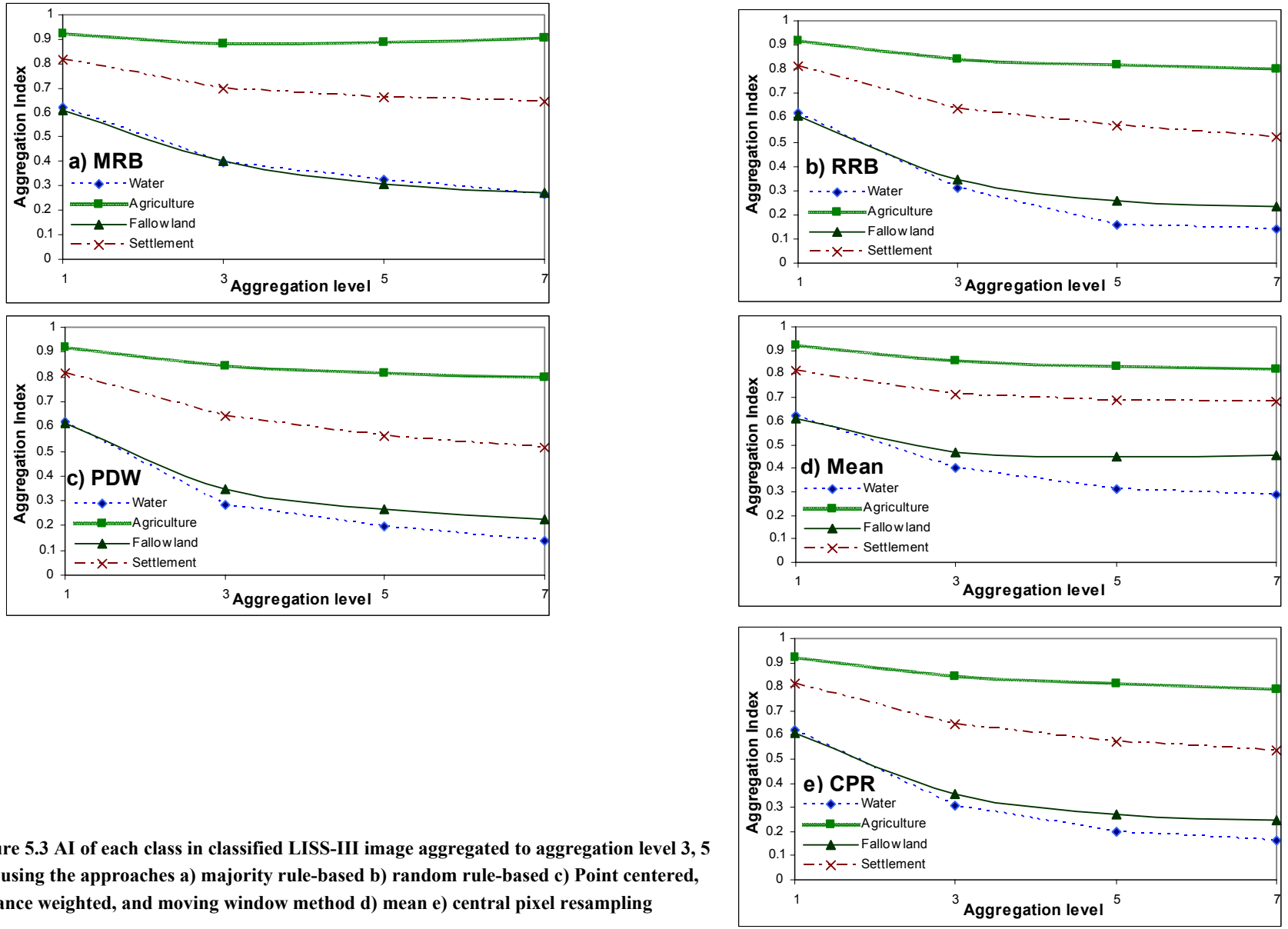

Figure 5.3 AI of each class in classified LISS-III image aggregated to aggregation level 3, 5 & 4 using the approaches a) majority rule-based b) random rule-based c) Point centered, distance weighted, and moving window method d) mean e) central pixel resampling

RRB, PDW and CPR affected the clumpiness of spatial pattern of all classes in almost similar manner (Figure 5.3 b, c & e). Both RRB and PDW randomly assign the class by selecting it from the classes present and their cumulative frequency distribution in specified cells of input grid respectively. It caused the less aggregated spatial pattern of each class with increasing level of aggregation. CPR assigns the central pixel (class) value of specified cells or window of input grid. It ignores the other pixels (class) value. In many cases, patches of one class may fall on the more than one contiguous window of input grid in which other classes may present at the central location. Selection of centrally located class caused the disaggregation of patches of that class and reduced the clumpiness of its spatial pattern. It occurred with all classes present in the landscape. This effect increased with increasing window size and accordingly caused the less aggregated spatial pattern of each class. Result showed that AI value of agriculture class was affected equally by all these three approaches and maximum of 13% decrease in its AI value was observed at aggregation level 7. The slope of decrease in AI value of agriculture class was slower than that of other classes. It was due to its dominant nature and highest clumped pattern in base image. At aggregation level 3, AI value of settlement class showed a decrease of 21% for all three approaches. But at higher level, it was affected less by CPR, but not more than 3%. Fallow and water class exhibited a highest decrease in their AI values for all three approaches and became more disaggregated through aggregation level as compared to other classes. But the slope of decrease in AI value of water was greater than the fallow class. It could be due to its less percentage (0.3%) at all aggregation levels, whose clumpiness of spatial pattern was interrupted greatly by other classes as a result of random or centre pixel selection of class. Overall, RRB, PDW and CPR decreased the clumpiness of spatial pattern of all classes, but less slowly for dominant class in landscape. He *et al.* (2002) also reported that AI of dominant class increased for MRB approach, but RRB approach caused decrease in AI of all classes in land-cover map of Landsat TM image.

Mean aggregation approach also decreased the AI values of all classes through the aggregation level. But the slope of decrease was less for all classes than that observed in the case of other aggregation approaches (Figure 5.3 d). It reflected that mean approach maintained more clumpiness of spatial pattern than other approaches. Mean approach filters out very small patches or reduces their interruptions on the clumpiness of spatial pattern of major class present in local region of image. This was not observed for RRB, PDW and CPR approach, where random or central pixel selection caused more interruption. Therefore mean approach exhibited more stability in aggregated pattern of each class, but the decreasing spatial resolution caused a decrease in the aggregated spatial pattern of each class. The result showed that AI value of agriculture class exhibited a maximum decrease of 10% at aggregation level 7. That was 25% and 16% for fallow and settlement class. Highest decrease (54%) was observed in the case of water class, but it was still lower than that observed in the case of other approaches. After the aggregation level 3, no significant decrease in AI value of dominant and moderately common classes was observed. It also reflected that mean approach even did not affect significantly the clumpiness of most dispersed class (fallow class) at higher levels.

5.2.3. Square pixel Index (SqP)

SqP indicates the degree of shape complexity of spatial pattern of a class in the landscape. Higher value indicates more deviation from perfect square, i.e. more complex shape. Figure 5.4 shows the SqP value of each class in base image. SqP value of agriculture and settlement class was nearly equal (0.983 and 0.982), which indicated that both classes were present in landscape with equal degree of their complexity in shape. Highest complex shape was represented by fallow class with a SqP value of 0.993. It is also apparent from Figure 5.1b that fallow class exhibited most dispersed pattern in the landscape. Whereas, water class shown lowest degree of shape complexity (0.949) than other classes.

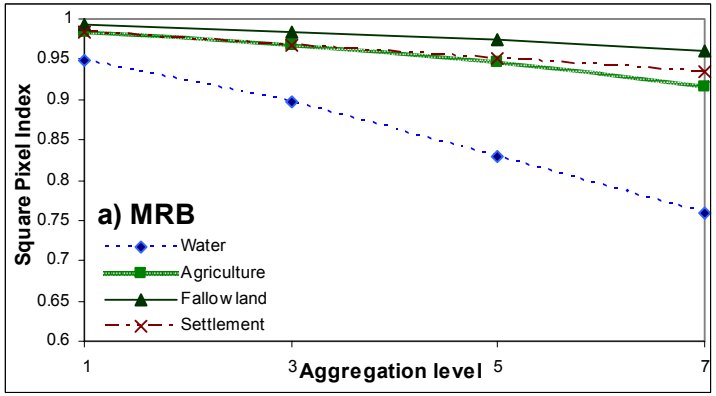

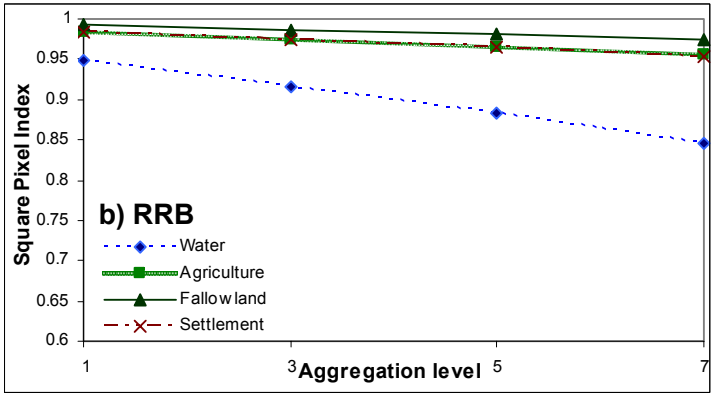

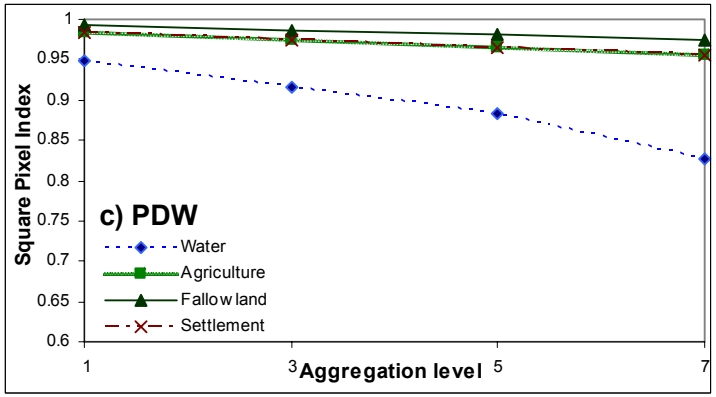

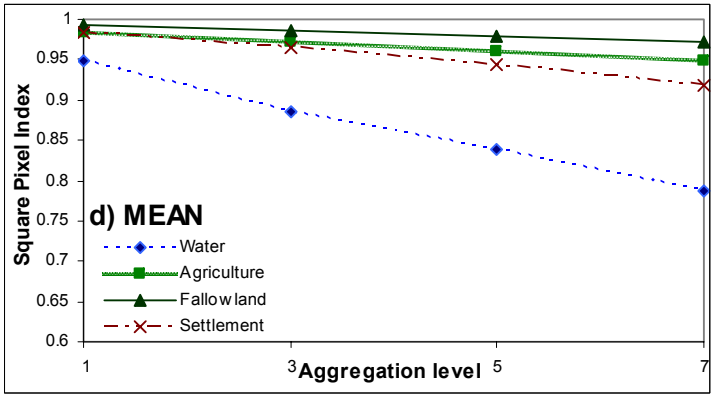

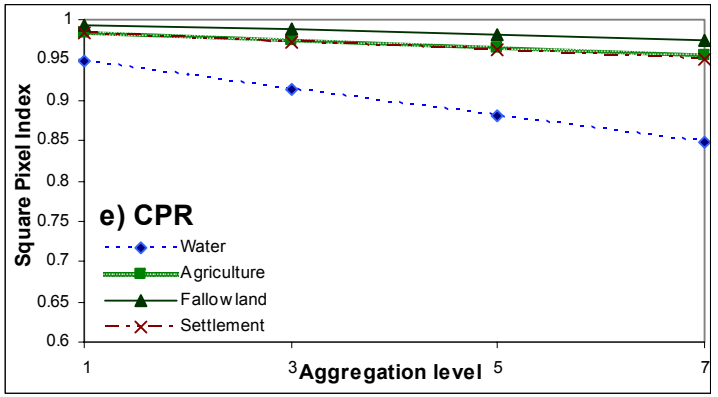

Figure 5.4 SqP of each class in classified LISS-III image aggregated to aggregation level 3, 5 & 4 using the approaches a) majority rule-based b) random rule-based c) Point centered, distance weighted, and moving window method d) mean e) central pixel resampling

The SqP values of each class was observed to have decreasing trend through the aggregation levels using MRB, RRB, PDW, CPR and mean approach. It reflected that degree of shape complexity reduced for all classes. In other words, shape of spatial pattern of each class became more generalized with increasing level of aggregation.

For all approaches, fallow class showed a less decrease in its SqP value at each aggregation level and exhibited a more complex shape than other classes. It occurred possibly due to the landscape configuration that made the less variability in SqP value of fallow class through aggregation level. RRB, PDW, CPR and mean approach affected the shape complexity of fallow land equally (Figure 5.4 b, c & e) and maximum of about 2% decrease in its SqP value was observed at aggregation level 7. The decrease in SqP value of fallow class was less than that observed in the case of MRB (Figure 5.4 a), where decrease of its SqP value was about 2% and 4% at aggregation level 3 and 5 respectively. In other words, MRB generalized more the shape of most complex shaped feature (fallow class).

RRB, PDW and CPR also responded same for the SqP values of agriculture, settlement and water class through aggregation levels. Agriculture and settlement class exhibited almost equal decrease in their SqP values in each of these three approaches (Figure 5.4 b, c & e) and a maximum of about 3% decrease in their SqP value was observed at aggregation level 7. Random and center pixel selection logic of these aggregation approaches maintained equal nature of their degree of shape complexity at each level of aggregation. MRB and mean approach did not respond in this manner, where difference in their shape complexity was observed with increasing level of aggregation. For MRB, the rate of decrease of SqP value of agriculture class was greater than that observed in the case of mean approach. But for settlement class, mean approach exhibited more decrease in its value (Figure 5.4a & d). At aggregation level 7, decrease in SqP value of agriculture and settlement class was about 7% and 5% for MRB approach, which was 4% and 7% for mean approach. MRB filtered out small patches of other classes from dominant agriculture class, but the mean approach reduced the effect of these small patches. It resulted in more decrease in shape complexity of agriculture class in MRB approach as compared to mean approach. In the base image, there are some patches of fallow class around the edge of settlement class patches (Figure 5.1). Mean approach increased the percentage of fallow class through aggregation levels. This increase caused increase in size of these fallow class patches around the edge of settlement class patches. It possibly made the edge of settlement class patches smoother with increasing levels of aggregation. This was not observed in the case of MRB approach. This is the main cause of the decrease in the shape complexity of settlement class using mean approach as compared to MRB approach.

For water class, degree of shape complexity is also reduced more by MRB and mean approach as compared to other approaches. But for all approaches, water exhibited a strong decrease in its SqP value than other classes. This was possibly due to its low occurrence (0.3%) and spatial pattern in base image.

The decrease in shape complexity with increasing level of aggregation was also reported by Frohn *et al.* (2006), where MRB was used to decrease the resolution of land Landsat TM map covering deforestation area.

Overall, RRB, PDW and CPR approach produced less distortion in shape complexity as compared to MRB and mean approach.

5.2.4. Calibration based model (slope estimator) for area correction

Slope estimator method is used to correct the class proportions that are distorted due to coarse resolution. Fine resolution image is aggregated to coarse resolution image and then the calibration based model is developed between them. This model is used to correct the class proportions when only coarse resolution image is available. Different aggregation approaches may be used to aggregate the fine resolution images and it will affect the derivation of calibration based model differently. This concept was used, in this study, to assess the effect of aggregation approaches. RRB, PDW and CPR did not distort the class proportion with increasing levels of aggregation. Therefore it is not relevant to apply the calibration based model for these approaches. Distortion in class proportions with respect to base image was observed only in the case of MRB and mean approaches. Hence only the result of MRB and mean approaches has been presented here.

Figure 5.6 and 5.8 show the class proportions (reference proportions) in base image, change in class proportions (uncorrected) due to aggregation and change in class proportions obtained after applying slope estimator method in the case of MRB and mean approach.

For MRB, slope estimator overcorrected (greater than reference proportion) the class proportion of agriculture, water and settlement class and undercorrected (lower than reference proportion) the fallow class proportion at all aggregation levels (Figure 5.6 a, b &c). Water class exhibited a highest overcorrection with respect its proportion than other classes at each aggregation levels. It may be due to its small percentage (0.3%) in base image, which decreased further using MRB aggregation. Agriculture class showed an increase in its proportion by 5% at aggregation level 3 and 13% at aggregation level 7, which after applying slope estimator was 0.7% and 2% respectively. For settlement class, slope estimator made an increase in its proportion with respect to reference proportion at each aggregation level, which on the contrary decreased due to MRB approach. But the increase in proportion was still lower than the decrease. At aggregation level 7, MRB decreased settlement class proportion by 11%, which was increased due to slope estimator by 6%. Slope estimator also corrected significantly the fallow class proportions, whose proportion was decreased strongly by MRB. Fallow class exhibited a decrease in its proportion by 53% at aggregation level 3, but this decrease became 36% after applying slope estimator method. Figure 5.5 shows the overall performance of slope estimator method at each aggregation level.

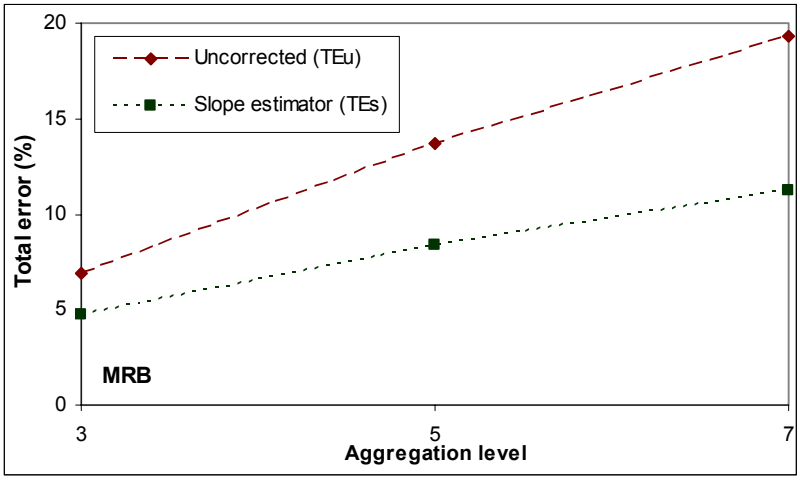

Figure 5.5 Total error produced before and after applying slope estimator method for MRB

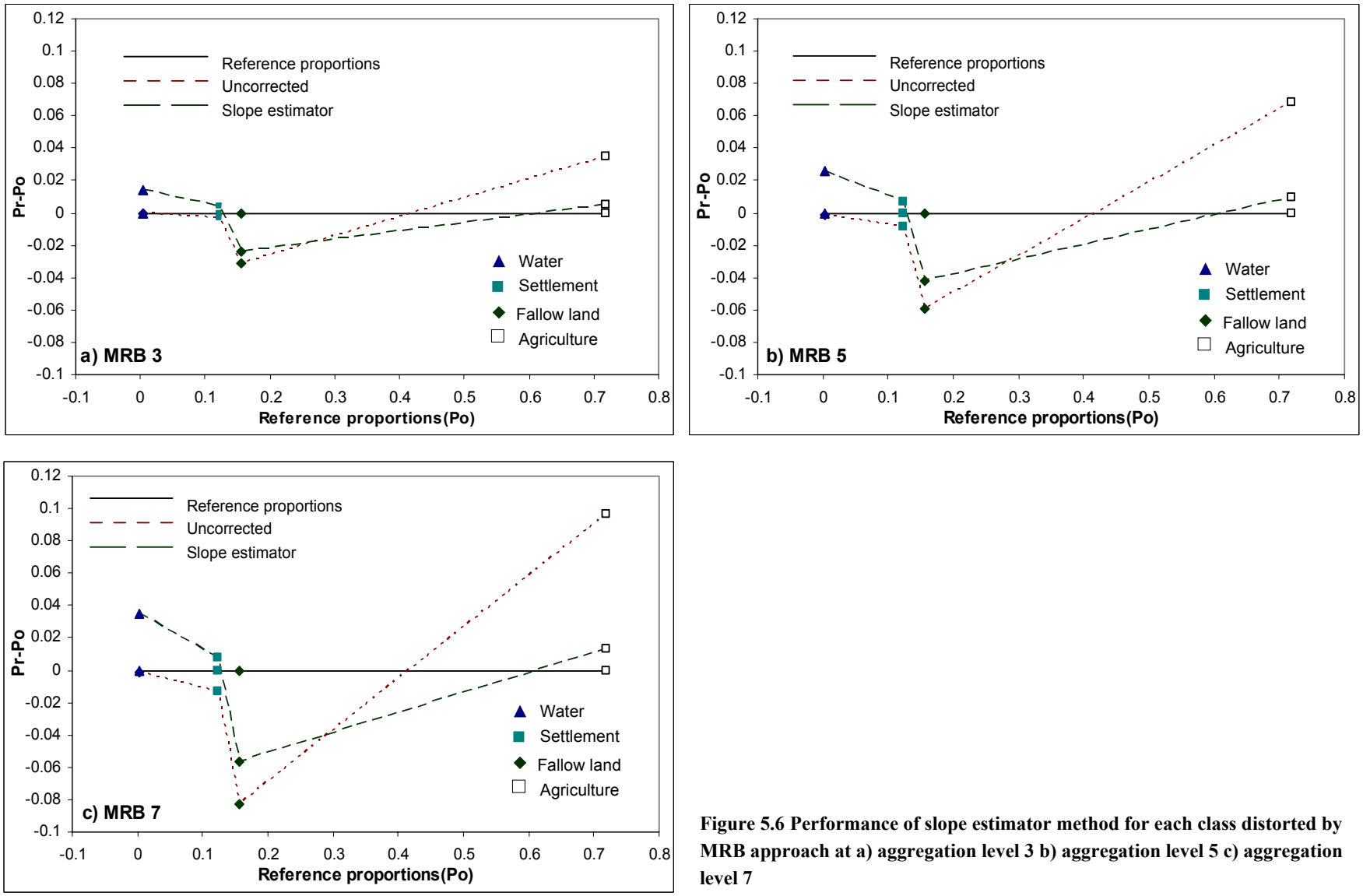

Figure 5.6 Performance of slope estimator method for each class distorted by MRB approach at a) aggregation level 3 b) aggregation level 5 c) aggregation level 7

In Figure 5.5, TEu is the total error calculated using the equation 4.6 before applying slope estimator method in the case of MRB approach at each aggregation level. TEs represent the total error after applying the slope estimator method. As the aggregation level increased, the improvement in slope estimator method for area correction was observed. At aggregation level 3, TEu and TEs was 7% and 5%, which became 19% and 11% at aggregation level 7. It shows that higher error was minimized more by slope estimator method. It can be seen as a gap between TEu and TEs lines at each aggregation level in figure 5.5. It can be also observed for each class, except water class, in figure 5.6, where uncorrected proportions was improved more with increasing level of aggregation level.

For Mean approach, slope estimator overcorrected the proportion of fallow class and undercorrected the proportion of agriculture, water and settlement class at all aggregation levels (Figure 5.8 a, b &c). Only at aggregation level 7, little overcorrection in agriculture class proportion was observed. Water class exhibited highest undercorrection compare to other classes. Amount of undercorrection of water class increased up to aggregation level 5 and it suddenly decreased at aggregation level 7. For fallow class, slope estimator did not make significant correction up to level 5 and overcorrected its proportion by 68% at aggregation level 7, while 56% decrease in its proportion was found due to mean approach. For settlement class, slope estimator undercorrected its proportion up to level 5, which was greater than decrease in its proportion due to mean aggregation. At aggregation level 7, correction in its proportion was observed and decrease in its proportion became 27%, which was 31% before applying slope estimator method. Above discussion reflects that inconsistence behaviour of slope estimator method was found for water, fallow land and settlement class. Slope estimator method responded well in the case of agriculture class. Up to aggregation level 5, slope estimator made its proportion 1% less from its reference proportion that was 3% and 5% at aggregation level 3 and 5 due to mean aggregation. Agriculture proportion was overcorrected by 1% at aggregation level 7. Figure 5.7 shows the overall performance of slope estimator method at each aggregation level.

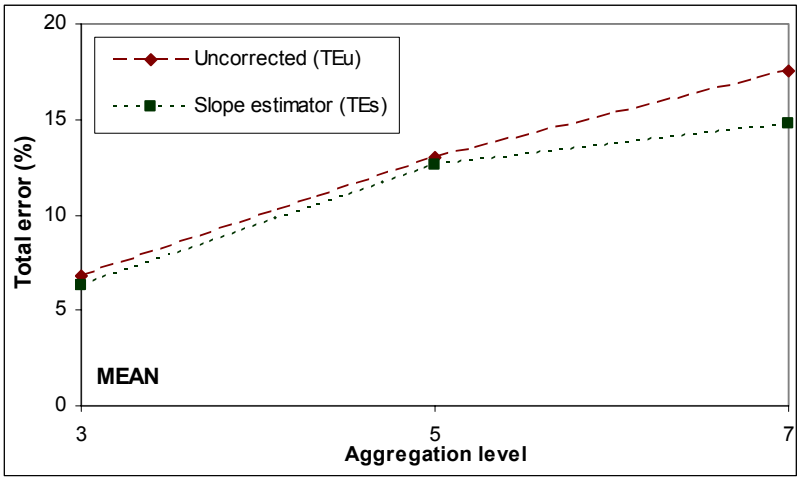

Figure 5.7 Total error produced before and after applying slope estimator method for Mean

Up to aggregation level 5, no significant decrease in TEu and TEs was observed. At aggregation level 7, slope estimator method reduced total error from 17% to 15%. The difference was still not large. It showed that slope estimator method did not make significant correction in distorted class proportions.

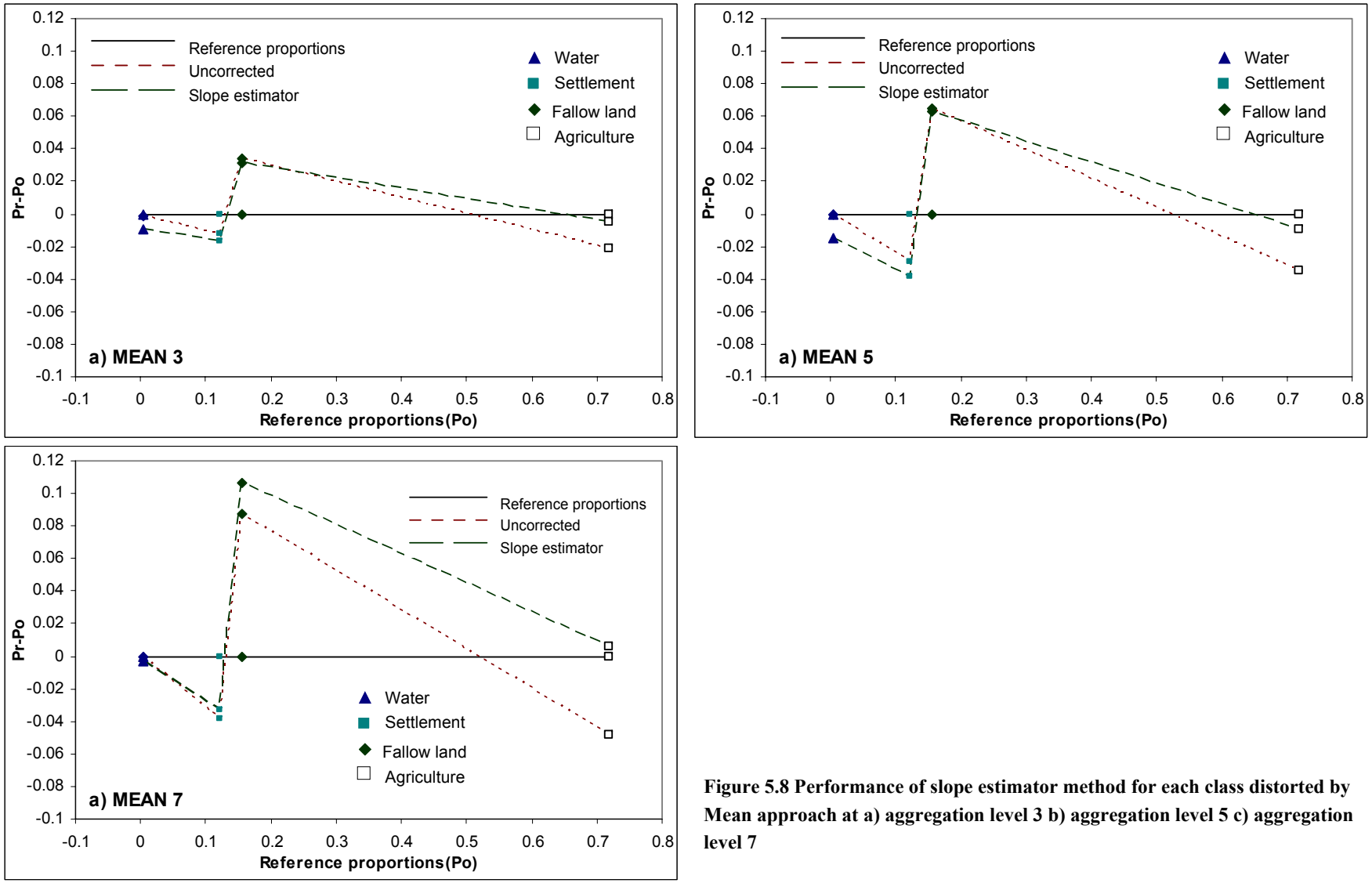

Figure 5.8 Performance of slope estimator method for each class distorted by Mean approach at a) aggregation level 3 b) aggregation level 5 c) aggregation level 7

Moody *et al.* (1996), in their study, explained that slope estimator method performs well, when there is a tendency of small classes to diminish and large classes to increase due to aggregation effect. MRB aggregation approach makes such effect. They found that the reduction in total error increased with increasing level of aggregation. Results presented here also shows that slope estimator method performed well in the case of MRB, where this method reduced the total error at each aggregation level. The increase in reduction of total error was observed with increasing level of aggregation. It was also reflected by the considerable correction in all dominant and moderately common class proportions for MRB approach. Slope estimator performed poorly for mean approach. That was verified by the estimation of total error before and after correction. On the whole, MRB approach performed better than mean approach in the derivation of calibration based model.

5.2.5. Local variance of classes

Local variance of image reflects the variability in image by considering the variation at local level. It is useful only when it is calculated for a scene in which one dominant feature is present. It will reduce the impact of other features in the measure of variability. Figure 5.9 shows the local variance of each class in NIR band at each aggregation level (as a function of resolution) as well as in base image (aggregation level 1), when the base image was aggregated by mean aggregation approach. Percentage of water class in the base image was very small and it was also distributed in image as a very small patches. Therefore no dominancy of this class was found in any region of image. The small patches of water was even smaller than 3×3 window (used to calculate local variance) in many region of images. Due to this, estimation of local variance of water class in many region of image may include much reflectance of other classes and therefore local variance value will not be the major representative of water class. It was not the case for other classes in image. For this reason, water class was excluded from analysis of local variance.

Figure 5.9 shows the local variance of class at different aggregation level. In the base image, local variance of agriculture, fallow and settlement class was 51.8, 100 and 50 respectively.

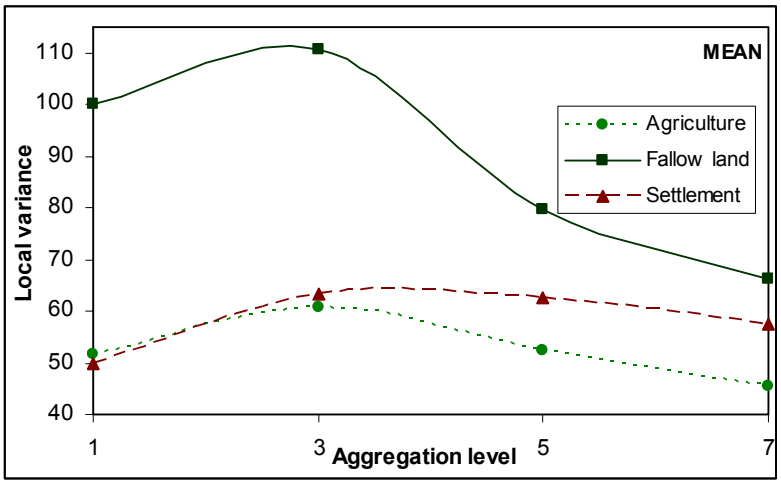

Figure 5.9 Local variance of each class for mean approach at aggregation level 3, 5 and 7

It showed that maximum variability was found for fallow class. It was due to the tonal variation of fallow class in its local region of image. Local variance of each class initially increased and it was found maximum at aggregation level 3 and thereafter decreased with respect to increase in aggregation level. It is possibly due to the reason that when the base image was aggregated to level 3, the objects in the

particular scene (a class) became nearly equal to the resolution of aggregated image. It decreases the likelihood of a pixel in each class with the neighbouring pixels, which results in increase in the local variance. When the resolution of base image was further decreased, many objects were mixed up in a single cell due to averaging (smoothening effect) of their reflectance values. This increased the likelihood with neighbouring pixels that resulted in the decrease in local variance of each class. Slope of decrease was higher for fallow and least for settlement class. Because of the maximum variability exhibited by fallow class in base image, smoothening effect of mean approach on fallow class reflectance was more at higher aggregation levels (5 & 7) as compared to other classes, which resulted in high decrease in fallow class local variance. Local variance of settlement class was small in base image compared to other classes meaning low variation in settlement. Due to this, smoothening in its variability was also low using mean approach at higher aggregation level. It resulted in slower decrease in its local variance compare to other classes. Mean approach decreased the local variance of agriculture more than settlement at higher aggregation level. Trend of local variance curve in the study was found consistent with the results by Woodcock and Strahler (1987) applied over settlement and agriculture scene (red band of Landsat TM image). The mean approach was used to aggregate the scene. The increase in local variance of both classes was found initially, and then subsequent decrease was observed thereafter with the decreasing resolution.

Figure 5.10 shows the local variance of each class at all aggregation level in the case of CPR approach. Local variance of each class increased with increasing level of aggregation.

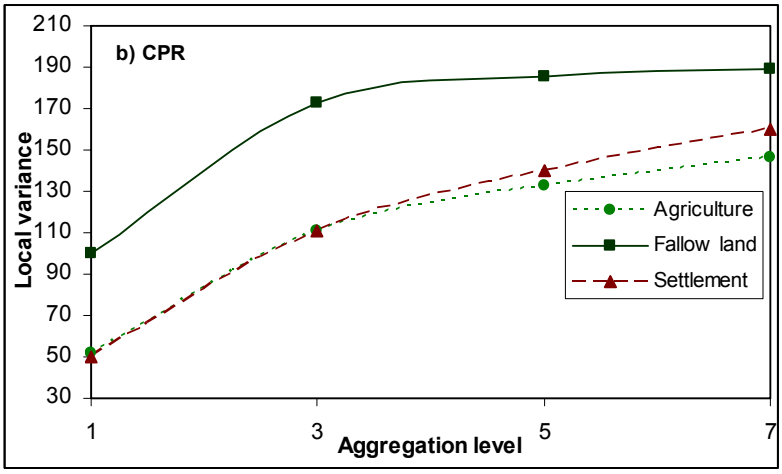

Figure 5.10 Local variance of each class for CPR approach at aggregation level 3, 5 and 7

The increase in local variance of each class shows that the CPR approach decreases the likelihood of a pixel in each class with its neighboring pixels. CPR approach assigns central pixel value of specified cells of input grid to the output aggregated pixel. In this way, CPR completely ignores the neighboring pixels in aggregation process. Within a class, a pixel shows more likelihood with its direct neighbors rather than the pixels farther from it. The ignorance of neighboring pixels due to CPR approach makes the two pixels contiguous, which are not direct neighbors. It decreased the likelihood of a pixel with neighboring pixels and resulted into increase in local variance of each class. CPR approach may also increase the chance of occurrence of different class reflectance values in a local region (3×3 pixels window, that has been used to compute local variance) of aggregated image. This may lead to strong variation in a local region and consequently increase in local variance of a particular class. The slope of increase in local variance of all classes was large at aggregation level 3, which decreased with further increase in aggregation levels. It showed that variability in a class tended towards consistency

with increasing levels of aggregation. At aggregation level 3, the increase in local variance was much higher than that observed for mean approach. CPR approach increased the local variance of agriculture, fallow and settlement class by 113%, 73% and 122% respectively at aggregation level 3, which was 17%, 10% and 26% for mean approach.

Decrease in local variance, at higher aggregation levels, reflected that the smoothening effect produced by the mean approach. The CPR produced increase in local variance of all classes, which was due to the complete ignorance of neighbouring pixels in aggregation process. It can be expected that heterogeneity (in terms of reflectance) in the local region of landscape should be reduced at coarse resolution, which will produce increase in likelihood and corresponding decrease in local variance. Response of local variance curve using mean approach exhibits this phenomenon. On the contrary, the CPR approach increases the local variance. Therefore it can be inferred that mean approach responded better for local variance than the CPR approach.

5.3. Realizations of RRB and PDW aggregation approach

RRB

RRB is based on the random selection of class from the specified cells of input grid. Therefore, each time the RRB is applied on the classified image, different realization of output aggregated image may be obtained. In order to assess the variability in realizations at each aggregation level, RRB was applied 100 times on base image to get 100 realization of each level. For each realization, the percent change in indicators such as each class proportion, AI and SqP with respect to that present in base image was estimated. The standard deviation (SD) of percent change in each indicator at each aggregation level was computed to report the variability in realizations.

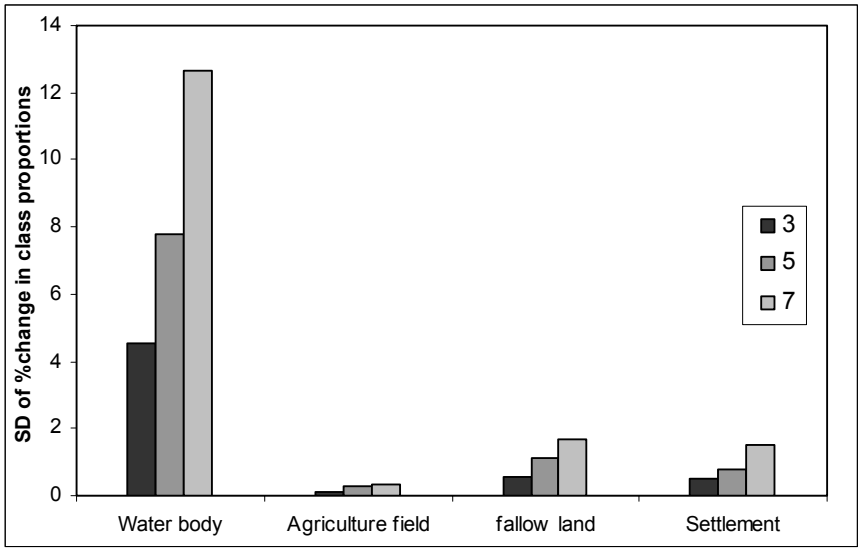

Figure 5.11 Variability in each class proportion due to different RRB realizations at aggregation levels 3, 5 & 7

Figure 5.11 shows the SD of percent change in class proportions at aggregation level 3, 5 and 7. Less than 1% variation (SD = 1) was observed for agriculture, fallow and settlement class at aggregation level 3 that increased with increasing level of aggregation. Change in fallow class proportion showed a

maximum variation among these three classes and agriculture class least. It was due to the disperse pattern of fallow class with very small patches at base image, where agriculture was present in most clumped pattern. But still change in fallow class proportion showed maximum variation of 2% at aggregation level 7 that was only 0.4% for agriculture class. SD of change in settlement proportion was in between agriculture and fallow class, which was due to its degree of clumped pattern between these two classes (Figure 5.3b). At aggregation level 7, SD was 1.4% for settlement class. Among all classes, maximum variation in change of water class proportion was observed. For this class, SD was 4.5% at aggregation level 3 that increased to 13% at aggregation level 7. Water class exhibited near same degree of clumpiness as fallow class (Figure 5.3b), but its proportion was very low (0.3%) in base image. Due to this, probability of random selection of water class from base image varied significantly for different realizations. This variation increased with increasing level of aggregation. It resulted in highest value of SD compare to other classes.

Figure 5.12 shows the SD of percent change in AI of each class at aggregation level 3, 5 and 7.
No significant variation in AI of agriculture, fallow and settlement class was observed at each level and it was maximum 1% at aggregation level 7 for fallow class. The change in AI of agriculture class exhibited a least variation among all classes, which was maximum 0.3% at aggregation level 7. Variation in AI of settlement class was in between agriculture and fallow class.

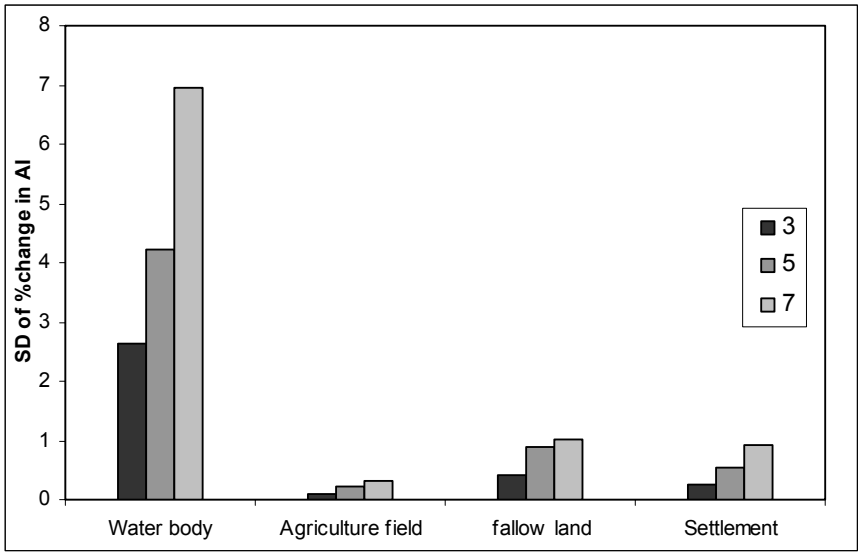

Figure 5.12 Variability in AI of each class due to different RRB realizations at aggregation levels 3, 5 & 7

These results were according to the degree of clumpiness of these classes at base image, i.e. more clumped pattern (agriculture) exhibited less variation. Maximum SD was observed for water class among all classes at each aggregation level.

Figure 5.13 shows the SD of percent change in SqP of each class at aggregation level 3, 5 and 7. It can be seen that change in SqP of agriculture, fallow and settlement class exhibited very small variation less than 0.05% at all aggregation levels. That reflects no variation in SqP. The change in SqP of water class showed some variation, but it is was 0.2% at aggregation level 3 that increased to only 1% at aggregation level 7.

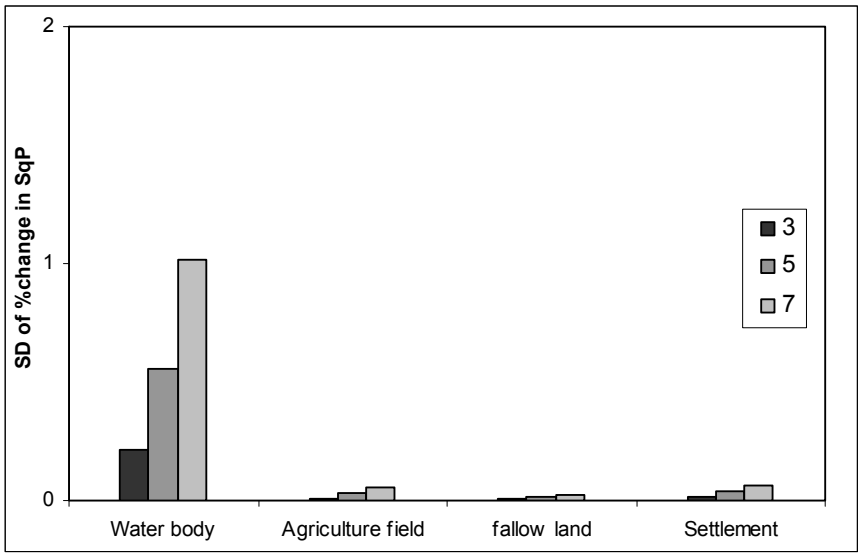

Figure 5.13 Variability in SqP of each class due to different RRB realizations at aggregation levels 3, 5, 7

RRB preserves the class proportions through aggregation levels (Figure 5.2b). SD of change in class proportions showed that there was not much distortion in proportions due to different realizations of RRB except least common class proportion (water). That may be ignored due to its very less percentage in base image. RRB decreases the clumpiness of spatial pattern of each class (Figure 5.3b) through aggregation level. SD of change in AI showed that this decrease was not considerably varied at any aggregation level due to different realizations. Only clumpiness of least common class (water) was distorted much. Shape complexity of classes also decreases due to RRB aggregation (Figure 5.4b). The variation in shape complexity was not found at any aggregation level due to different realizations. Least common class did not show also significant variation and it was less than 1%. According to the results, it can be inferred that RRB behaves similarly for each realization.

PDW

Aggregated image generated by PDW depends on the choice of *n*, *r*, *w* and random number seed. The choice of *n* and *r* was kept fixed at each aggregation level (described in section 4.4.1.3). But different realization can be still achieved by changing the choice of *w* and random number seed. First, the effect of different choices of *w* (0, 1 or 2) on indicators such as class proportion, AI and SqP was assessed by keeping the random number seed fixed (-17161817). Then the 100 random number seed were used to generate 100 realizations at each aggregation level for each choice of *w*. In this way, total 900 realizations were generated. For each realization, the percent change in each indicator with respect to that present in base image was estimated, whose SD was computed to report the variability in realizations due to different random number seed and *w*.

PDW maintains the class proportions through aggregation levels, but decreases the value of AI and SqP. For w = 1 and random number seed = -17161817, the result has been shown in Figure 5.2c, 5.3c and 5.4c. When random number seed was kept fixed, different choice of *w* did not affected the proportions at particular level of aggregation. The amount of decrease in AI and SqP, that was observed for *w* = 1 at particular aggregation level, was also not affected by another choices of *w*. Only small deviation in the case of water was observed. Figure 5.14 shows one of the indicators, AI value of each class, at each aggregation level for different choices of *w*, which shows no effect of *w* on AI. For w = 0, water class showed slow decrease in its AI value at aggregation level 3.

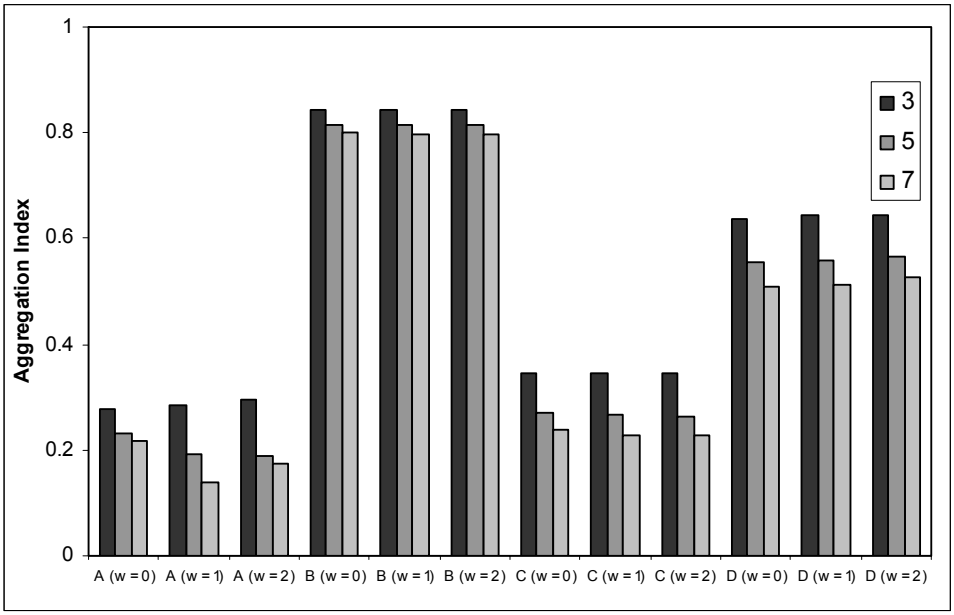

Figure 5.14 Aggregation Index of each class at aggregation level 3, 5 and 7 for choices of w, 0, 1 & 2

Figure 5.15 shows the SD of percent change in class proportions for each 100 realizations. For $w = 0$, the change in all class proportions exhibited similar variation, that was observed in the case of RRB (Figure 5.11). SD increased for all classes with increasing level of aggregation, but decreased with increasing value of w (from 0 to 2) for each aggregation level. Change in water proportion here also showed highest variation among all classes that was least for agriculture proportion. The strong decrease in SD was observed for $w = 2$ for all classes at all aggregation levels. At aggregation level 7, the SD of change in water proportion was 12% for $w = 0$, which decreased to 2% for $w = 2$. The variation in fallow and settlement class was also decreased from 1.7% and 1.5% ($w = 0$) to 0.3% and 0.2% ($w = 2$) at aggregation level 7. For $w = 2$, almost no variation was observed for all classes except water, for which variation was also very small.

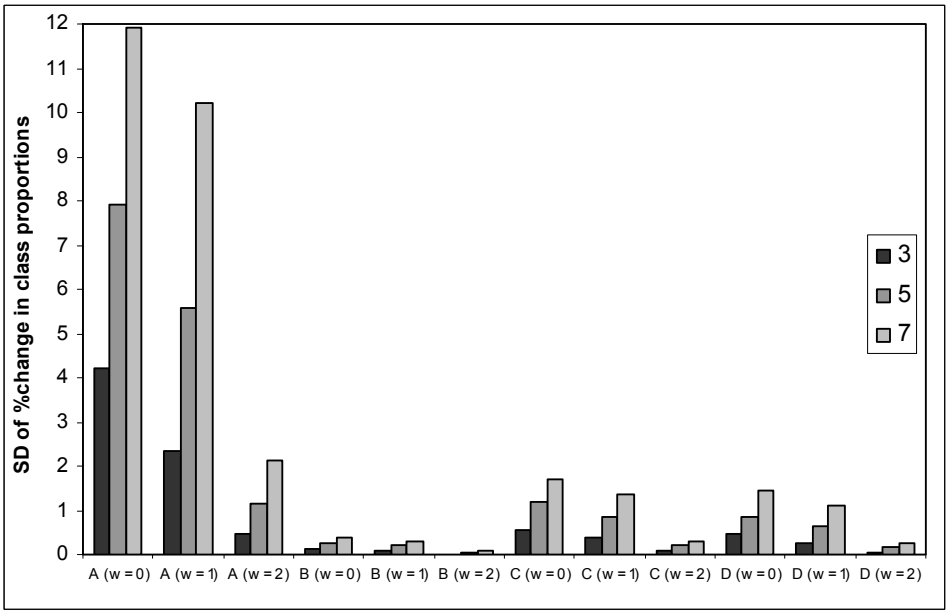

Figure 5.15 Variability in each class proportion due to different PDW realizations at aggregation levels 3, 5 & 7

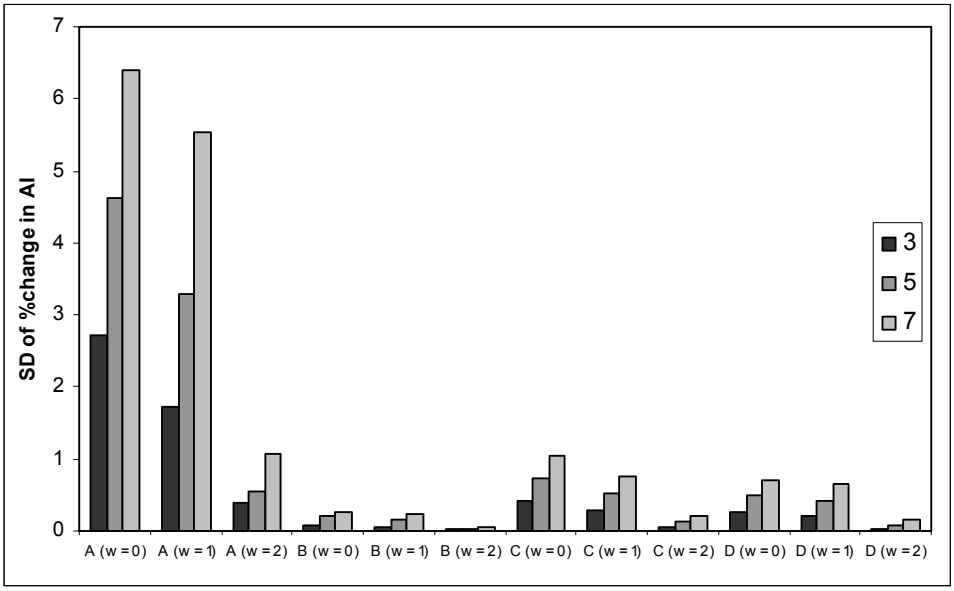

Figure 5.16 Variability in AI of each class due to different PDW realizations at aggregation levels 3, 5 & 7

Figure 5.16 shows the SD of percent change in AI of each class for each 100 realizations. For $w = 0$, the change in AI exhibited similar variation, that was observed in the case of RRB (Figure 5.12) and less than 1% variation was shown by agriculture, fallow and settlement class. SD decreased for all classes with increasing value of w from 0 to 2 at each aggregation level. But strong decrease was observed for $w = 2$. Less than 1% variation in agriculture, fallow and settlement class is itself not a significant variation and increase in the value of w made it negligible. At aggregation level 7, SD for water class decreased from 6.3% (w = 0) to 1% (w = 2), i.e. no significant variation in AI of water class for w = 2 was observed.

SD of percent change in SqP of each class, for each 100 realizations has been shown in Figure 5.17. For $w = 0$, resemblance with RRB was again observed. Agriculture, fallow land and settlement class exhibited lass than 0.05% variation for $w = 0$, which was further decreased by increasing value of w. It showed that no variation in change of SqP value was observed for all choices of w at each aggregation level.

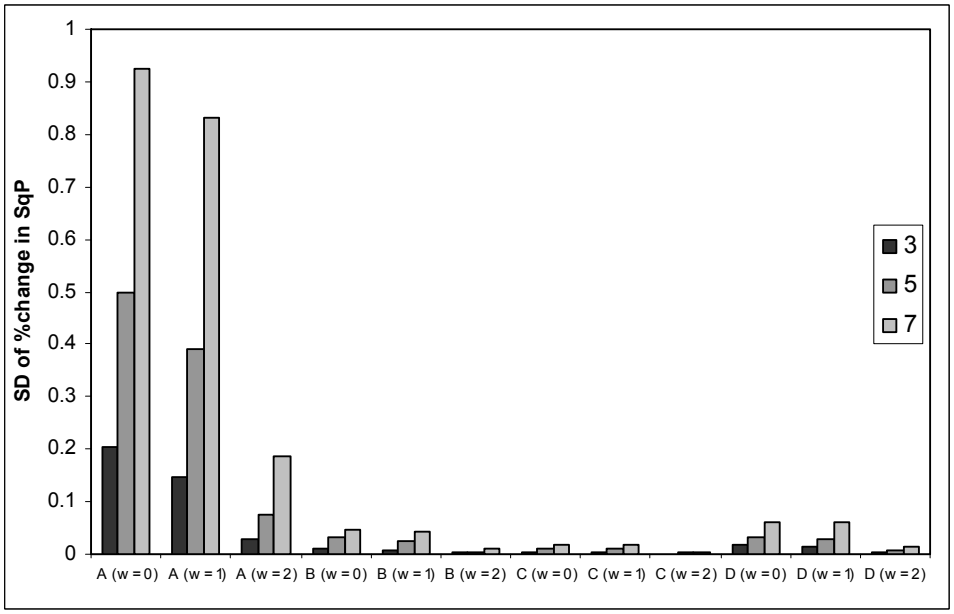

Figure 5.17 Variability in SqP of each class due to different PDW realizations at aggregation level 3, 5 & 7

Water class also showed variation less than 1% for w = 0 at aggregation level 7, that decreased to 0.18% for *w* = 2. It showed that no significant variation in change of SqP value of water was also observed for any value of *w* at all aggregation level.

The change in the value of *w*, for fixed random number seed, did not affect the value of indicators such as proportions, AI and SqP of classes, which was obtained at different aggregation level. But variations in their values were observed for each *w* due to the use of different random number seed. Variations was maximum for *w* = 0 and least for *w* = 2 for all classes. Except least common class (water), the maximum variation of other class proportions for w = 0 was not large (less than 2%). But for *w* = 2, all classes showed small variation in their proportions. Change in AI and SqP of dominant and moderately common class (agriculture, fallow and settlement) were also not significantly varied for all value of *w*. Variation in AI of least common class was also not significant for *w* = 2. These results showed that the variation due to the use of different random number seed can be best minimized by choosing *w* = 2.

5.4. Summary of results

The results presented here can be summarized as following points.

1. Random rule-based (RRB), Point centered distance weighted moving window method (PDW) and Central Pixel Resampling (CPR) approach preserved the class proportion with decreasing spatial resolution. Majority rule-based (MRB) increased the proportion of dominant class (agriculture) and decreased the proportions of other classes. Mean approach also increased the proportion of one class (fallow), but it was not a dominant class. The proportion of other classes was decreased by mean approach. The results of MRB, RRB, PDW and mean approach were consistence with the results found elsewhere (Moody *et al.* 1995, He *et al.* 2002, Gupta *et al.* 2000, Gardner *et al.* 2008)

2. MRB approach increased the Aggregation Index (AI) of dominant class and decreased AI of other classes. RRB, PDW and CPR decreased AI of all classes in almost similar manner. Mean approach also decreased the AI values of all classes through the aggregation level, but the slope of decrease was less for all classes as compared to other aggregation approaches. The results of RRB and MRB approach found here were also observed in the study of He *et al.* 2002.

3. All aggregation approaches decreased SqP value of each class through aggregation levels. It showed that the shape complexity of each class was reduced by each aggregation approach. RRB, PDW and CPR approach behaved similarly for SqP value of each class, but produced less distortion in shape complexity as compared to MRB and mean approach. The decrease in shape complexity due to MRB aggregation was also reported by Frohn *et al.* (2006).

4. MRB approach performed better than mean approach in deriving the calibration based model (slope estimator method) for area correction. The reduction in total error was observed using MRB approach and this reduction increased with increasing level of aggregation. It was not in the case of mean approach, where significant decrease in total error was not observed at any aggregation level. Response of MRB approach to the total error was also reported by Moody *et al.* (1996).

5. Mean approach increased the local variance of each class at aggregation level 3 and decreased with further increase in aggregation levels. The CPR approach produced strong increase in local variance of each class. At aggregation level 3, the increase in local variance was higher using CPR approach as compared to mean approach. Response of mean approach to the trend of local variance curve of settlement and agriculture class was also reported by Woodcock and Strahler (1987).

6. RRB approach did not produced significant change in class proportions, AI and SqP value for its different realizations. RRB approach behaved similarly for all classes in each realization except water class, whose occurrence was low in image (0.3%).

7. For PDW approach, different choice of weight '*w*' parameter did not affect the class proportions, AI and SqP value at fixed random number seed. But the use of different random number seed produced the variation in class proportions, AI and SqP value of each class for each choice of *w*. These variations were highest for $w = 0$ and least for $w = 2$. It showed that effect of different random number seeds were best minimized using $w = 2$. Resemblance between PDW and RRB approach was observed for $w = 0$.

6. Conclusions & Recommendations

Spatial resolution of satellite images can be made coarse using variety of aggregation approaches. Some aggregation approaches (categorical aggregation) like majority rule-based (MRB), random rule-based (RRB) and point centered distance weighted moving window method (PDW), have been applied on classified image. Some aggregation approaches (numerical aggregation) like mean and central pixel resampling (CPR), are applied directly on continuous images. The work attempted here was to analyze the effect of both categorical and numerical aggregation approaches in depth. The 23.5m LISS-III image (base image) was taken as base image using and aggregation approaches were applied to get coarse resolution images at aggregation level 3 (70.5m), 5 (117.5m) and 7 (164.5m). Four land use/cover classes were defined from base image namely agriculture (dominant class, 72%), fallow land and settlement (moderately common class, 16% &12%) and water (least common class, 0.3%). Most of the previous studies to assess the effect of aggregation were carried out by taking land-cover classes. Moody *et al.* (1995), in their study, had used land-cover classes namely barren, brush, hard-wood, conifer and water. He *et al.* (2002), in their study, had taken land-cover classes such as maple, mixed deciduous and coniferous forest, water and oak. The study area used in this present work was mainly comprised of land-use classes and the effect of different aggregation approaches were found consistent with the results reported in previous studies. It shows that the similar effect is produced by different aggregation approaches over wide variety of classes in landscape.

To meet the objective of present study, aggregation effect was examined for each land use/cover class and the following questions were answered.

As a function of resolution and aggregation approaches and aggregation levels, what changes are observed in land use/cover proportions?

It was found that MRB approach increased the proportion of dominant classes with decreasing spatial resolution of base image and its proportion increased by 13% up to aggregation level 7. Proportions of moderately and least common class decreased, but the rate of decrease of fallow class proportion was greater than settlement class proportion due to its dispersed pattern in landscape. In general, MRB filters out the minor classes from landscape and reveals the general pattern of broad classes, for example, it may be helpful in delineation of dominant agriculture class distributions by filtering out small patches of other classes such as settlement and fallow class. It can be used in regional as well as national level agriculture land monitoring and management, where conceptualization of broad agriculture distribution is required. MRB may also be useful in other studies such as forest monitoring at regional or national level by delineation of broad forest cover distribution. It is important to note that both RRB and PDW approach preserved each class proportions at all aggregation levels. It was seen from the analysis that the PDW approach preserved the class proportions precisely than RRB approach. PDW approach showed the increase or decrease in all class proportions except least common class (water class in this case) by 0.3%, which was found little greater (0.5%) for RRB approach. CPR approach also preserved the class proportions, but it showed more distortion in class proportions than RRB and PDW approach. This was again not greater than 8% for moderately common classes and was less than 1% for dominant class. RRB approach is based on random selection and thus it may produce somewhat different realizations each time it is used to aggregate image, which will not be produced by CPR. Therefore, CPR can be better substitute for RRB approach. The information acquired by remote sensor incorporates the additional degree of spatial correlation between pixels. As important aspect of

PDW approach is that the output generated by PDW depends on different parameters, which can be used to incorporate the spatial correlation between pixels (Gardner *et al.* 2008). For this reason, the aggregation by PDW may produce resemblance with the image acquired by actual remote sensors. Therefore PDW can be best substitute for RRB and CPR approach even though the effect of these three approaches was found similar. In this present work, spatial correlation was not incorporated in aggregation process using PDW approach. Only the attempt has been made to assess the effect of PDW on aggregation of fine resolution image. All these three approaches can preserve the class proportions and therefore can be used in the studies such as ecological resource management where the accuracy of land cover proportions at coarse resolution is required. Mean approach is not suitable for such studies as it distorted each class proportion. Mean approach increased the proportions of one class (fallow class, i.e. not dominant) and this resulted in decrease in other class proportions through all aggregation levels. As the proportion of dominant class (agriculture) was decreased and mean approach also resulted into less clumped pattern of dominant class (mentioned in next question), therefore this approach is not suitable to delineate the broad cover type distribution.

How do the spatial properties of land use/covers change using different aggregation approaches through aggregation levels?

Aggregation Index (AI, quantify clumpiness of spatial pattern of class) and Square Pixel Index (SqP, quantify the shape complexity of class) was used to assess the spatial properties of each class at all aggregation levels and base image as well. AI of dominant class increased whereas moderately and least common classes decreased due to MRB aggregation approach through all aggregation levels. It showed that MRB made the dominant class more aggregated or clumped and thus again shows its suitability for delineation of broad cover type distribution. RRB, PDW and CPR approach behaved near similarly for AI and decreased the AI value of each class through all aggregation levels. It was due to the reason that random selection logic of RRB and PDW approach and central pixel selection logic of CPR approach resulted in less clumped pattern of each class through all aggregation levels. Mean approach decreased more slowly the AI value of each class through aggregation levels as compared to RRB, PDW and CPR approach and thus exhibited more stability in aggregated pattern of each class. SqP Index was decreased by each aggregation approach. It reflected that all aggregation approaches generalized the shape complexity of each class. But RRB, PDW and CPR approach produced low distortion in shape complexity and thus carried the spatial information regarding shape complexity more than MRB and mean approach.

What variations are found in statistical property of continuous aggregated images through aggregation levels?

Local variance of each class was computed to assess the statistical property of images at class specific level. It was found that mean approach first increased the local variance of each class at aggregation level 3 and then decrease in local variance was observed. Woodcock and Strahler (1987) explained that the peak in local variance curve is related to size of the objects in the scene and it occurs when the size of the object becomes nearly equal to the pixel size. As the resolution increases, the mix up of objects in a single cell occurs. This increases the likelihood of a pixel with its neighbouring pixels and results in decrease of local variance. In the original coarse resolution, decrease in local variance may also be expected due to decrease in heterogeneity in terms of reflectance value. Pattern in local variance curve of each class using mean approach exhibited such phenomena. On the contrary, CPR approach produced strong increase in local variance of each class through aggregation levels. It was due to the complete ignorance of neighbours of central pixels, which is not expected even at original

coarse resolution image. At aggregation level 3 also, the increase in local variance by CPR approach was much higher than mean approach. For these, mean approach responded well for local variance of each class at different aggregation levels.

What is the impact of different aggregation approaches in deriving calibration based model for area correction?

As the distortion in class proportion was observed for MRB and mean aggregation approach and therefore calibration based model for area correction was applied for these approaches only. For mean approach, difference in the total error curve of uncorrected proportions (TEu) and proportions modified by model (TEs) increased with increasing levels of aggregation. At aggregation level 3, TEu and TEs was found 7% and 5%, which became 19% and 11% at aggregation level 7. For CPR approach, there was no significant difference in TEu and TEs up to aggregation level 5. It was again only 2% at aggregation level 7. For these reasons, MRB performed well in the derivation of calibration based model.

Is it possible to optimize the PDW parameters?

Output of PDW depends on the choices of parameters n, r, w and random number seed. The choices of n and r have been kept fixed according to the aggregation levels to ensure that sampling points should not lie outside the window size (3×3, 5×5 and 7×7). For even window size, it is difficult to choose the value of n and r. In these cases, sampling points will certainly lie outside the window size and analysis of output aggregated classified image will not be the representative of measurement scale that is being considered.

Keeping n, r and random number seed fixed at all aggregation levels, analysis was performed for different choices of w. It was found that different choice of w did not affect the values of class proportions, AI and SqP. Different random number seed and choice of w were used to obtain different realizations of PDW at each aggregation levels. The results of standard deviation of percent change in class proportions, AI and SqP showed that random number seed produced variations for each choice of w and these variation were best minimized for $w = 2$ (inverse square distance weighting) at each aggregation level. The selection of one random number seed is again problematic and difficult to achieve and optimize. For this reason, it is difficult to optimize the PDW parameters.

What variability is found in different realization of random rule aggregation approach on classified map?

100 realizations of RRB approach were obtained at each aggregation levels. Maximum standard deviation of percent change in class proportions was found around 2% except water class, for which it was maximum of 13%. Variation in AI and SqP values was found small (less than 1%) for each class. For AI, only water class exhibited a maximum variation of 7%. It can be concluded that different realizations of RRB did not affect significantly the class proportions and spatial properties of classes. Large variation for water class was due to its low occurrence (0.3%) in landscape.

Recommendations:

1. In the present study, landscape metric (AI and SqP) at class level were considered to assess the effect of different aggregation approaches. Assessment of metrics at patch level as well as at landscape level may also be considered in order to improve the understanding of aggregation approaches and their effects.
2. Landscape metric also depend on the extent of landscape and the level of classification of landscape. These factors may also be considered to assess the effect of aggregation of satellite images.
3. Although different realizations of RRB did not affect the class proportions and spatial properties of classes, different realization tends to change the spatial patterning of aggregated images. Thus an optimization technique for random selection of class is required to stabilize the output of RRB.
4. Information of spatial correlation of pixels in landscape can be useful to select the PDW parameter. But the selection of random number seed is problematic and requires further attentions.
5. The development of models to correct the landscape metrics values (AI and SqP), distorted due to aggregation effect, can be useful to get the idea about the spatial properties of fine resolution image using coarse resolution image.

7. References

Bezdek, J.C.; Ehrlich, R.; & Full, W.(1984). FCM: the fuzzy *c*-means clustering algorithm: *Computers & Geosciences*: **10**(2-3): 191-203

Bierkens, M.P.; Finke P.A.; & Willigen P.D. (2000). *Upscaling and Downscaling Methods for Environmental Research*: Kluwer Academic Publishers, The Netherlands: 1-27

Bian, L.; & Butler, R. (1999). Comparing effects of aggregation methods on statistical and spatial properties of simulated spatial data: *Photogrammetric Engineering & remote Sensing*: **65**(1): 73-84

Bian, L. (1997). Multiscale nature of spatial data in scaling up environmental models: In: D.A. Quattrochi and M.F. Goodchild, Editors, Scale in Remote Sensing and GIS, Lewis Publishers, Boca Raton (1997): 13–26

Bogaert, J.; Myneni, R.b.; & Knyazikhin, Y. (2002). A mathematical comment on the formulae for the aggregation index and shape index: *Landscape Ecology*: **17**: 87-90

Congalton, R.G. (1991). A review of assessing the accuracy of classification of remotely sensed data: *Remote Sensing of Environment*: **37**: 35-47

Cullinan, V.I.; & Thomas, J.M. (1992). A comparison of quantitative methods for examining landscape pattern and scale: *Landscape Ecology*: **7**(3): 211-227

Dungan, J.L.; Perry, J.N.; Dale, M.R.T.; Legendre, P.; Citron-Pousty, S.; Fortin, M.J.; Jakomulska, A.; Miriti, M.; & Rosenberg, M.S. (2002). A balance view of scale in spatial statistical analysis: *Ecography*: **25**: 626-640

Frohn, R.C. (1998). *Remote Sensing for Landscape Ecology*: Lewis publishers, Boca Raton: 1-47

Frohn, R.C.; & Hao, Y. (2006). Landscape metric performance in analysing two decades of deforestation in Amazon Basin of Rondomia, Brazil: *Remote Sensing of Environment*: **100**: 237-251

Foody, G.M. (1996). Approaches for the production and evaluation of fuzzy land cover classifications from remotely-sensed data: *International Journal of Remote Sensing*: **17**(7): 1317–1340

Foody, G.M. (2002). Status of land cover classification accuracy assessment: *Remote Sensing of Environment*: **80**: 185– 201

Gopal, S.; & Woodcock, C. (1994). Theory and methods for accuracy assessment of thematic maps using fuzzy sets: *Photogrammetric Engineering and Remote Sensing*: **60**(2): 181–188

Gupta, R.K.; Prasad, T.S.; Rao, P.V.K.; & Manikavelu, P.M.B. (2000). Problems in upscaling of high resolution remote sensing data to coarse spatial resolution over land surface: *Advances in Space Research*: **26**(7):1111-1121

Gupta, R.K.; Prasad, T.S.; & Vijayan, D. (2002). Upscaling aspects of multi-resolution satellite data in spatial and frequency domains: *Advances in Space Research.*: **29**(1): 57-61

Gardner, R.H.; Lookingbill, T.R.; Townsend, P.A.; & Ferrari, J. (2008). A new approach for rescaling land cover data: *Landscape Ecology*: **23**: 513-526

Gardner, R.H. (2007). PDW documentation: www.al.umces.edu/PDW.htm

He, H.S.; DeZonia B.E.; & Mladenoff D.J. (2000). An aggregation index (AI) to quantify spatial patterns of landscapes: *Landscape Ecology*: **15** : 591-601

He, H.S.; Ventura, S.J.; & Mladenoff, D.J. (2002). Effects of spatial aggregation approaches on classified satellite imagery: *International Journal of Geographical Information Science*: **16**(1): 93-109

Kumar, A.K.; Ghosh, S.K.; & Dadhwal, V.K. (2007). Full fuzzy land cover mapping using remote sensing data based on fuzzy c-means and density estimation: *Canadian Journal of Remote Sensing*: **33(**2**)**: 81-87

Leibowitz, S.G.; & Hyman, J. B. (1999). Use of scale invariance in evaluating judgment indicators: *Environmental Monitoring and Assessment*: **58**: 283–303

Lucieer, A. (2003). PARBAT version 0.24: http:// parbat.lucieer.net

Lucieer, A. (2004). *Uncertainties in Segmentation and their Visualization*: PhD thesis: University of Utrecht and ITC, The Netherlands

Li, H.; & Wu, J. (2004). Use and misuse of landscape indices: *Landscape Ecology*: 19: 389-399

Longley P.A.; Goodchild, M.F.; Maguire, D.J.; & Rhind D.W. (2005). *Geographical Information System and Science*: John Wiley & Sons, England: 128-153

Marceau, D.J.; & Hay, G.J. (1999). Remote sensing contributions to the scale issue: *Canadian Journal of Remote Sensing*: **25(**4**)**: 357-366

Moody, A.; & Woodcock, C.E. (1994). Scale-dependent errors in the estimation of land-cover proportions-implications for global land-cover dataset: *Photogrammetric Engineering & Remote Sensing*: **60**(5): 585-594

Moody, A.; & Woodcock, C.E. (1995). The influence of scale and the spatial characteristics of landscapes on land-cover mapping using remote sensing: *Landscape Ecology*: **10**(6): 363-379

Moody, A.; & Woodcock, C.E. (1996). Calibration-based models for correction of area estimates derived from coarse resolution land-cover data: *Remote Sensing of Environment*: **58**: 225-241

Moody, A. (1998). Using landscape spatial relationships to improve estimates of land-cover area from coarse resolution remote sensing: *Remote Sensing of Environment*: **64**: 202-220

McGarigal, K.; Cushman, S. A.; Neel, M. C.; & Ene, E. (2002)**.** FRAGSTATS: Spatial Pattern Analysis Program for Categorical Maps. Computer software program produced by the authors at the University of Massachusetts, Amherst. Available at the following web site: www.umass.edu/landeco/research/fragstats/fragstats.html

O'Neill, R.V.; Krumme, J.R.; Gardner, R.H.; Sugihara, G.; Jackson, B.; DeAngelist, D.L.; Milne, B.T.; Turner, M.G.; Zygmunt, B.; Christensen, S.W.; Dal, V.H.; & Graham, R.L. (1988). Indices in landscape pattern: *Landscape Ecology*: **1**(3): 153-162

Quattrochi, D.A.; & Goodchild, M.F. (1997). *Scale in Remote Sensing and GIS*: Lewis publishers, Boca Raton: 1-72

Rastetter, E.B.; King, A.W.; Cosby, B.J.; Hornberger, G.M.; & O'Neill, R.V. (1992). Aggregating fine-scale ecological knowledge to model coarser-scale attributes of ecosystems: *Ecological Applications*: **2**: 55–70

Riitters, K.H.; O'Neil1, R.V.; Hunsaker, C.T.; Wickham, J.D.; Yankee, D.H.; Timmins, S.P.; Jones, K.B.; & Jackson, B.L. (1995). A factor analysis of landscape pattern and structure metrics: *Landscape Ecology*: **10**(1): 23-39

Stein, A.; Riley, J.; & Halberg, N. (2001). Issues of scale for environmental indicators: *Agriculture, Ecosystem and Environment*: **87**: 215-232

Saura, S. (2004). Effects of remote sensor spatial resolution and data aggregation on selected fragmentation indices: *Landscape Ecology*: **19**: 197-209

Tso, B.; & Mather, P.M. (2001). *Classification Methods for Remotely Sensed Data*: Taylor & Francis, London

Turner, M.G.; O'Neill, R.V.; Gardner, R.H.; & Milne, B.T. (1989). Effect of changing spatial scale on the analysis of landscape pattern: *Landscape Ecology*: **3**(3/4): 153-162

Wickham, J.D.; & Ritters, K.H. (1995). Sensitivity of landscape metrics to pixel size: *International Journal of Remote Sensing*: 16(18): 3585-3594

Woodcock, C.E.; & Strahler, A.H. (1987). The factor of scale in remote sensing: *Remote Sensing of Environment*: 21: 311-332

Wu, J. (2004). Effect of changing scale on landscape pattern analysis: scaling relations: *Landscape Ecology*: **19**: 125-138

Wu, J.; Shen, W.; Sun, W.; & Tueller, P.T. (2002). Empirical patterns of the effects of changing scale on landscape metrics: *Landscape Ecology*: **17**: 761-782

Appendix 1

Class proportions observed for each aggregation approach at each aggregation level

		Water	Agriculture	Fallow land	Settlement
Reference image →		0.0031	0.7189	0.1556	0.1223
MRB	3	0.0027	0.7534	0.1247	0.1192
	5	0.0021	0.7873	0.0968	0.1137
	7	0.0018	0.8154	0.0732	0.1096
RRB	3	0.0031	0.7191	0.1560	0.1218
	5	0.0032	0.7192	0.1524	0.1251
	7	0.0034	0.7189	0.1563	0.1214
PDW	3	0.0030	0.7190	0.1559	0.1222
	5	0.0034	0.7179	0.1560	0.1227
	7	0.0027	0.7181	0.1552	0.1240
Mean	3	0.0022	0.6980	0.1894	0.1103
	5	0.0023	0.6845	0.2205	0.0927
	7	0.0024	0.6705	0.2431	0.0840
CPR`	3	0.0031	0.7143	0.1665	0.1160
	5	0.0033	0.7164	0.1650	0.1153
	7	0.0036	0.7133	0.1681	0.1149

Aggregation Index of each class for each aggregation approach at each aggregation level

		Water	Agriculture	Fallow land	Settlement
Reference image →		0.62	0.921	0.611	0.814
MRB	3	0.398	0.884	0.402	0.697
	5	0.325	0.889	0.31	0.664
	7	0.267	0.903	0.273	0.646
RRB	3	0.312	0.845	0.346	0.637
	5	0.16	0.817	0.26	0.567
	7	0.14	0.801	0.236	0.522
PDW	3	0.286	0.845	0.346	0.643
	5	0.194	0.813	0.265	0.558
	7	0.139	0.796	0.227	0.512
Mean	3	0.403	0.859	0.469	0.715
	5	0.31	0.835	0.449	0.686
	7	0.286	0.821	0.457	0.684
CPR`	3	0.307	0.843	0.358	0.644
	5	0.197	0.813	0.274	0.571
	7	0.16	0.792	0.244	0.535

Square Pixel index of each class for each aggregation approach at each aggregation level

		Water	Agriculture	Fallow land	Settlement
Reference image →		0.9488	0.9834	0.9927	0.9829
MRB	3	0.8969	0.9675	0.9841	0.9684
	5	0.8295	0.9451	0.9738	0.9517
	7	0.7595	0.9164	0.9602	0.9353
RRB	3	0.9147	0.9748	0.9870	0.9737
	5	0.8838	0.9646	0.9805	0.9638
	7	0.8453	0.9548	0.9739	0.9536
PDW	3	0.9154	0.9749	0.9869	0.9733
	5	0.8823	0.9652	0.9806	0.9642
	7	0.8274	0.9557	0.9742	0.9550
Mean	3	0.8855	0.9720	0.9855	0.9651
	5	0.8384	0.9598	0.9783	0.9431
	7	0.7874	0.9483	0.9708	0.9185
CPR`	3	0.9144	0.9751	0.9871	0.9726
	5	0.8798	0.9652	0.9809	0.9620
	7	0.8477	0.9564	0.9746	0.9510

Slope estimator assessment of class proportions for majority rule-based and mean aggregation approach at each aggregation level

			Agriculture	Fallow land	Settlement
Reference image →			0.7189	0.1556	0.1223
MRB	3	Uc	0.7534	0.1247	0.1192
		SE	0.7242	0.1319	0.1267
	5	Uc	0.7873	0.0968	0.1137
		SE	0.7283	0.1137	0.1287
	7	Uc	0.8154	0.0732	0.1096
		SE	0.7320	0.0993	0.1304
Mean	3	Uc	0.6980	0.1894	0.1103
		SE	0.7137	0.1873	0.1054
	5	Uc	0.6845	0.2205	0.0927
		SE	0.7096	0.2188	0.0837
	7	Uc	0.6705	0.2431	0.0840
		SE	0.7254	0.2616	0.0891

Uc → Uncorrected (before applying slope estimator)

SE → Slope estimator assessment

Total error (TE) before and after applying slope estimator method

		TE (%) Uc	TE (%) SE
MRB	3	6.90	4.73
	5	13.68	8.40
	7	19.30	11.27
Mean	3	6.77	6.35
	5	12.98	12.63
	7	17.50	14.81

Local variance of each class for mean and CPR approach at each aggregation level

		Agriculture	Fallow land	Settlement
Reference image →		51.77	100.13	50.01
Mean	3	60.69	110.46	63.27
	5	52.23	79.55	62.43
	7	45.45	66.25	57.56
CPR	3	110.48	173.10	111.01
	5	132.80	185.59	140.21
	7	145.99	189.24	160.36

Standard deviation of percent change in class proportions, Aggregation Index and Square Pixel Index

RRB realizations

		Water	Agriculture	Fallow land	Settlement
Class proportions	3	4.54	0.13	0.54	0.49
	5	7.78	0.27	1.12	0.80
	7	12.65	0.36	1.66	1.49
Aggregation Index	3	2.65	0.08	0.42	0.26
	5	4.23	0.21	0.89	0.55
	7	6.95	0.31	1.00	0.92
Square Pixel Index	3	0.22	0.01	0.00	0.02
	5	0.55	0.03	0.01	0.04
	7	1.02	0.06	0.02	0.06

PDW realizations using 100 random number seeds

Class proportions				
	Weight	Aggregation level		
		3	5	7
Water	0	4.22	7.90	11.91
	1	2.35	5.58	10.21
	2	0.49	1.15	2.14
Agriculture	0	0.12	0.25	0.37
	1	0.08	0.19	0.31
	2	0.02	0.04	0.06
Fallow land	0	0.54	1.19	1.68
	1	0.37	0.87	1.37
	2	0.08	0.20	0.28
Settlement	0	0.46	0.85	1.45
	1	0.27	0.64	1.10
	2	0.05	0.15	0.25

Aggregation Index				
	Weight	Aggregation level		
		3	5	7
Water	0	2.71	4.63	6.40
	1	1.72	3.30	5.55
	2	0.38	0.54	1.08
Agriculture	0	0.08	0.20	0.26
	1	0.06	0.15	0.24
	2	0.01	0.03	0.06
Fallow land	0	0.42	0.72	1.03
	1	0.29	0.52	0.77
	2	0.06	0.13	0.21
Settlement	0	0.25	0.51	0.70
	1	0.20	0.41	0.66
	2	0.04	0.08	0.15

Square Pixel Index				
	Weight	Aggregation level		
		3	5	7
Water	0	0.205	0.496	0.924
	1	0.147	0.389	0.833
	2	0.030	0.076	0.185
Agriculture	0	0.011	0.031	0.046
	1	0.008	0.023	0.042
	2	0.002	0.005	0.010
Fallow land	0	0.005	0.012	0.019
	1	0.003	0.010	0.019
	2	0.001	0.002	0.005
Settlement	0	0.016	0.034	0.062
	1	0.013	0.029	0.061
	2	0.003	0.007	0.014

Appendix 2

Code of majority rule-based aggregation approach

```
################################################
#    import ASCII file of classified image
################################################
Path <- 'D:\\MRB\\'
Inputfile <- paste(Path, 'classified','.txt', sep='')
temp <- read.table(Inputfile, skip = 5)
d <- dim(temp)
nri <- d[1]
nci <- d[2]
img <- array(0, c(nri,nci))
img[,] <- as.matrix(temp)

#####################################################################
##### setting window size and number of class
#####################################################################
nc <- 4
ws <- 3

#####################################################################
## Number of row and number of column of ouput aggregated image
#####################################################################
nro <- trunc(nri/ws)
nco <- trunc(nci/ws)

#############################################################################################
# initialization of vector that contain the frequency of each class in a specified block
#############################################################################################
frq <- array(0,nc)

#############################################################################################
### Initialization of vector that holds the output of each block after processing
#############################################################################################
out <- array(0,(nro*nco))

################################################
### initialization of some variables
################################################
mcl <- array(0,nc)
r1 <- 0
r2 <- 0
c1 <- 0
```

```
c2 <- 0
x1 <- 0
x2 <- 0
tmp <- 0

##############################################################################################
### ‘sr’ stores sequence along vertical direction.          'sc' stores sequence along horizontal direction.
##############################################################################################
for(i in 1:nro)
{
 r2 <- r2+ws
 r1 <- r2-(ws-1)
  sr <- seq(from = r1,to = r2,by = 1)
   for(j in 1:nco)
     {
     c2 <- c2+ws
     c1 <- c2-(ws-1)
     sc <- seq(from = c1,to = c2,by = 1)

        for(k in sr)
          {
          for(l in sc)
            {
             tmp <- img[k,l]
              frq[tmp] <- frq[tmp]+1
            }
          }

          maxfr <- max(frq)
          for(m in 1:nc)
            {
             if(frq[m] == maxfr)
               {
                 clb <- m
               }
            }
             mcl[1] <- clb
             x1 <- 2
             cond <- 0
            for(n in 1:nc)
              {
                if(maxfr == frq[n] &&  n != clb)
                 {
                 mcl[x1] <- n
                 x1 <- x1+1
                 cond <- 1
                 }
              }
```

```
            if(cond == 1)
            {
             rn <- round(runif(1,min = 1, max = (x1-1)))
             clb <- mcl[rn]
            }
           frq <- array(0,nc)
           mcl <- array(0,nc)

           x2 <- x2+1
           out[x2] <- clb
      }
       c1 <- 0
       c2 <- 0
}

#############################################################################################
#### converting vector that contains majority class of each block to matrix
#############################################################################################
z1 <- 0
z2 <- 0
z3 <- 0
agg <- array(0,c(nro,nco))
for(m in 1:nro)
 {
  z1 <- z1+1
     for(n in 1:nco)
       {
       z2 <- z2+1
       z3 <- z3+1
       agg[z1,z2] <- out[z3]
       }
       z2 <- 0
 }

#########################################################################
### writing output aggregated matrix to text file
#########################################################################

 write.table(agg[,], file = paste(Path,'output','.txt',sep=''),append=FALSE,quote=TRUE,sep ="
",eol="\n",na="NA",dec=".",row.names=FALSE,col.names=FALSE,qmethod=c("escape","double"))
```

Code of random rule-based aggregation approach

```
################################################
#    import ASCII file of classified image
################################################
Path <- 'D:\\RRB\\'
Inputfile <- paste(Path, 'classified','.txt', sep='')
temp <- read.table(Inputfile, skip = 5)
d <- dim(temp)
nri <- d[1]
nci <- d[2]
img <- array(0, c(nri,nci))
img[,] <- as.matrix(temp)

#####################################################
### setting block size (it can be odd or even)
#####################################################
ws <- 3

#####################################################################
## number of row and number of column of ouput aggregated image
#####################################################################
nro <- trunc(nri/ws)
nco <- trunc(nci/ws)

#############################################################################################
## initialization of vector that holds the matrix elements of one block (ex when ws = 3 then block size
## is 3*3, so it holds 9 matrix elements that fall within block
#############################################################################################
g <- array(0,(ws*ws))

#############################################################################################
### initialization of vector that holds the randomly selected elements of each block
#############################################################################################
a <- array(0,(nro*nco))

################################################
### initialization of some variables
################################################
r1 <- 0
r2 <- 0
c1 <- 0
c2 <- 0
x1 <- 0
x2 <- 0
```

```
##############################################################################################
#### 'sr' stores sequence along vertical direction.          'sc' stores sequence along horizontal direction.
####'rp' stores randomly selected position within a block.     vector 'a' stores all randomly selected
##elements.
##############################################################################################

for(i in 1:nro)
{
 r2 <- r2+ws
 r1 <- r2-(ws-1)
 sr <- seq(from = r1,to = r2,by = 1)
  for(j in 1:nco)
    {
    c2 <- c2+ws
    c1 <- c2-(ws-1)
    sc <- seq(from = c1,to = c2,by = 1)
       for(k in sr)
         {
         for(l in sc)
           {
            x1 <- x1+1
            g[x1] <- img[k,l]
            }
          }
          x1 <- 0
          rp <- round(runif(1,min=1,max=(ws*ws)))
          x2 <- x2+1
          a[x2] <- g[rp]
     }
     c1 <- 0
     c2 <- 0
}

##############################################################################################
#### converting vector that contains randomly slected elements to matrix
##############################################################################################

z1 <- 0
z2 <- 0
z3 <- 0
agg <- array(0,c(nro,nco))
for(m in 1:nro)
 {
  z1 <- z1+1
    for(n in 1:nco)
     {
     z2 <- z2+1
     z3 <- z3+1
```

```
      agg[z1,z2] <- a[z3]
      }
      z2 <- 0
}

#####################################################################
### writing output aggregated matrix to text file
#####################################################################

 write.table(agg[,], file = paste(Path,'output','.txt',sep=''),append=FALSE,quote=TRUE,sep ="
",eol="\n",na="NA",dec=".",row.names=FALSE,col.names=FALSE,qmethod=c("escape","double"))
```

Explanation of PDW aggregation approach

The more detailed explanation of aggregation using PDW approach has been presented in this section. This explanation is based on the PDW code available on website www.al.umces.edu/PDW.htm. For simplicity, the example presented here is based on the aggregation of 6m classified image to 18m resolution.

Selection of class from input image and its assignment to output aggregated pixel in PDW is based on random selection from cumulative frequency distribution of land cover types. Cumulative frequency distribution is just the addition of frequency of given cover type with the frequency of other cover types.

As for example in PDW, it is implemented like that.

	1	2	3
1	1	**1**	2
2	**4**	**2**	**1**
3	4	**2**	4

Figure 1: 3×3 block of 6m resolution map

Let the resolution of input image = 6m. To achieve the resolution of 18m, 3*3 block will move over the image. One block has been shown in Fig 1, which contains the classes 1, 2 and 4.

Steps to assign cover type in one pixel of 18m aggregated image.

A. If number of points in the sampling net is 5, then pixels at (1, 2), (2, 1), (2, 2), (2, 3), (3, 2) are considered for processing.

B. Coordinate of each considered pixel is defined as

Pixel coordinate $[R_1 (i, j)]$	Coordinate $[R_2 (i, j)]$ set by PDW algorithm	Coordinate $[R_3 (i, j)]$ after multiplying resolution of input image (6 m)
(2, 2)	(0, 0)	(0, 0)
(2, 3)	(1, 0)	(6, 0)
(2, 1)	(-1, 0)	(-6, 0)
(1, 2)	(0, 1)	(0, 6)
(3, 2)	(0, -1)	(0, -6)

If we take resolution of sampling net *r* equal to resolution of input image, then 6 is multiplied to each coordinate. We may take any value of *r*. As for example if *r* = 12 and number of sampling points *n* is 5, then the sampling scheme will be like that as shown in Figure 2.

1	4	**1**	2	1
4	1	1	2	1
4	4	**2**	1	**2**
4	4	2	4	2
1	1	**4**	4	4

Figure 2: Sampling scheme for *r* = 12 and *n* = 5

Coordinate of central pixel is considered at origin to aggregate image using odd window size (such as 3×3, 5×5). In order to aggregate the image using even window size (such as 2×2, 4×4), the bottom right corner is considered at origin. Coordinates of other pixels are assigned accordingly.

C. Weight *w* of each pixel (that lies on sampling point) from the center is assigned according to linear or exponential decay. For this, distance of each pixel from center is calculated and **'1'** is added to each distance (just to avoid the 0 distance, which will be at centre). Inverse of distance in the case of linear decay and inverse square of distance in the case of exponential decay give the weight of each pixel and then each weight is divided by sum of total weight in order to normalize it.

Calculation of weight of each pixel in Figure 1

If we take *w* = 1 (inverse distance decay)
First the distance of each pixel that fall within sampling net is calculated from origin ($R_1 (i, j) = (2, 2)$ or $R_3 (i, j) = (0, 0)$)

a. Distance of pixel (class – 2) at pixel coordinates (2, 2) (i.e. at origin according to $R_3 (i, j)$) from origin

$D_1(2) = 0$

Weight of this pixel is

$W_1(2) = (D_1(2)+1)^{-w} = (0+1)^{-1} = 1$ (1 is added to distance and then its inverse is calculated to find out weight)

b. Distance of pixel (class – 1) at pixel coordinates (2, 3) (i.e. at (6, 0) according to R_3 (i, j)) from origin

$D_2(1)$ = sqrt((6 - 0)^2+(0 - 0)^2) = 6

$W_2(1) = (6+1)^{-1} = 1/ 7$

c. Distance of pixel (class – 4) at pixel coordinates (2, 1) (i.e. at (-6, 0) according to R_3 (i, j)) from origin

$D_3(4)$ = sqrt((-6 - 0)^2+(0 - 0)^2) = 6

$W_3(4) = (6+1)^{-1} = 1/ 7$

d. Distance of pixel (class – 1) at pixel coordinates (1, 2) (i.e. at (0, 6) according to R_3 (i, j)) from origin

$D_4(1)$ = sqrt((0 - 0)^2+(6 - 0)^2) = 6

$W_4(1) = (6+1)^{-1} = 1/ 7$

e. Distance of pixel (class – 2) at pixel coordinates (3, 2) (i.e. at (0, -6) according to R_3 (i, j)) from origin)

$D_5(2)$ = sqrt((0 - 0)^2+(0 + 6)^2) = 6

$W_5(2) = (6+1)^{-1} = 1/ 7$

All estimated weights are added and then divided by each weight in order to normalize it.

Wtsum = 1+ 1/7 + 1/7 + 1/7 + 1/7 = 11/7

$W_1(2) = 1/(11/7) = 7/11$

$W_2(1) = 1/11$

$W_3(4) = 1/ 11$

$W_4(1) = 1/ 11$

$W_5(2) = 1/ 11$

D. Normalized weight of all pixels having same cover type within sampling net is added. That gives the frequency of each cover type within sampling net.

It is calculated as

frq(1) -- $W_2(1) + W_4(1) = 1/11 + 1/11 = 2/11$

frq(2) – $W_1(2) + W_5(2) = 7/11 + 1/11 = 8/11$

frq(4) -- $W_4(1) = 1/11$

Each frequency is divided by the sum of total frequency in order to normalize it. Here the sum is 1 therefore same normalized frequency distribution is obtained for each cover type.

E. Frequency distribution is made cumulative (to get cumulative frequency distribution) in this way

cfd(1) --- frq(1) +frq(0)
2/11 + 0 (since frq(0) is 0 as it is not present)

cfd (2) --- frq(2) + frq(1)
8/11 + 2/11

cfd (4) --- frq(4) + frq(3)
1/11 + 0 (since frq(3) is 0 as it is not present)

Note – If equal weight (w = 0)is given to all points of sampling net, then frequency of each class will be simply its count within sampling net.

Random number seed

Random number seed is set to obtain the uniform random deviate so that each time the program is run to get same aggregation level, it will give the same output. In PDW program random number seed has been used to obtain the uniform random deviate between 0 and 1.

The concept behind this is simple that random number generation is really a not a random process in computer, it is based on certain rule. Therefore the generation of random number can be controlled (to get same number each time) by providing random number seed.

The same concept has been used in PDW program. It is based on the program provided in Numerical Recipes Software (PDW documentation). The requirement of this program is to take the random number seed which should always be negative and less than 2^10.

The uniform random deviate is compared with cumulative frequency distribution obtained in step 5. If its value is just lower than the 'cfd' of any cover type, then that cover type will be selected and assigned to output aggregated pixel (pixel of 18m resolution in given example)

Code of central pixel resampling approach

```
##########################################
### setting number of bands
##########################################
nb <- 4
Path <- 'D:\\CPR\\'

#########################################################
### importing each band of image
#########################################################
i<-1
input <- paste(Path, 'band_',i,'.txt', sep='')
temp <- read.table(input, skip = 5)
d <- dim(temp)
nri <- d[1]
nci <- d[2]
img <- array(0, c(nri,nci,nb))
img[,,i] <- as.matrix(temp)
for(i in 1:nb)
{
 input <- paste(Path, 'band_',i,'.txt', sep='')
 temp <- read.table(input, skip = 5)
 img[,,i] <- as.matrix(temp)
}

##############################################
#### setting window size (it should be odd)
##############################################
ws <- 3

#############################################################################
### number of row and column of output aggregated image
#############################################################################
nro <- trunc(nri/ws)
nco <- trunc(nci/ws)

#####################################################################
### initialization of output image matrix
#####################################################################
g <- array(0, c(nro,nco,nb))

#################################################################
### initialization of some variables
#################################################################
l<- 0
m <- 0
```

```
##############################################################################################
#### 'cr' and 'cc' hold the total number of rows and columns in original image which are to be used
####during aggregation
##############################################################################################
cr <- nro*ws
cc <- nco*ws

##############################################################################################
### 'sr' and 'sc' hold the sequence in vertical and horizantal direction respectively, which retrict the
###'for' loop to execute in sequence that is required to obtain central pixel value
##############################################################################################
sr <- seq(from=(ws+1)/2, to = (cr-((ws-1)/2)), by = ws)
sc <- seq(from=(ws+1)/2, to = (cc-((ws-1)/2)), by = ws)

for(i in 1:nb)
{
   for(j in sr)
     {
     l <- l+1
       for(k in sc)
        {
         m <- m+1
         g[l,m,]=img[j,k,]

        }
       m <- 0
     }
   l <- 0
}

#############################################################
### writing aggregeted matrix of all band to text file
#############################################################
for(i in 1:nb)
write.table(g[,,i], file = paste(Path,'output_band',i,'.txt',sep=''),append=FALSE,quote=TRUE,sep ="
",eol="\n",na="NA",dec=".",row.names=FALSE,col.names=FALSE,qmethod=c("escape","double"))
```

Code of Aggregation Index

```
Path <- 'D:\\AI\\'

Inputfile <- paste(Path, 'classified','.txt', sep='')
temp <- read.table(Inputfile, skip = 5)
d <- dim(temp)
nri <- d[1]
nci <- d[2]
img <- array(0, c(nri,nci))
img[,] <- as.matrix(temp)

nc <- 4
AI <- array(0,nc)
AIr <- array(0,nc)
edg <- array(0,nc)
frq <- array(0,nc)

for(k in 1:nc)
{
 for(i in 1:nri)
   {
    for(j in 1:nci)
       {
        if(k == 1)
          {
           temp <- img[i,j]
           frq[temp] <- frq[temp]+1
          }
        if(i == 1)
          {
           if(j != nci)
             {
              if(img[i,j] == k && img[i,j+1]== k)
                {
                 edg[k] <- edg[k]+1
                }
             }
          }
         if(i != 1)
           {
           if(j != nci)
             {
              if(img[i,j] == k && img[i,j+1]== k)
               {
                 edg[k] <- edg[k]+1
               }
```

```
            if(img[i,j] == k && img[i-1,j] == k)
              {
              edg[k] <- edg[k] +1
              }
            }
           if(j == nci)
            {
             if(img[i,j] == k && img[i-1,j] == k)
              {
              edg[k] <- edg[k] +1
              }
            }
          }
        }
    }
     maxsq <- trunc(sqrt(frq[k]))
     m <- frq[k] - (maxsq*maxsq)
     if(m == 0)
     maxedg <- (2*maxsq)*(maxsq-1)
     if(m != 0 && m < maxsq)
     maxedg <-  ((2*maxsq)*(maxsq-1))+((2*m)-1)
     if( m >= maxsq)
     maxedg <-  ((2*maxsq)*(maxsq-1))+((2*m)-2)
     AI[k] <- edg[k]/maxedg
     AIr[k] <- round(AI[k],digits = 3)
}
  sfrq <- sum(frq)
  LAI <- 0
  for(k in 1:nc)
    {
     tem <- AI[k]*(frq[k]/sfrq)
     LAI <- LAI + tem
    }
      LAIr <- round(LAI, digits = 3)

#################################################################
### writing AI values of each class in text file
#################################################################

write.table(c('Aggregation Index of class 1,2,3 and 4 respectively',AIr[], 'Landscape Aggregation In-
dex',LAIr), file =paste(Path,'Aggregation_Index_mean7','.txt',sep=''),append=FALSE,quote=TRUE,sep
="",eol="\n\n",na="NA",dec=".",row.names=FALSE,col.names=FALSE,qmethod=c("escape","double
"))
```

Some limitations of code

All the code given above has been written in R programming language. Before running code user should keep in mind the following points.

1. All the code has been written to apply only on square images. It needs modification to apply on non-square images.
2. The code of majority rule-based, random rule-based and Aggregation Index should be applied on classified image having class labels in sequence starting from '1'. It needs again modification to apply on the classified image having class labels with any numbers.